

# Displacement and Stress Associated with Distributed Anelastic Deformation in a Half-Space

by Sylvain Barbot, James D. P. Moore, and Valère Lambert

**Abstract** We present a suite of analytical and semianalytical solutions for the displacements, strains, and stress due to distributed anelastic deformation of finite strain volumes in a half-space for cuboid sources. We provide the solutions in the cases of antiplane strain, plane strain, and 3D deformation. These expressions represent powerful tools for the analysis of deformation data to image distributed strain in the Earth's interior and for the dynamic modeling of distributed deformation off faults, including thermoelasticity, poroelasticity, and viscoelasticity. We include computer programs that evaluate these expressions free of major singular points. Combined with formulas that describe the deformation around faults, these solutions represent a comprehensive description of quasi-static deformation throughout the earthquake cycle within the lithosphere–asthenosphere system.

*Electronic Supplement:* Animations of displacement and stress.

## Introduction

The last few decades have witnessed an explosion of studies on fault processes, from kinematic modeling of geodetic data to dynamic modeling of fault rheology. These studies were made possible by fundamental solutions that describe the stress and displacements incurred by the rocks surrounding moving faults (Steketee, 1958; Chinnery, 1963; Savage and Hastie, 1966; Sato and Matsu'ura, 1974; Iwasaki and Sato, 1979; Okada, 1985, 1992). In contrast, off-fault and distributed deformation have received little attention. For example, the dynamic modeling of viscoelastic relaxation or poroelastic rebound still relies on computationally intensive numerical methods (e.g., Barbot and Fialko, 2010a). In addition, the direct imaging of distributed deformation using inverse methods is still impractical, severely limiting our insight on potentially important processes of stress evolution. To remedy this, we describe the displacement and stress incurred on the surrounding rocks by distributed anelastic strain. These solutions provide the building blocks to constrain the kinematics of deformation in the Earth's interior using deformation data. Our description of stress interactions enables the dynamic modeling of stress evolution, including distributed deformation in the crust due to the flow of fluids or the diffusion of temperature, or viscoelastic flow of the lower crust and asthenosphere. Combined with formulations that describe stress interactions around faults, the result is a comprehensive representation of the kinematics and dynamics of deformation in the lithosphere–asthenosphere system.

Our goal is to describe closed-form analytic solutions for the displacement and stress occasioned by an arbitrary distribution of anelastic deformation in the Earth's interior. Here, anelastic deformation refers to any thermodynamically irreversible process of deformation, which includes thermoelasticity, poroelasticity, and viscoelasticity. To make the problem tractable, we focus on anelastic deformation confined in finite cuboid volumes. More complex deformation can be reproduced by a linear combination of these elementary solutions. Being the first to tackle this problem, we seek alternative descriptions that cross validate each other. In addition to providing analytic solutions, we describe several numerical approximations that constitute independent points of comparison. To make our results most useful, we provide computer codes to evaluate the mathematical expressions free of major numerical artifacts. These expressions contain singular points solely at the corners of each anelastic strain region.

This article describes the derivation of the analytic and numerical solutions and provides some illustrative examples. We start with a short introduction to the concepts of eigenstrain and equivalent body forces that are central to describing anelastic deformation. We then derive the displacement and stress kernels for the case of antiplane strain. In the next two sections, we derive the solutions for the cases of plane strain and 3D deformation.

## Eigenstrain and Equivalent Body Forces

To represent the effect of distributed strain in the volume, we employ the method of equivalent body forces (Barbot and Fialko, 2010a,b). We assume that the total strain in the medium is the sum of the elastic and anelastic contributions

$$\boldsymbol{\epsilon} = \boldsymbol{\epsilon}^e + \boldsymbol{\epsilon}^i, \quad (1)$$

in which  $\boldsymbol{\epsilon}^i$  represents the cumulative anelastic strain. The constitutive stress strain relationship applies for elastic strain, so in general we have

$$\boldsymbol{\sigma} = \mathbf{C} : \boldsymbol{\epsilon}^e, \quad (2)$$

in which  $\boldsymbol{\sigma}$  is the Cauchy stress and  $\mathbf{C}$  is the elastic moduli tensor, assumed independent of anelastic strain. Many aspects of the Earth's quasi-static deformation throughout the earthquake cycle may be encapsulated in this formulation (Barbot and Fialko, 2010a), including thermoelasticity, Newtonian, Burgers or power-law viscoelasticity (Masuti *et al.*, 2016), poroelasticity, and even faulting. Isotropic anelastic strain may represent thermoelastic and poroelastic processes or bulk viscosity. Deviatoric anelastic strain may be due to viscoelastic flow.

In this framework, anelastic strain can be associated with equivalent body forces as follows. The conservation of linear momentum at steady state can be written:

$$\nabla \cdot \boldsymbol{\sigma} = \nabla \cdot (\mathbf{C} : \boldsymbol{\epsilon}^e) = \mathbf{0}, \quad (3)$$

in which the single dot indicates the vector dot product. Substituting  $\boldsymbol{\epsilon}^e = \boldsymbol{\epsilon} - \boldsymbol{\epsilon}^i$ , we get the inhomogeneous equation for the total strain:

$$\nabla \cdot (\mathbf{C} : \boldsymbol{\epsilon}) - \nabla \cdot (\mathbf{C} : \boldsymbol{\epsilon}^i) = \mathbf{0}. \quad (4)$$

As  $\boldsymbol{\epsilon}^i$  is given, we define a moment density

$$\mathbf{m} = \mathbf{C} : \boldsymbol{\epsilon}^i, \quad (5)$$

that is independent of the dynamic variables. As a result, for any distribution of anelastic strain (or eigenstrain)  $\boldsymbol{\epsilon}^i$ , we can associate a distribution of fixed equivalent body forces

$$\mathbf{f} = -\nabla \cdot (\mathbf{C} : \boldsymbol{\epsilon}^i) = -\nabla \cdot \mathbf{m}. \quad (6)$$

The total displacement due to anelastic strain and the elastic response of the medium can be obtained by solving the momentum equations. For a homogeneous and isotropic material, the total displacement is obtained by solving Navier's equation:

$$(\lambda + \mu)\nabla\nabla \cdot \mathbf{u} + \mu\nabla^2\mathbf{u} + \mathbf{f} = \mathbf{0}, \quad (7)$$

in which  $\lambda$  and  $\mu$  are the Lamé parameters and  $\mu$  is the rigidity. Given the total displacement  $\mathbf{u}$ , we can obtain the total strain with

$$\boldsymbol{\epsilon} = \frac{1}{2}(\nabla\mathbf{u} + \nabla\mathbf{u}^T), \quad (8)$$

in which  $\nabla\mathbf{u}^T$  is the transpose of the displacement gradient. Finally, the stress field is derived by removing the anelastic strain contribution:

$$\boldsymbol{\sigma} = \mathbf{C} : (\boldsymbol{\epsilon} - \boldsymbol{\epsilon}^i). \quad (9)$$

Navier's equation allows us to model elastoplastic deformation due to an arbitrary distribution of anelastic strain under the infinitesimal strain approximation. The moment density is an arbitrary tensor field, and the displacement field can be obtained with

$$\mathbf{u}(\mathbf{x}) = \int_{\Omega} \mathbf{G}(\mathbf{x}, \mathbf{y}) \cdot \mathbf{f}(\mathbf{y}) d\mathbf{y}, \quad (10)$$

in which  $\mathbf{G}$  are the Green's functions for a point force. To keep the problem tractable, we assume anelastic strain distributions that are piecewise homogeneous in cuboid volumes  $\Omega_k$  (or in rectangular areas for 2D solutions), so we can write the displacement solution as

$$\mathbf{u}(\mathbf{x}) \approx \sum_k \int_{\Omega_k} \mathbf{G}(\mathbf{x}, \mathbf{y}) \cdot \mathbf{f}_k(\mathbf{y}) d\mathbf{y}, \quad (11)$$

in which  $\mathbf{f}_k$  is the equivalent body force for a homogeneous anelastic strain in the domain  $\Omega_k$ . This simplifying assumption allows us to solve equation (7) analytically in closed form using the displacement kernels

$$\mathbf{u}_k(\mathbf{x}) = \int_{\Omega_k} \mathbf{G}(\mathbf{x}, \mathbf{y}) \cdot \mathbf{f}_k(\mathbf{y}) d\mathbf{y}. \quad (12)$$

Arbitrary source distributions can then be obtained by linear superposition. The displacement kernels  $\mathbf{u}_k(\mathbf{x})$  form the basic ingredients for forward (e.g., Lambert and Barbot, 2016) and inverse modeling of deformation data. The following sections describe the solution method for antiplane strain, plane strain, and 3D deformation.

## Distributed Deformation of Finite Shear Zones in Antiplane Strain

The antiplane strain framework is relevant to modeling deformation at transform plate boundaries (e.g., Barbot *et al.*, 2008). In this context, distributed deformation comes about in the damage zone surrounding faults, the shear zone that develops at the down-dip extension of faults (Moore and Parsons, 2015), and the viscoelastic flow that accommodates the transport of rigid plates (Lambert and Barbot, 2016).

### Problem Definition

We consider the elastic deformation in antiplane strain caused by distributed anelastic strain in an elementary rectangular area, which we refer to as a shear zone. We consider

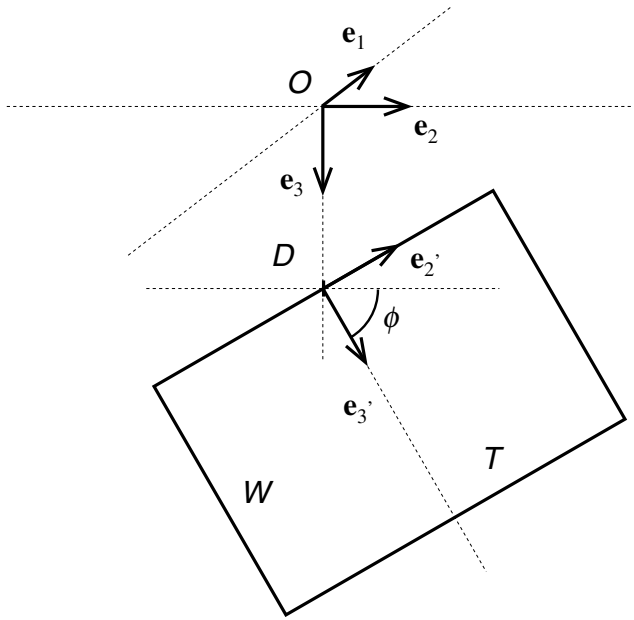


**Figure 1.** Position and orientation of a shear zone of thickness  $T$  and width  $W$ , buried at depth  $D$ , dipping an angle  $\phi$ , and striking in the  $\mathbf{e}_1$  direction. The prime coordinate system is aligned with the shear zone. Both systems of coordinates point in the strike direction, such as  $\mathbf{e}'_1 = \mathbf{e}_1$ . For  $\phi = \pi/2$ ; the two systems are identical except for a translation.

two systems of coordinates. The unprimed system of coordinates is aligned with the free surface and in the strike direction of the shear zone (Fig. 1). The primed system of coordinates is aligned with the fault. In the case of antiplane strain, we have  $u_{i,1} = 0$  for  $i = 1, 2, 3$  and  $u_2 = u_3 = 0$ . We apply anelastic deformation in a rectangular area of width  $W$  in the dip direction  $\mathbf{e}'_3$ , and of thickness  $T$  in the normal direction  $\mathbf{e}'_2$ . The relationships between the primed and unprimed coordinates are:

$$\begin{aligned} x'_1 &= x_1 \\ x'_2 &= x_2 \sin \phi - (x_3 - D) \cos \phi \\ x'_3 &= x_2 \cos \phi + (x_3 - D) \sin \phi \end{aligned} \quad (13)$$

and

$$\begin{aligned} x_1 &= x'_1 \\ x_2 &= +x'_2 \sin \phi + x'_3 \cos \phi \\ x_3 &= -x'_2 \cos \phi + x'_3 \sin \phi + D. \end{aligned} \quad (14)$$

The shear zone is buried at a depth  $D$  in the  $\mathbf{e}_3$  direction. The volume is subjected to two independent eigenstrain components  $\epsilon'_{12}$  and  $\epsilon'_{13}$ , which are expressed in the unprimed system of coordinates.

The spatial extent of the eigenstrain can be defined with the generalized functions  $S(x) = \Pi(x - 1/2)$ , with  $S'(x) = \delta(x) - \delta(x - 1)$  and  $\Pi(x) = H(x + 1/2) - H(x - 1/2)$ ,  $H(x)$  being the Heaviside function. Using a combination

of primed and unprimed coordinates for convenience, we can write the distribution of eigenstrain as

$$\epsilon'_{ij}(x_2, x_3) = \epsilon'_{ij} \Pi\left(\frac{x'_2}{T}\right) S\left(\frac{x'_3}{W}\right) \equiv \epsilon'_{ij} \Omega(x_2, x_3), \quad (15)$$

with  $x'_2 = x'_2(x_2, x_3)$  and  $x'_3 = x'_3(x_2, x_3)$ . Or, more explicitly

$$\begin{aligned} \epsilon'_{ij}(x_2, x_3) &= \epsilon'_{ij} \Pi\left(\frac{x_2 \sin \phi - (x_3 - D) \cos \phi}{T}\right) \\ &\times S\left(\frac{x_2 \cos \phi + (x_3 - D) \sin \phi}{W}\right). \end{aligned} \quad (16)$$

We have defined the functions

$$\begin{aligned} \Omega(x_2, x_3) &= \Pi\left(\frac{x'_2(x_2, x_3)}{T}\right) S\left(\frac{x'_3(x_2, x_3)}{W}\right) \\ \Omega'(x'_2, x'_3) &= \Pi\left(\frac{x'_2}{T}\right) S\left(\frac{x'_3}{W}\right), \end{aligned} \quad (17)$$

which describe where the strain is applied. The deformation in the half-space due to elastic coupling can be attributed to the equivalent body forces

$$f_1 = 2\mu\epsilon'_{12,2} + 2\mu\epsilon'_{13,3}, \quad (18)$$

with  $f_2 = f_3 = 0$ . Because of the presence of two systems of reference, we use the chain rule. The equivalent body force becomes

$$\begin{aligned} f_1 &= -2\mu\epsilon'_{12}(\Omega'_{,2} \sin \phi + \Omega'_{,3} \cos \phi) \\ &+ 2\mu\epsilon'_{13}(-\Omega'_{,2} \cos \phi + \Omega'_{,3} \sin \phi) \\ &= -\sin \phi(2\mu\epsilon'_{12}\Omega'_{,2} + 2\mu\epsilon'_{13}\Omega'_{,3}) \\ &- \cos \phi(2\mu\epsilon'_{12}\Omega'_{,3} - 2\mu\epsilon'_{13}\Omega'_{,2}). \end{aligned} \quad (19)$$

To be clear, we use the notation

$$\Omega'_{,i} = \frac{\partial \Omega'(x'_1, x'_2, x'_3)}{\partial x'_i}. \quad (20)$$

So we have the equivalent body forces:

$$\begin{aligned} f_1(x_2, x_3) &= \sin \phi \left\{ 2\mu\epsilon'_{12} \frac{1}{T} \left[ \delta\left(\frac{x'_2}{T} - \frac{1}{2}\right) - \delta\left(\frac{x'_2}{T} + \frac{1}{2}\right) \right] S\left(\frac{x'_3}{W}\right) \right. \\ &+ 2\mu\epsilon'_{13} \Pi\left(\frac{x'_2}{T}\right) \frac{1}{W} \left[ \delta\left(\frac{x'_3}{W} - 1\right) - \delta\left(\frac{x'_3}{W}\right) \right] \left. \right\} \\ &+ \cos \phi \left\{ 2\mu\epsilon'_{12} \Pi\left(\frac{x'_2}{T}\right) \frac{1}{W} \left[ \delta\left(\frac{x'_3}{W} - 1\right) - \delta\left(\frac{x'_3}{W}\right) \right] \right. \\ &- 2\mu\epsilon'_{13} \frac{1}{T} \left[ \delta\left(\frac{x'_2}{T} - \frac{1}{2}\right) - \delta\left(\frac{x'_2}{T} + \frac{1}{2}\right) \right] S\left(\frac{x'_3}{W}\right) \left. \right\}. \end{aligned} \quad (21)$$

Analytic Solution

The displacement field can be obtained by solving Navier’s equation, which simplifies to the inhomogeneous Poisson’s equation in antiplane strain:

$$u_{1,22} + u_{1,33} + \frac{1}{\mu}f_1 = 0. \tag{22}$$

We will solve Poisson’s equation using the Green’s function method, where the displacement in the direction  $i$  due to forces pointing in the direction  $j$  are given by the point-source Green’s functions  $G_{ji}(x_1, x_2, x_3)$ . By double integration in cylindrical coordinates and after using the method of images, we find the Green’s function in antiplane for a point source located at  $(y_2, y_3)$ :

$$G_{11}(x_2, x_3) = -\frac{1}{4\pi\mu}[\ln((x_2 - y_2)^2 + (x_3 - y_3)^2) + \ln((x_2 - y_2)^2 + (x_3 + y_3)^2)]. \tag{23}$$

Then, the displacements are obtained using the convolution

$$u_1(x_2, x_3) = \frac{-1}{4\pi\mu} \iint_{-\infty}^{\infty} f_1(y_2, y_3) \ln((x_2 - y_2)^2 + (x_3 - y_3)^2) dy_2 dy_3 - \frac{-1}{4\pi\mu} \iint_{-\infty}^{\infty} f_1(y_2, y_3) \ln((x_2 - y_2)^2 + (x_3 + y_3)^2) dy_2 dy_3. \tag{24}$$

Using the spatial distribution of equivalent body forces (equation 21), we can write the displacement field explicitly:

$$u_1 = + \sin \phi \left\{ 2\mu\epsilon_{12} \iint_{-\infty}^{\infty} \frac{1}{T} \left[ \delta\left(\frac{y'_2}{T} - \frac{1}{2}\right) - \delta\left(\frac{y'_2}{T} + \frac{1}{2}\right) \right] S\left(\frac{y'_3}{W}\right) G_{11}(y_2, y_3) dy_2 dy_3 + 2\mu\epsilon_{13} \iint_{-\infty}^{\infty} \Pi\left(\frac{y'_2}{T}\right) \frac{1}{W} \left[ \delta\left(\frac{y'_3}{W} - 1\right) - \delta\left(\frac{y'_3}{W}\right) \right] G_{11}(y_2, y_3) dy_2 dy_3 \right\} + \cos \phi \left\{ 2\mu\epsilon_{12} \iint_{-\infty}^{\infty} \Pi\left(\frac{y'_2}{T}\right) \frac{1}{W} \left[ \delta\left(\frac{y'_3}{W} - 1\right) - \delta\left(\frac{y'_3}{W}\right) \right] G_{11}(y_2, y_3) dy_2 dy_3 - 2\mu\epsilon_{13} \iint_{-\infty}^{\infty} \frac{1}{T} \left[ \delta\left(\frac{y'_2}{T} - \frac{1}{2}\right) - \delta\left(\frac{y'_2}{T} + \frac{1}{2}\right) \right] S\left(\frac{y'_3}{W}\right) G_{11}(y_2, y_3) dy_2 dy_3 \right\}. \tag{25}$$

To simplify the problem, we now change the variables of integration from  $dy_2 dy_3$  to  $dy'_2 dy'_3$ :

$$u_1 = \sin \phi \left\{ 2\mu\epsilon_{12} \iint_{-\infty}^{\infty} \frac{1}{T} \left[ \delta\left(\frac{y'_2}{T} - \frac{1}{2}\right) - \delta\left(\frac{y'_2}{T} + \frac{1}{2}\right) \right] S\left(\frac{y'_3}{W}\right) G_{11}(y_2, y_3) dy'_2 dy'_3 + 2\mu\epsilon_{13} \iint_{-\infty}^{\infty} \Pi\left(\frac{y'_2}{T}\right) \frac{1}{W} \left[ \delta\left(\frac{y'_3}{W} - 1\right) - \delta\left(\frac{y'_3}{W}\right) \right] G_{11}(y_2, y_3) dy'_2 dy'_3 \right\} + \cos \phi \left\{ 2\mu\epsilon_{12} \iint_{-\infty}^{\infty} \Pi\left(\frac{y'_2}{T}\right) \frac{1}{W} \left[ \delta\left(\frac{y'_3}{W} - 1\right) - \delta\left(\frac{y'_3}{W}\right) \right] G_{11}(y_2, y_3) dy'_2 dy'_3 - 2\mu\epsilon_{13} \iint_{-\infty}^{\infty} \frac{1}{T} \left[ \delta\left(\frac{y'_2}{T} - \frac{1}{2}\right) - \delta\left(\frac{y'_2}{T} + \frac{1}{2}\right) \right] S\left(\frac{y'_3}{W}\right) G_{11}(y_2, y_3) dy'_2 dy'_3 \right\}, \tag{26}$$

in which the expression  $G_{11}(y_2, y_3)$  is short for  $G_{11}[y_2(y'_2, y'_3), y_3(y'_2, y'_3)]$ . We simplify the bounds of integration again by integrating over the delta functions:

$$u_1 = \sin \phi \left\{ 2\mu\epsilon_{12} \int_0^W G_{11}[y_2(y'_2, y'_3), y_3(y'_2, y'_3)] \Big|_{y'_2=-T/2}^{y'_2=T/2} dy'_3 + 2\mu\epsilon_{13} \int_{-T/2}^{T/2} G_{11}[y_2(y'_2, y'_3), y_3(y'_2, y'_3)] \Big|_{y'_3=0}^{y'_3=W} dy'_2 \right\} + \cos \phi \left\{ 2\mu\epsilon_{12} \int_{-T/2}^{T/2} G_{11}[y_2(y'_2, y'_3), y_3(y'_2, y'_3)] \Big|_{y'_3=0}^{y'_3=W} dy'_2 - 2\mu\epsilon_{13} \int_0^W G_{11}[y_2(y'_2, y'_3), y_3(y'_2, y'_3)] \Big|_{y'_2=-T/2}^{y'_2=T/2} dy'_3 \right\}. \tag{27}$$

(Here, the relation  $\int_{-\infty}^{\infty} \delta(ax) dx = 1/|a|$  has been useful.)

We then expand the expression in terms of primed variables

$$\begin{aligned}
 u_1 = & \sin \phi \left\{ 2\mu \epsilon_{12}^i \int_0^W G_{11} \left[ y_2' \sin \phi + y_3' \cos \phi, -y_2' \cos \phi + y_3' \sin \phi + D \right] \Big|_{y_2'=-T/2}^{y_2'=T/2} dy_3' \right. \\
 & \left. + 2\mu \epsilon_{13}^i \int_{-T/2}^{T/2} G_{11} \left[ y_2' \sin \phi + y_3' \cos \phi, -y_2' \cos \phi + y_3' \sin \phi + D \right] \Big|_{y_3'=0}^{y_3'=W} dy_2' \right\} \\
 & + \cos \phi \left\{ 2\mu \epsilon_{12}^i \int_{-T/2}^{T/2} G_{11} \left[ y_2' \sin \phi + y_3' \cos \phi, -y_2' \cos \phi + y_3' \sin \phi + D \right] \Big|_{y_3'=0}^{y_3'=W} dy_2' \right. \\
 & \left. - 2\mu \epsilon_{13}^i \int_0^W G_{11} \left[ y_2' \sin \phi + y_3' \cos \phi, -y_2' \cos \phi + y_3' \sin \phi + D \right] \Big|_{y_2'=-T/2}^{y_2'=T/2} dy_3' \right\}, \tag{28}
 \end{aligned}$$

and we substitute the Green's function for its definition (equation 23) to get

$$\begin{aligned}
 u_1 = & \frac{-1}{2\pi} \left[ \sin \phi \left\{ \epsilon_{12}^i \int_0^W \ln((x_2 - y_2' \sin \phi - y_3' \cos \phi)^2 + (x_3 + y_2' \cos \phi - y_3' \sin \phi - D)^2) \Big|_{y_2'=-T/2}^{y_2'=T/2} dy_3' \right. \right. \\
 & + \epsilon_{12}^i \int_0^W \ln((x_2 - y_2' \sin \phi - y_3' \cos \phi)^2 + (x_3 - y_2' \cos \phi + y_3' \sin \phi + D)^2) \Big|_{y_2'=-T/2}^{y_2'=T/2} dy_3' \\
 & + \epsilon_{13}^i \int_{-T/2}^{T/2} \ln((x_2 - y_2' \sin \phi - y_3' \cos \phi)^2 + (x_3 + y_2' \cos \phi - y_3' \sin \phi - D)^2) \Big|_{y_3'=0}^{y_3'=W} dy_2' \\
 & \left. + \epsilon_{13}^i \int_{-T/2}^{T/2} \ln((x_2 - y_2' \sin \phi - y_3' \cos \phi)^2 + (x_3 - y_2' \cos \phi + y_3' \sin \phi + D)^2) \Big|_{y_3'=0}^{y_3'=W} dy_2' \right\} \\
 & + \cos \phi \left\{ \epsilon_{12}^i \int_{-T/2}^{T/2} \ln((x_2 - y_2' \sin \phi - y_3' \cos \phi)^2 + (x_3 + y_2' \cos \phi - y_3' \sin \phi - D)^2) \Big|_{y_3'=0}^{y_3'=W} dy_2' \right. \\
 & + \epsilon_{12}^i \int_{-T/2}^{T/2} \ln((x_2 - y_2' \sin \phi - y_3' \cos \phi)^2 + (x_3 - y_2' \cos \phi + y_3' \sin \phi + D)^2) \Big|_{y_3'=0}^{y_3'=W} dy_2' \\
 & - \epsilon_{13}^i \int_0^W \ln((x_2 - y_2' \sin \phi - y_3' \cos \phi)^2 + (x_3 + y_2' \cos \phi - y_3' \sin \phi - D)^2) \Big|_{y_2'=-T/2}^{y_2'=T/2} dy_3' \\
 & \left. - \epsilon_{13}^i \int_0^W \ln((x_2 - y_2' \sin \phi - y_3' \cos \phi)^2 + (x_3 - y_2' \cos \phi + y_3' \sin \phi + D)^2) \Big|_{y_2'=-T/2}^{y_2'=T/2} dy_3' \right\}, \tag{29}
 \end{aligned}$$

which represents only four separate indefinite integrals. The solution is obtained in closed form as follows:

$$\begin{aligned}
 u_1 = & \frac{-1}{2\pi} \left[ \sin \phi \left\{ \epsilon_{12}^i (J_{12} + K_{12}) + \epsilon_{13}^i (J_{13} + K_{13}) \right\} \right. \\
 & \left. + \cos \phi \left\{ \epsilon_{12}^i (J_{13} + K_{13}) - \epsilon_{13}^i (J_{12} + K_{12}) \right\} \right], \tag{30}
 \end{aligned}$$

in which the integrals  $J_{12}, K_{12}, J_{13},$  and  $K_{13}$  are defined below. To simplify the expressions, we make use of the Chinnery (1963) notation, defined here as:

$$\begin{aligned}
 f(y_2', y_3') \Big| \Big| = & f(T/2, W) - f(-T/2, W) \\
 & - f(T/2, 0) + f(-T/2, 0). \tag{31}
 \end{aligned}$$

We have the following integrals in closed form:

$$\begin{aligned}
 J_{12} = & -2r_2' \arctan\left(\frac{r_3'}{r_2'}\right) - r_3' \ln(r_2'^2 + r_3'^2) \Big| \Big| \\
 K_{12} = & -2s_2' \arctan\left(\frac{s_3'}{s_2'}\right) - s_3' \ln(r_2'^2 + s_3'^2) \Big| \Big| \\
 J_{13} = & -2r_3' \arctan\left(\frac{r_2'}{r_3'}\right) - r_2' \ln(r_2'^2 + r_3'^2) \Big| \Big| \\
 K_{13} = & -2s_3' \arctan\left(\frac{s_2'}{s_3'}\right) - s_2' \ln(r_2'^2 + s_3'^2) \Big| \Big|, \tag{32}
 \end{aligned}$$

with the substitutions

$$\begin{aligned}
 r_2 = & x_2 - y_2 = x_2 - y_2' \sin \phi - y_3' \cos \phi \\
 r_3 = & x_3 - y_3 = x_3 + y_2' \cos \phi - y_3' \sin \phi - D, \tag{33}
 \end{aligned}$$

also including

$$\begin{aligned} r'_2 &= r_2 \sin \phi - r_3 \cos \phi \\ r'_3 &= r_2 \cos \phi + r_3 \sin \phi, \end{aligned} \quad (34)$$

for the source, and

$$\begin{aligned} s_3 &= x_3 - y'_2 \cos \phi + y'_3 \sin \phi + D \\ s'_2 &= r_2 \sin \phi + s_3 \cos \phi \\ s'_3 &= r_2 \cos \phi - s_3 \sin \phi, \end{aligned} \quad (35)$$

for its image. Examples of displacement fields in the  $(x_2, x_3)$  plane are shown in Figure 2. The displacement field for a wide range of anelastic strain orientations and shear-zone geometries are shown in [\(E\) Movie S1](#), available in the electronic supplement to this article.

We note that the elastic displacements due to distributed anelastic strain in a finite shear zone converges to those due to a pair of screw dislocations with slip  $s$  in the limit of  $\epsilon'_{13} = 0$ , vanishing thickness  $T$ , and infinite anelastic strain  $\epsilon'_{12} = s/T$ . Our solution (equation 30) for the displacements due to distributed anelastic deformation therefore represents a unified expression for plastic deformation from localized to more distributed. This is illustrated in Figure 2. This result holds true for deformation in plane strain or 3D.

#### Numerical Solution with the tanh Quadrature

The displacement field can be obtained with arbitrary accuracy using a double exponential numerical quadrature (Haber, 1977), which is particularly useful when integrating singular expressions. We implement this numerical solution to provide us with an independent validation of our analytical solutions. We therefore convolve the Green's functions with the equivalent body forces (equation 21) numerically. To do so, we write the integral in the canonical form of the tanh quadrature using the change of variable  $y'_2 = v'T/2$  and  $y'_3 = (1 + w')W/2$ . We get

$$\begin{aligned} u_1 &= \sin \phi \left\{ 2\mu\epsilon'_{12} \frac{W}{2} \int_{-1}^1 G_{11} \left[ y'_2 \sin \phi + (1 + w')W/2 \cos \phi, -y'_2 \cos \phi + (1 + w')W/2 \sin \phi + D \right] \Big|_{y'_2=-T/2}^{y'_2=T/2} dw' \right. \\ &\quad \left. + 2\mu\epsilon'_{13} \frac{T}{2} \int_{-1}^1 G_{11} \left[ v'T/2 \sin \phi + y'_3 \cos \phi, -v'T/2 \cos \phi + y'_3 \sin \phi + D \right] \Big|_{y'_3=0}^{y'_3=W} dv' \right\} \\ &\quad + \cos \phi \left\{ 2\mu\epsilon'_{12} \frac{T}{2} \int_{-1}^1 G_{11} \left[ v'T/2 \sin \phi + y'_3 \cos \phi, -v'T/2 \cos \phi + y'_3 \sin \phi + D \right] \Big|_{y'_3=0}^{y'_3=W} dv' \right. \\ &\quad \left. - 2\mu\epsilon'_{13} \frac{W}{2} \int_{-1}^1 G_{11} \left[ y'_2 \sin \phi + (1 + w')W/2 \cos \phi, -y'_2 \cos \phi + (1 + w')W/2 \sin \phi + D \right] \Big|_{y'_2=-T/2}^{y'_2=T/2} dw' \right\}. \end{aligned} \quad (36)$$

As expected, the numerical integration converges to the analytic solution (equation 30) with increasing integration points, to the limit of double-precision floating-point accuracy. The analytical solution is most convenient however, because it is calculated several orders of magnitude faster.

#### Stress and Strain

In antiplane strain, the nonzero components of the total strain are  $\epsilon_{12} = u_{1,2}/2$  and  $\epsilon_{13} = u_{1,3}/2$ . The elastic strains are

$$\begin{aligned} \epsilon^e_{12} &= \epsilon_{12} - \epsilon^i_{12}, \\ \epsilon^e_{13} &= \epsilon_{13} - \epsilon^i_{13}. \end{aligned} \quad (37)$$

So following equation (9), the corresponding stress components are

$$\begin{aligned} \sigma_{12} &= \mu u_{1,2} - 2\mu\epsilon^i_{12}, \\ \sigma_{13} &= \mu u_{1,3} - 2\mu\epsilon^i_{13}. \end{aligned} \quad (38)$$

Here, we describe the analytic solution for stress in the case of vertical shear zones (the stress components for dipping shear zones can be obtained by differentiating the corresponding displacement field). In this case, the Chinnery (1963) notation is

$$\begin{aligned} f(y'_2, y'_3) &= f(T/2, D + W) - f(-T/2, D + W) \\ &\quad - f(T/2, D) + f(-T/2, D) \end{aligned} \quad (39)$$

and the stress components are as follows:

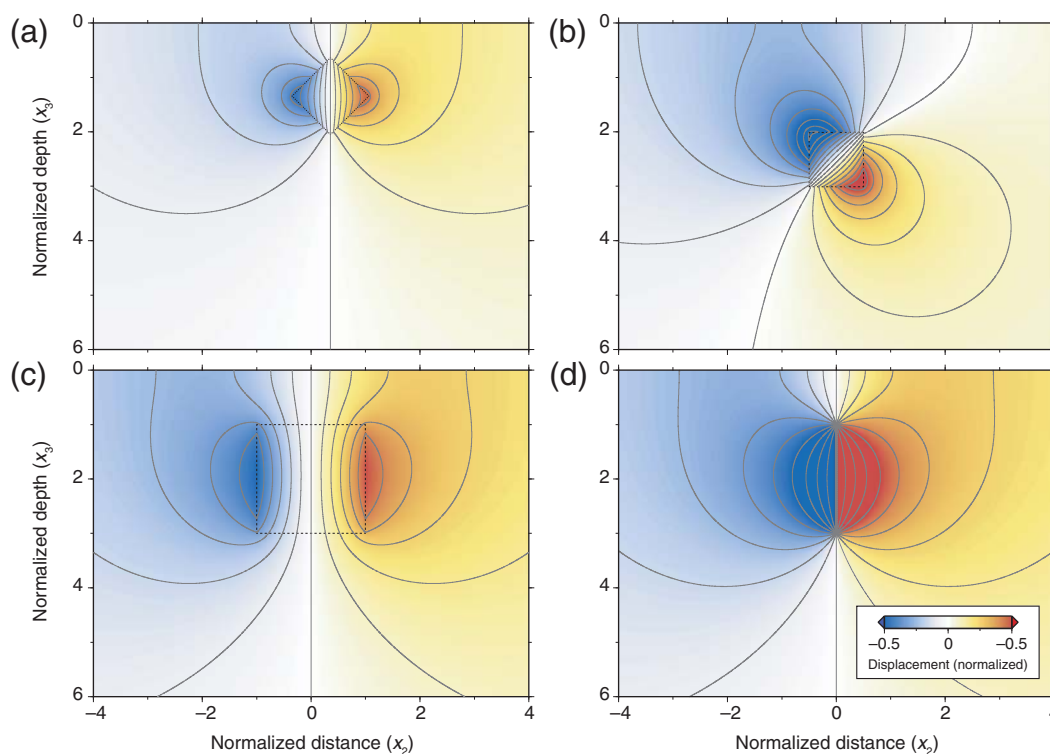


**Figure 2.** Antiplane displacement due to anelastic strain in a rectangular shear zone (black dashed box). The displacement due to shear in the  $\epsilon_{12}$  direction in a rectangular shear-zone dipping  $45^\circ$  is shown in the upper left quadrant. The displacement due to shear in  $\epsilon_{12}$  and  $\epsilon_{13}$  in equal contributions in a vertical shear zone is in the upper right quadrant. The bottom figures illustrate the convergence of a vertical shear zone to a pair of screw dislocations for small thickness for anelastic strain  $\epsilon_{12}$ . The normalization distance is proportional to the width of the shear zone.

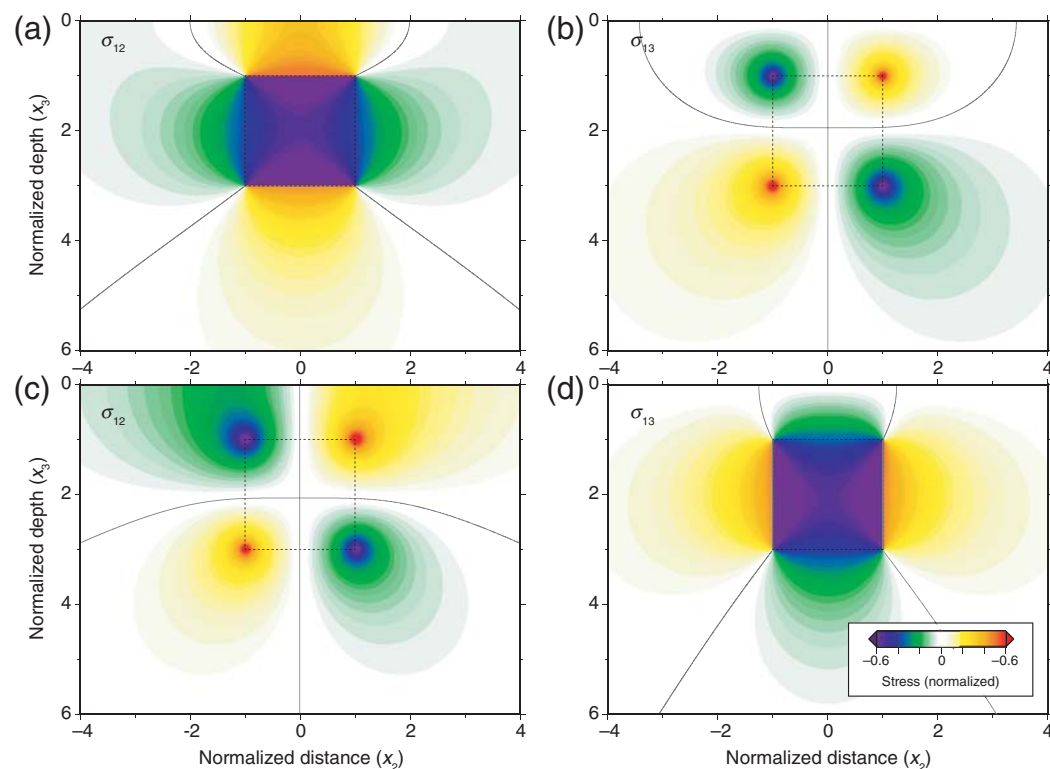


**Figure 3.** (a,c) Stress components  $\sigma_{12}$  and (b,d)  $\sigma_{13}$  due to anelastic strain (a,b)  $\epsilon_{12}^i$  and (c,d)  $\epsilon_{13}^i$  in a rectangular shear zone (black dashed box). Anelastic strain in the direction  $\mathbf{e}_i \otimes \mathbf{e}_j$  corresponds to a stress reduction in the direction  $\mathbf{e}_i \otimes \mathbf{e}_j$  inside the shear zone. The vertical stress vanishes at the surface.

$$\begin{aligned}
\sigma_{12} &= \frac{\mu\epsilon_{13}^i}{2\pi} \left[ \ln((x_2 - y_2)^2 + (x_3 - y_3)^2) + \ln((x_2 - y_2)^2 + (x_3 + y_3)^2) \right] \Big\| \Big\| \\
&\quad + \frac{\mu\epsilon_{12}^i}{\pi} \left[ \arctan \frac{x_3 - y_3}{x_2 - y_2} - \arctan \frac{x_3 + y_3}{x_2 - y_2} \right] \Big\| \Big\| \\
&\quad - 2\mu\epsilon_{12}^i \Pi\left(\frac{x_2}{T}\right) \Pi\left(\frac{x_3 - D}{W} - \frac{1}{2}\right) \\
\sigma_{13} &= \frac{\mu\epsilon_{12}^i}{2\pi} \left[ \ln((x_2 - y_2)^2 + (x_3 - y_3)^2) - \ln((x_2 - y_2)^2 + (x_3 + y_3)^2) \right] \Big\| \Big\| \\
&\quad + \frac{\mu\epsilon_{13}^i}{\pi} \left[ \arctan \frac{x_2 - y_2}{x_3 - y_3} + \arctan \frac{x_2 - y_2}{x_3 + y_3} \right] \Big\| \Big\| \\
&\quad - 2\mu\epsilon_{13}^i \Pi\left(\frac{x_2}{T}\right) \Pi\left(\frac{x_3 - D}{W} - \frac{1}{2}\right). \tag{40}
\end{aligned}$$

Eigenstrain  $\epsilon_{13}^i$  causes shear in the  $\sigma_{13}$  and  $\sigma_{12}$  components and vice versa (Fig. 3). Importantly, the stress change caused by distributed anelastic strain in the same tensor direction is always negative. This is a key element of the solution that allows dynamic simulations of distributed deformation. Strain in the direction of stress relaxes the stress in the shear zone and loads its neighbors.

### Distributed Deformation of Finite Regions in Plane Strain

Many aspects of crustal- and mantle-distributed deformation may be investigated under the plane strain approximation. This includes diffuse deformation in the mantle around subduction zones, rifts, and spreading centers. Plastic flow instabilities may also result in acceleration of the seismic cycle or in other episodic deformation. The diffusion of temperature and pore pressure modulates stress evolution, which may have important implications on the earthquake cycle. All these processes and their coupling may be modeled using the anelastic deformation of elementary rectangular volumes.

#### Problem Definition

We consider the elastic deformation in plane strain caused by distributed anelastic strain in an elementary rectangular area. We use the same system of coordinates as the previous section, but in plane strain we have  $u_{1,i} = 0$  for  $i = 1, 2, 3$ , and  $u_1 = 0$ . We define a system of coordinates  $\mathbf{e}_i^i$  aligned with the strain region and centered on the top middle point (Fig. 1). We consider a rectangular area of thickness  $T$  and width  $W$  buried at depth  $D$  subjected to the eigenstrains  $\epsilon_{22}^i$ ,  $\epsilon_{23}^i$ ,  $\epsilon_{32}^i$ , and  $\epsilon_{33}^i$ , with  $\epsilon_{23}^i = \epsilon_{32}^i$ . We define the dip angle of the strain region as the angle between the horizontal and the width direction  $\mathbf{e}_3^i$ . Hence, the strain region is vertical, and the primed and unprimed systems of coordinates are parallel for  $\phi = \pi/2$ . The relationships between primed and unprimed coordinates are

given by equations (13) and (14). Using a combination of primed and unprimed coordinates for convenience, we can write the distribution of eigenstrain as

$$\begin{aligned}
\epsilon_{22}^i(x_2, x_3) &= \epsilon_{22}^i \Pi\left(\frac{x_2'}{T}\right) S\left(\frac{x_3'}{W}\right) \equiv \epsilon_{22}^i \Omega(x_2, x_3) \\
\epsilon_{23}^i(x_2, x_3) &= \epsilon_{23}^i \Pi\left(\frac{x_2'}{T}\right) S\left(\frac{x_3'}{W}\right) \equiv \epsilon_{23}^i \Omega(x_2, x_3) \\
\epsilon_{33}^i(x_2, x_3) &= \epsilon_{33}^i \Pi\left(\frac{x_2'}{T}\right) S\left(\frac{x_3'}{W}\right) \equiv \epsilon_{33}^i \Omega(x_2, x_3), \tag{41}
\end{aligned}$$

with  $x_2' = x_2'(x_2, x_3)$  and  $x_3' = x_3'(x_2, x_3)$ . Or, more explicitly

$$\begin{aligned}
\epsilon_{22}^i(x_2, x_3) &= \epsilon_{22}^i \Pi\left(\frac{x_2 \sin \phi - (x_3 - D) \cos \phi}{T}\right) \\
&\quad \times S\left(\frac{x_2 \cos \phi + (x_3 - D) \sin \phi}{W}\right) \\
\epsilon_{23}^i(x_2, x_3) &= \epsilon_{23}^i \Pi\left(\frac{x_2 \sin \phi - (x_3 - D) \cos \phi}{T}\right) \\
&\quad \times S\left(\frac{x_2 \cos \phi + (x_3 - D) \sin \phi}{W}\right) \\
\epsilon_{33}^i(x_2, x_3) &= \epsilon_{33}^i \Pi\left(\frac{x_2 \sin \phi - (x_3 - D) \cos \phi}{T}\right) \\
&\quad \times S\left(\frac{x_2 \cos \phi + (x_3 - D) \sin \phi}{W}\right). \tag{42}
\end{aligned}$$

The  $\Omega$  and  $\Omega'$  functions are described in equation (17). We obtain the equivalent body forces from partial differentiation of the moment density using the chain rule. The equivalent body forces become



$$\begin{aligned} \mathbf{f} &= - \begin{pmatrix} 0 \\ \lambda \epsilon_{kk,2}^i + 2\mu \epsilon_{22,2}^i + 2\mu \epsilon_{23,3}^i \\ 2\mu \epsilon_{23,2}^i + \lambda \epsilon_{kk,3}^i + 2\mu \epsilon_{33,3}^i \end{pmatrix} = - \begin{pmatrix} 0 \\ (\lambda \epsilon_{kk}^v + 2\mu \epsilon_{22}^v)(\Omega'_{,2} \sin \phi + \Omega'_{,3} \cos \phi) + 2\mu \epsilon_{23}^i(-\Omega'_{,2} \cos \phi + \Omega'_{,3} \sin \phi) \\ 2\mu \epsilon_{23}^i(\Omega'_{,2} \sin \phi + \Omega'_{,3} \cos \phi) + (\lambda \epsilon_{kk}^i + 2\mu \epsilon_{33}^i)(-\Omega'_{,2} \cos \phi + \Omega'_{,3} \sin \phi) \end{pmatrix} \\ &= - \sin \phi \begin{pmatrix} 0 \\ (\lambda \epsilon_{kk}^v + 2\mu \epsilon_{22}^v)\Omega'_{,2} + 2\mu \epsilon_{23}^i\Omega'_{,3} \\ 2\mu \epsilon_{23}^i\Omega'_{,2} + (\lambda \epsilon_{kk}^i + 2\mu \epsilon_{33}^i)\Omega'_{,3} \end{pmatrix} - \cos \phi \begin{pmatrix} 0 \\ (\lambda \epsilon_{kk}^v + 2\mu \epsilon_{22}^v)\Omega'_{,3} - 2\mu \epsilon_{23}^i\Omega'_{,2} \\ 2\mu \epsilon_{23}^i\Omega'_{,3} - (\lambda \epsilon_{kk}^i + 2\mu \epsilon_{33}^i)\Omega'_{,2} \end{pmatrix}. \end{aligned} \tag{43}$$

So after combining with equation (42), we obtain the equivalent body forces

$$\begin{aligned} f_2 &= \sin \phi \left\{ (\lambda \epsilon_{kk}^i + 2\mu \epsilon_{22}^i) \frac{1}{T} \left[ \delta \left( \frac{x'_2}{T} - \frac{1}{2} \right) - \delta \left( \frac{x'_2}{T} + \frac{1}{2} \right) \right] S \left( \frac{x'_3}{W} \right) + 2\mu \epsilon_{23}^i \Pi \left( \frac{x'_2}{T} \right) \frac{1}{W} \left[ \delta \left( \frac{x'_3 - W}{W} \right) - \delta \left( \frac{x'_3}{W} \right) \right] \right\} \\ &\quad + \cos \phi \left\{ (\lambda \epsilon_{kk}^i + 2\mu \epsilon_{22}^i) \Pi \left( \frac{x'_2}{T} \right) \frac{1}{W} \left[ \delta \left( \frac{x'_3 - W}{W} \right) - \delta \left( \frac{x'_3}{W} \right) \right] - 2\mu \epsilon_{23}^i \frac{1}{T} \left[ \delta \left( \frac{x'_2}{T} - \frac{1}{2} \right) - \delta \left( \frac{x'_2}{T} + \frac{1}{2} \right) \right] S \left( \frac{x'_3}{W} \right) \right\} \\ f_3 &= \sin \phi \left\{ (\lambda \epsilon_{kk}^i + 2\mu \epsilon_{33}^i) \Pi \left( \frac{x'_2}{T} \right) \frac{1}{W} \left[ \delta \left( \frac{x'_3 - W}{W} \right) - \delta \left( \frac{x'_3}{W} \right) \right] + 2\mu \epsilon_{23}^i \frac{1}{T} \left[ \delta \left( \frac{x'_2}{T} - \frac{1}{2} \right) - \delta \left( \frac{x'_2}{T} + \frac{1}{2} \right) \right] S \left( \frac{x'_3}{W} \right) \right\} \\ &\quad + \cos \phi \left\{ -(\lambda \epsilon_{kk}^i + 2\mu \epsilon_{33}^i) \frac{1}{T} \left[ \delta \left( \frac{x'_2}{T} - \frac{1}{2} \right) - \delta \left( \frac{x'_2}{T} + \frac{1}{2} \right) \right] S \left( \frac{x'_3}{W} \right) + 2\mu \epsilon_{23}^i \Pi \left( \frac{x'_2}{T} \right) \frac{1}{W} \left[ \delta \left( \frac{x'_3 - W}{W} \right) - \delta \left( \frac{x'_3}{W} \right) \right] \right\}, \end{aligned} \tag{44}$$

with  $f_1 = 0$ .

### Analytic Solution

The displacement field can be obtained by solving Navier's equation using the Green's function approach. For a line force in the  $\mathbf{e}_2$  direction acting at  $(y_2, y_3)$ , the resulting displacement at  $(x_2, x_3)$  is

$$\begin{aligned} G_{22} &= \frac{-1}{2\pi\mu(1-\nu)} \left[ \frac{3-4\nu}{4} \ln r_1 + \frac{8\nu^2-12\nu+5}{4} \ln r_2 + \frac{(x_3-y_3)^2}{4r_1^2} + \frac{(3-4\nu)(x_3+y_3)^2 + 2y_3(x_3+y_3) - 2y_3^2}{4r_2^2} - \frac{y_3x_3(x_3+y_3)^2}{r_2^4} \right] \\ G_{23} &= \frac{1}{2\pi\mu(1-\nu)} \left[ (1-2\nu)(1-\nu) \arctan \frac{x_2-y_2}{x_3+y_3} + \frac{(x_3-y_3)(x_2-y_2)}{4r_1^2} + (3-4\nu) \frac{(x_3-y_3)(x_2-y_2)}{4r_2^2} - \frac{y_3x_3(x_2-y_2)(x_3+y_3)}{r_2^4} \right], \end{aligned} \tag{45}$$

in which

$$\begin{aligned} r_1^2 &= (x_2 - y_2)^2 + (x_3 - y_3)^2 \\ r_2^2 &= (x_2 - y_2)^2 + (x_3 + y_3)^2. \end{aligned} \tag{46}$$

For a line force in the  $\mathbf{e}_3$  direction acting at  $(y_2, y_3)$ , the resulting displacement at  $(x_2, x_3)$  is

$$\begin{aligned} G_{32} &= \frac{1}{2\pi\mu(1-\nu)} \left[ -(1-2\nu)(1-\nu) \arctan \frac{x_2-y_2}{x_3+y_3} + \frac{(x_3-y_3)(x_2-y_2)}{4r_1^2} + (3-4\nu) \frac{(x_3-y_3)(x_2-y_2)}{4r_2^2} + \frac{y_3x_3(x_2-y_2)(x_3+y_3)}{r_2^4} \right] \\ G_{33} &= \frac{1}{2\pi\mu(1-\nu)} \left[ -\frac{3-4\nu}{4} \ln r_1 - \frac{8\nu^2-12\nu+5}{4} \ln r_2 - \frac{(x_2-y_2)^2}{4r_1^2} + \frac{2y_3x_3 - (3-4\nu)(x_2-y_2)^2}{4r_2^2} - \frac{y_3x_3(x_2-y_2)^2}{r_2^4} \right]. \end{aligned} \tag{47}$$

Generally, the displacement field is given by

$$u_i(\mathbf{x}) = \iint_{-\infty}^{\infty} f_j G_{ji}(\mathbf{x}, \mathbf{y}) d\mathbf{y}, \quad (48)$$

$$\begin{aligned} u_2 &= \iint_{-\infty}^{\infty} f_2(y_2, y_3) G_{22}(y_2, y_3) dy_2 dy_3 \\ &\quad + \iint_{-\infty}^{\infty} f_3(y_2, y_3) G_{32}(y_2, y_3) dy_2 dy_3 \\ u_3 &= \iint_{-\infty}^{\infty} f_2(y_2, y_3) G_{23}(y_2, y_3) dy_2 dy_3 \\ &\quad + \iint_{-\infty}^{\infty} f_3(y_2, y_3) G_{33}(y_2, y_3) dy_2 dy_3. \end{aligned} \quad (49)$$

in which Einstein's summation convention is implied. Expanding the sum, the displacement field is given by

Using the spatial distribution of equivalent body forces, we can write the displacement field in the  $\mathbf{e}_2$  direction explicitly:

$$\begin{aligned} u_2 = \sin \phi &\left\{ (\lambda \epsilon_{kk}^i + 2\mu \epsilon_{22}^i) \iint_{-\infty}^{\infty} \frac{1}{T} \left[ \delta \left( \frac{y_2'}{T} - \frac{1}{2} \right) - \delta \left( \frac{y_2'}{T} + \frac{1}{2} \right) \right] S \left( \frac{y_3'}{W} \right) G_{22}(y_2, y_3) dy_2 dy_3 \right. \\ &\quad + 2\mu \epsilon_{23}^i \iint_{-\infty}^{\infty} \Pi \left( \frac{y_2'}{T} \right) \frac{1}{W} \left[ \delta \left( \frac{y_3' - W}{W} \right) - \delta \left( \frac{y_3'}{W} \right) \right] G_{22}(y_2, y_3) dy_2 dy_3 \\ &\quad + (\lambda \epsilon_{kk}^i + 2\mu \epsilon_{33}^i) \iint_{-\infty}^{\infty} \Pi \left( \frac{y_2'}{T} \right) \frac{1}{W} \left[ \delta \left( \frac{y_3' - W}{W} \right) - \delta \left( \frac{y_3'}{W} \right) \right] G_{32}(y_2, y_3) dy_2 dy_3 \\ &\quad \left. + 2\mu \epsilon_{23}^i \iint_{-\infty}^{\infty} \frac{1}{T} \left[ \delta \left( \frac{y_2'}{T} - \frac{1}{2} \right) - \delta \left( \frac{y_2'}{T} + \frac{1}{2} \right) \right] S \left( \frac{y_3'}{W} \right) G_{32}(y_2, y_3) dy_2 dy_3 \right\} \\ + \cos \phi &\left\{ (\lambda \epsilon_{kk}^i + 2\mu \epsilon_{22}^i) \iint_{-\infty}^{\infty} \Pi \left( \frac{y_2'}{T} \right) \frac{1}{W} \left[ \delta \left( \frac{y_3' - W}{W} \right) - \delta \left( \frac{y_3'}{W} \right) \right] G_{22}(y_2, y_3) dy_2 dy_3 \right. \\ &\quad - 2\mu \epsilon_{23}^i \iint_{-\infty}^{\infty} \frac{1}{T} \left[ \delta \left( \frac{y_2'}{T} - \frac{1}{2} \right) - \delta \left( \frac{y_2'}{T} + \frac{1}{2} \right) \right] S \left( \frac{y_3'}{W} \right) G_{22}(y_2, y_3) dy_2 dy_3 \\ &\quad - (\lambda \epsilon_{kk}^i + 2\mu \epsilon_{33}^i) \iint_{-\infty}^{\infty} \frac{1}{T} \left[ \delta \left( \frac{y_2'}{T} - \frac{1}{2} \right) - \delta \left( \frac{y_2'}{T} + \frac{1}{2} \right) \right] S \left( \frac{y_3'}{W} \right) G_{32}(y_2, y_3) dy_2 dy_3 \\ &\quad \left. + 2\mu \epsilon_{23}^i \iint_{-\infty}^{\infty} \Pi \left( \frac{y_2'}{T} \right) \frac{1}{W} \left[ \delta \left( \frac{y_3' - W}{W} \right) - \delta \left( \frac{y_3'}{W} \right) \right] G_{32}(y_2, y_3) dy_2 dy_3 \right\}. \end{aligned} \quad (50)$$

To simplify the problem, we now change the variables of integration from  $dx_2 dx_3$  to  $dx_2' dx_3'$ . So we write

$$\begin{aligned} u_2 = \sin \phi &\left\{ (\lambda \epsilon_{kk}^i + 2\mu \epsilon_{22}^i) \iint_{-\infty}^{\infty} \frac{1}{T} \left[ \delta \left( \frac{y_2'}{T} - \frac{1}{2} \right) - \delta \left( \frac{y_2'}{T} + \frac{1}{2} \right) \right] S \left( \frac{y_3'}{W} \right) G_{22}(y_2, y_3) dy_2' dy_3' \right. \\ &\quad + 2\mu \epsilon_{23}^i \iint_{-\infty}^{\infty} \Pi \left( \frac{y_2'}{T} \right) \frac{1}{W} \left[ \delta \left( \frac{y_3' - W}{W} \right) - \delta \left( \frac{y_3'}{W} \right) \right] G_{22}(y_2, y_3) dy_2' dy_3' \\ &\quad + (\lambda \epsilon_{kk}^i + 2\mu \epsilon_{33}^i) \iint_{-\infty}^{\infty} \Pi \left( \frac{y_2'}{T} \right) \frac{1}{W} \left[ \delta \left( \frac{y_3' - W}{W} \right) - \delta \left( \frac{y_3'}{W} \right) \right] G_{32}(y_2, y_3) dy_2' dy_3' \\ &\quad \left. + 2\mu \epsilon_{23}^i \iint_{-\infty}^{\infty} \frac{1}{T} \left[ \delta \left( \frac{y_2'}{T} - \frac{1}{2} \right) - \delta \left( \frac{y_2'}{T} + \frac{1}{2} \right) \right] S \left( \frac{y_3'}{W} \right) G_{32}(y_2, y_3) dy_2' dy_3' \right\} \\ + \cos \phi &\left\{ (\lambda \epsilon_{kk}^i + 2\mu \epsilon_{22}^i) \iint_{-\infty}^{\infty} \Pi \left( \frac{y_2'}{T} \right) \frac{1}{W} \left[ \delta \left( \frac{y_3' - W}{W} \right) - \delta \left( \frac{y_3'}{W} \right) \right] G_{22}(y_2, y_3) dy_2' dy_3' \right. \\ &\quad - 2\mu \epsilon_{23}^i \iint_{-\infty}^{\infty} \frac{1}{T} \left[ \delta \left( \frac{y_2'}{T} - \frac{1}{2} \right) - \delta \left( \frac{y_2'}{T} + \frac{1}{2} \right) \right] S \left( \frac{y_3'}{W} \right) G_{22}(y_2, y_3) dy_2' dy_3' \\ &\quad - (\lambda \epsilon_{kk}^i + 2\mu \epsilon_{33}^i) \iint_{-\infty}^{\infty} \frac{1}{T} \left[ \delta \left( \frac{y_2'}{T} - \frac{1}{2} \right) - \delta \left( \frac{y_2'}{T} + \frac{1}{2} \right) \right] S \left( \frac{y_3'}{W} \right) G_{32}(y_2, y_3) dy_2' dy_3' \\ &\quad \left. + 2\mu \epsilon_{23}^i \iint_{-\infty}^{\infty} \Pi \left( \frac{y_2'}{T} \right) \frac{1}{W} \left[ \delta \left( \frac{y_3' - W}{W} \right) - \delta \left( \frac{y_3'}{W} \right) \right] G_{32}(y_2, y_3) dy_2' dy_3' \right\}, \end{aligned} \quad (51)$$

in which the expression  $G_{ij}(y_2, y_3)$  is short for  $G_{ij}[y_2(y'_2, y'_3), y_3(y'_2, y'_3)]$ . We simplify the bounds of integration again:

$$\begin{aligned}
 u_2 = & \sin \phi \left\{ (\lambda e_{kk}^i + 2\mu e_{22}^i) \int_0^W G_{22}[y_2(T/2, y'_3), y_3(T/2, y'_3)] - G_{22}[y_2(-T/2, y'_3), y_3(-T/2, y'_3)] dy'_3 \right. \\
 & + 2\mu e_{23}^i \int_{-T/2}^{T/2} G_{22}[y_2(y'_2, W), y_3(y'_2, W)] - G_{22}[y_2(y'_2, 0), y_3(y'_2, 0)] dy'_2 \\
 & + (\lambda e_{kk}^i + 2\mu e_{33}^i) \int_{-T/2}^{T/2} G_{32}[y_2(y'_2, W), y_3(y'_2, W)] - G_{32}[x_2(y'_2, 0), x_3(y'_2, 0)] dy'_2 \\
 & \left. + 2\mu e_{23}^i \int_0^W G_{32}[y_2(T/2, y'_3), y_3(T/2, y'_3)] - G_{32}[y_2(-T/2, y'_3), y_3(-T/2, y'_3)] dy'_3 \right\} \\
 + & \cos \phi \left\{ (\lambda e_{kk}^i + 2\mu e_{22}^i) \int_{-T/2}^{T/2} G_{22}[y_2(y'_2, W), y_3(y'_2, W)] - G_{22}[y_2(y'_2, 0), y_3(y'_2, 0)] dy'_2 \right. \\
 & - 2\mu e_{23}^i \int_0^W G_{22}[y_2(T/2, y'_3), y_3(T/2, y'_3)] - G_{22}[y_2(-T/2, y'_3), y_3(-T/2, y'_3)] dy'_3 \\
 & - (\lambda e_{kk}^i + 2\mu e_{33}^i) \int_0^W G_{32}[y_2(T/2, y'_3), y_3(T/2, y'_3)] - G_{32}[y_2(-T/2, y'_3), y_3(-T/2, y'_3)] dy'_3 \\
 & \left. + 2\mu e_{23}^i \int_{-T/2}^{T/2} G_{32}[y_2(y'_2, W), y_3(y'_2, W)] - G_{32}[y_2(y'_2, 0), y_3(y'_2, 0)] dy'_2 \right\}. \tag{52}
 \end{aligned}$$

The solution for  $u_3$  can be obtained using the proper Green's functions. To be complete, we write

$$\begin{aligned}
 u_3 = & \sin \phi \left\{ (\lambda e_{kk}^i + 2\mu e_{22}^i) \int_0^W G_{23}[y_2(T/2, y'_3), y_3(T/2, y'_3)] - G_{23}[y_2(-T/2, y'_3), y_3(-T/2, y'_3)] dy'_3 \right. \\
 & + 2\mu e_{23}^i \int_{-T/2}^{T/2} G_{23}[y_2(y'_2, W), y_3(y'_2, W)] - G_{23}[y_2(y'_2, 0), y_3(y'_2, 0)] dy'_2 \\
 & + (\lambda e_{kk}^i + 2\mu e_{33}^i) \int_{-T/2}^{T/2} G_{33}[y_2(y'_2, W), y_3(y'_2, W)] - G_{33}[x_2(y'_2, 0), x_3(y'_2, 0)] dy'_2 \\
 & \left. + 2\mu e_{23}^i \int_0^W G_{33}[y_2(T/2, y'_3), y_3(T/2, y'_3)] - G_{33}[y_2(-T/2, y'_3), y_3(-T/2, y'_3)] dy'_3 \right\} \\
 + & \cos \phi \left\{ (\lambda e_{kk}^i + 2\mu e_{22}^i) \int_{-T/2}^{T/2} G_{23}[y_2(y'_2, W), y_3(y'_2, W)] - G_{23}[y_2(y'_2, 0), y_3(y'_2, 0)] dy'_2 \right. \\
 & - 2\mu e_{23}^i \int_0^W G_{23}[y_2(T/2, y'_3), y_3(T/2, y'_3)] - G_{23}[y_2(-T/2, y'_3), y_3(-T/2, y'_3)] dy'_3 \\
 & - (\lambda e_{kk}^i + 2\mu e_{33}^i) \int_0^W G_{33}[y_2(T/2, y'_3), y_3(T/2, y'_3)] - G_{33}[y_2(-T/2, y'_3), y_3(-T/2, y'_3)] dy'_3 \\
 & \left. + 2\mu e_{23}^i \int_{-T/2}^{T/2} G_{33}[y_2(y'_2, W), y_3(y'_2, W)] - G_{33}[y_2(y'_2, 0), y_3(y'_2, 0)] dy'_2 \right\}. \tag{53}
 \end{aligned}$$

We then obtain the displacement field in closed form with

$$\begin{aligned}
 u_2 = & \frac{1}{8\pi\mu(1-\nu)} \left[ \sin \phi \left\{ (\lambda e_{kk}^i + 2\mu e_{22}^i) I_{223}' + 2\mu e_{23}^i (I_{222}' + I_{323}') + (\lambda e_{kk}^i + 2\mu e_{33}^i) I_{322}' \right\} \right. \\
 & \left. + \cos \phi \left\{ (\lambda e_{kk}^i + 2\mu e_{22}^i) I_{222}' + 2\mu e_{23}^i (I_{322}' - I_{223}') - (\lambda e_{kk}^i + 2\mu e_{33}^i) I_{323}' \right\} \right] \\
 u_3 = & \frac{1}{8\pi\mu(1-\nu)} \left[ \sin \phi \left\{ (\lambda e_{kk}^i + 2\mu e_{22}^i) I_{233}' + 2\mu e_{23}^i (I_{232}' + I_{333}') + (\lambda e_{kk}^i + 2\mu e_{33}^i) I_{332}' \right\} \right. \\
 & \left. + \cos \phi \left\{ (\lambda e_{kk}^i + 2\mu e_{22}^i) I_{232}' + 2\mu e_{23}^i (I_{332}' - I_{233}') - (\lambda e_{kk}^i + 2\mu e_{33}^i) I_{333}' \right\} \right], \tag{54}
 \end{aligned}$$

in which we have defined the integrals

$$\begin{aligned}
I_{223'} &= 8\pi\mu(1-\nu) \int_0^W G_{22}[y_2(T/2, y_3'), y_3(T/2, y_3')] - G_{22}[y_2(-T/2, y_3'), y_3(-T/2, y_3')] dy_3' \\
I_{222'} &= 8\pi\mu(1-\nu) \int_{-T/2}^{T/2} G_{22}[y_2(y_2', W), y_3(y_2', W)] - G_{22}[y_2(y_2', 0), y_3(y_2', 0)] dy_2' \\
I_{322'} &= 8\pi\mu(1-\nu) \int_{-T/2}^{T/2} G_{32}[y_2(y_2', W), y_3(y_2', W)] - G_{32}[x_2(y_2', 0), x_3(y_2', 0)] dy_2' \\
I_{323'} &= 8\pi\mu(1-\nu) \int_0^W G_{32}[y_2(T/2, y_3'), y_3(T/2, y_3')] - G_{32}[y_2(-T/2, y_3'), y_3(-T/2, y_3')] dy_3' \\
I_{233'} &= 8\pi\mu(1-\nu) \int_0^W G_{23}[y_2(T/2, y_3'), y_3(T/2, y_3')] - G_{23}[y_2(-T/2, y_3'), y_3(-T/2, y_3')] dy_3' \\
I_{232'} &= 8\pi\mu(1-\nu) \int_{-T/2}^{T/2} G_{23}[y_2(y_2', W), y_3(y_2', W)] - G_{23}[y_2(y_2', 0), y_3(y_2', 0)] dy_2' \\
I_{332'} &= 8\pi\mu(1-\nu) \int_{-T/2}^{T/2} G_{33}[y_2(y_2', W), y_3(y_2', W)] - G_{33}[y_2(y_2', 0), y_3(y_2', 0)] dy_2' \\
I_{333'} &= 8\pi\mu(1-\nu) \int_0^W G_{33}[y_2(T/2, y_3'), y_3(T/2, y_3')] - G_{33}[y_2(-T/2, y_3'), y_3(-T/2, y_3')] dy_3', \tag{55}
\end{aligned}$$

and where in this case Chinnery's notation  $||$  refers to

$$f(y_2', y_3') || = f\left(\frac{T}{2}, W\right) - f\left(-\frac{T}{2}, W\right) + f\left(-\frac{T}{2}, 0\right) - f\left(\frac{T}{2}, 0\right). \tag{56}$$

Using the following substitutions

$$\begin{aligned}
y_2 &= +y_2' \sin \phi + y_3' \cos \phi \\
y_3 &= -y_2' \cos \phi + y_3' \sin \phi + D \\
r_1'^2 &= (x_3 - y_3)^2 + (x_2 - y_2)^2 \\
r_2'^2 &= (x_3 + y_3)^2 + (x_2 - y_2)^2 \\
p_2 &= +(x_3 - D) \cos \phi - x_2 \sin \phi + y_2' \\
p_3 &= -(x_3 - D) \sin \phi - x_2 \cos \phi + y_3' \\
p_2' &= -(x_3 + D) \cos \phi - x_2 \sin \phi + y_2' \\
p_3' &= +(x_3 + D) \sin \phi - x_2 \cos \phi + y_3', \tag{57}
\end{aligned}$$

we write the integrals in closed form as

$$\begin{aligned}
I_{223'} &= \frac{x_3}{r_2'^2} \left[ (x_2^2 + x_3^2 - D^2) \sin \phi + \sin(2\phi)(3Dy_2' + x_3y_2' - x_2y_3') \right. \\
&\quad - \sin(3\phi)((D + x_3)^2 + x_2^2 + 2(y_2')^2) + \sin(4\phi)((D + x_3)y_2' + x_2y_3') \\
&\quad - 2Dx_2 \cos \phi + \cos(2\phi)(Dy_3' + 3x_2y_2' - x_3y_3') \\
&\quad \left. - 2y_2'y_3' \cos(3\phi) + \cos(4\phi)((D + x_3)y_3' - x_2y_2') \right] \\
&\quad + \frac{1}{2} \arctan\left(\frac{p_3'}{p_2'}\right) \left[ \cos(\phi)(16\nu^2(D + x_3) - 28\nu(D + x_3) + 13D + 11x_3) \right. \\
&\quad \quad + \cos(3\phi)(-4\nu(D + x_3) + 3D + 5x_3) + (4\nu(4\nu - 5) + 7)x_2 \sin(\phi) \\
&\quad \quad \left. + (3 - 4\nu)x_2 \sin(3\phi) + 2(4\nu - 3)y_2' \cos(2\phi) - 2(4\nu(2\nu - 3) + 5)y_2' \right] \\
&\quad - p_2 \arctan\left(\frac{p_3}{p_2}\right) [3 - 4\nu + \cos(2\phi)] \\
&\quad + \frac{1}{4} \log(r_2'^2) \left[ \sin(3\phi)(4\nu(D + x_3) - 3D - 5x_3) \right. \\
&\quad \quad \left. - \sin(\phi)(16\nu^2(D + x_3) - 28\nu(D + x_3) + 13D + 11x_3) \right]
\end{aligned}$$

$$\begin{aligned}
 & + (4\nu(4\nu - 5) + 7)x_2 \cos \phi + (3 - 4\nu)x_2 \cos(3\phi) \\
 & + 2(3 - 4\nu)y'_2 \sin(2\phi) - 2(4\nu(2\nu - 3) + 5)y'_3 \Big] \\
 & + \frac{1}{4} \log(r_1'^2) \Big[ (5 - 8\nu)x_2 \cos \phi + x_2 \cos(3\phi) - 2(D - x_3)(4 - 4\nu + \cos(2\phi)) \sin \phi \\
 & + 8\nu y'_3 + 2y'_2 \sin(2\phi) - 6y'_3 \Big], \tag{58}
 \end{aligned}$$

$$\begin{aligned}
 I_{222'} = & \frac{x_3}{r_2'^2} \Big[ -\cos \phi(x_2^2 + x_3^2 - D^2) + \sin(4\phi)(x_2 y'_2 - (D + x_3)y'_3) + \sin(2\phi)((3D + x_3)y'_3 + x_2 y'_2) \\
 & + \cos(4\phi)((D + x_3)y'_2 + x_2 y'_3) + \cos(2\phi)(-Dy'_2 + x_3 y'_2 + 3x_2 y'_3) \\
 & - \cos(3\phi)((D + x_3)^2 + x_2^2 + 2(y'_3)^2) - 2Dx_2 \sin \phi - 2y'_2 y'_3 \sin(3\phi) \Big] \\
 & + \frac{1}{2} \arctan\left(\frac{p_2'}{p_3}\right) \Big[ -4\nu(4\nu - 7)(D + x_3) \sin \phi - \sin(3\phi)(4\nu(D + x_3) - 3D - 5x_3) \\
 & - (13D + 11x_3) \sin \phi - (4(5 - 4\nu)\nu - 7)x_2 \cos \phi - (3 - 4\nu)x_2 \cos(3\phi) \\
 & - 2(4\nu - 3)y'_3 \cos(2\phi) - 2(4\nu(2\nu - 3) + 5)y'_3 \Big] \\
 & + p_3 \arctan\left(\frac{p_2}{p_3}\right) \Big[ 4\nu + \cos(2\phi) - 3 \Big] \\
 & + \frac{1}{4} \log(r_2'^2) \Big[ \cos \phi(16\nu^2(D + x_3) - 28\nu(D + x_3) + 13D + 11x_3) \\
 & + \cos(3\phi)(4\nu(D + x_3) - 3D - 5x_3) + (4\nu(4\nu - 5) + 7)x_2 \sin \phi \\
 & + (4\nu - 3)x_2 \sin(3\phi) + 2(3 - 4\nu)y'_3 \sin(2\phi) - 2(4\nu(2\nu - 3) + 5)y'_2 \Big] \\
 & + \frac{1}{4} \log(r_1'^2) \Big[ -2(D - x_3) \cos(\phi)(4\nu + \cos(2\phi) - 4) \\
 & - 2x_2 \sin(\phi)(4\nu + \cos(2\phi) - 2) + 8\nu y'_2 + 2y'_3 \sin(2\phi) - 6y'_2 \Big] \tag{59}
 \end{aligned}$$

and

$$\begin{aligned}
 I_{233'} = & \frac{x_3}{r_2'^2} \Big[ (-D^2 + x_2^2 + x_3^2) \cos(\phi) + \sin(2\phi)(-Dy'_3 - 3x_2 y'_2 + x_3 y'_3) \\
 & + \sin(4\phi)(x_2 y'_2 - (D + x_3)y'_3) - \cos(3\phi)((D + x_3)^2 + x_2^2 + 2(y'_2)^2) \\
 & + \cos(2\phi)(3Dy'_2 + x_3 y'_2 - x_2 y'_3) + \cos(4\phi)((D + x_3)y'_2 + x_2 y'_3) \\
 & + 2Dx_2 \sin(\phi) + 2y'_2 y'_3 \sin(3\phi) \Big] \\
 & + 4(\nu - 1)(2\nu - 1) \arctan\left(\frac{p_2'}{p_3}\right) [x_2 \cos(\phi) - (D + x_3) \sin(\phi)] \\
 & - \sin(\phi) \arctan\left(\frac{p_3'}{p_2}\right) \Big[ (4\nu - 3)(D + x_2 \sin(2\phi) - x_3) \\
 & + \cos(2\phi)(4\nu(D + x_3) - 3D - x_3) + 2(3 - 4\nu)y'_2 \cos(\phi) \Big] \\
 & + 4(\nu - 1)(2\nu - 1)y'_3 \arctan\left(\frac{x_2 - y_2}{x_3 + y_3}\right) \\
 & - \frac{1}{2} p_2 \log(r_1'^2) \cos(2\phi) \\
 & - p_2 \arctan\left(\frac{p_3}{p_2}\right) \sin(2\phi) \\
 & + \frac{1}{4} \log(r_2'^2) \Big[ \cos \phi(16\nu^2(D + x_3) - 4\nu(7D + 3x_3) + 11D + x_3)
 \end{aligned}$$

$$\begin{aligned}
& + \cos(3\phi)(-4\nu(D + x_3) + 3D + x_3) + (4\nu(4\nu - 5) + 5)x_2 \sin(\phi) \\
& + (3 - 4\nu)x_2 \sin(3\phi) + 2(4\nu - 3)y_2' \cos(2\phi) - 8(\nu - 1)(2\nu - 1)y_2', \tag{60}
\end{aligned}$$

$$\begin{aligned}
I_{232'} &= \frac{x_3}{r_2^2} \left[ (x_2^2 + x_3^2 - D^2) \sin(\phi) + \sin(2\phi)(Dy_2' - x_3y_2' - 3x_2y_3') \right. \\
&\quad - \sin(4\phi)((D + x_3)y_2' + x_2y_3') + \sin(3\phi)((D + x_3)^2 + x_2^2 + 2(y_3')^2) \\
&\quad + \cos(2\phi)(3Dy_3' + x_2y_2' + x_3y_3') + \cos(4\phi)(x_2y_2' - (D + x_3)y_3') \\
&\quad \left. - 2Dx_2 \cos(\phi) - 2y_2'y_3' \cos(3\phi) \right] \\
&\quad - 4(\nu - 1)(2\nu - 1) \arctan\left(\frac{p_3'}{p_2}\right) \left[ (D + x_3) \cos(\phi) + x_2 \sin(\phi) \right] \\
&\quad - \cos(\phi) \arctan\left(\frac{p_2'}{p_3}\right) \left[ \cos(2\phi) \times (3D + x_3 - 4\nu(D + x_3)) \right. \\
&\quad \quad \left. + (4\nu - 3)(D - x_2 \sin(2\phi) - x_3 + 2y_3' \sin(\phi)) \right] \\
&\quad + 4(\nu - 1)(2\nu - 1)y_2' \arctan\left(\frac{x_2 - y_2}{x_3 + y_3}\right) \\
&\quad + p_3 \arctan\left(\frac{p_2}{p_3}\right) \sin(2\phi) \\
&\quad + \frac{1}{4} \log(r_2'^2) \left[ \sin(\phi)(16\nu^2(D + x_3) - 4\nu(7D + 3x_3) + 11D + x_3) \right. \\
&\quad \quad + \sin(3\phi)(4\nu(D + x_3) - 3D - x_3) + (4(5 - 4\nu)\nu - 5)x_2 \cos(\phi) + (3 - 4\nu)x_2 \cos(3\phi) \\
&\quad \quad \left. + 2(4\nu - 3)y_3' \cos(2\phi) + 8(\nu - 1)(2\nu - 1)y_3' \right] \\
&\quad - \frac{1}{2} p_3 \cos(2\phi) \log(r_1'^2), \tag{61}
\end{aligned}$$

$$\begin{aligned}
I_{323'} &= \frac{x_3}{r_2^2} \left[ (D^2 - x_2^2 - x_3^2) \cos(\phi) + \sin(2\phi)(Dy_3' + 3x_2y_2' - x_3y_3') + \sin(4\phi)((D + x_3)y_3' - x_2y_2') \right. \\
&\quad + \cos(3\phi)((D + x_3)^2 + x_2^2 + 2(y_2')^2) - \cos(4\phi)((D + x_3)y_2' + x_2y_3') \\
&\quad \left. + \cos(2\phi)(x_2y_3' - (3D + x_3)y_2') - 2Dx_2 \sin(\phi) - 2y_2'y_3' \sin(3\phi) \right] \\
&\quad - 4(\nu - 1)(2\nu - 1) \arctan\left(\frac{p_2'}{p_3}\right) \left[ x_2 \cos(\phi) \times -(D + x_3) \sin(\phi) \right] \\
&\quad - p_2 \arctan\left(\frac{p_3}{p_2}\right) \sin(2\phi) \\
&\quad - \sin(\phi) \arctan\left(\frac{p_3'}{p_2}\right) \left[ (4\nu - 3)(D + x_2 \sin(2\phi) - x_3) \right. \\
&\quad \quad \left. + \cos(2\phi)(4\nu(D + x_3) - 3D - 5x_3) + 2(3 - 4\nu)y_2' \cos(\phi) \right] \\
&\quad - 4(\nu - 1)(2\nu - 1)y_3' \arctan\left(\frac{x_2 - y_2}{x_3 + y_3}\right) \\
&\quad + \frac{1}{4} \log(r_2'^2) \left[ -\cos(\phi)(D(4\nu(4\nu - 5) + 5) + (4\nu(4\nu - 9) + 19)x_3) \right. \\
&\quad \quad + \cos(3\phi)(-4\nu(D + x_3) + 3D + 5x_3) + (4(7 - 4\nu)\nu - 11)x_2 \sin(\phi) + (3 - 4\nu)x_2 \sin(3\phi) \\
&\quad \quad \left. + 2(4\nu - 3)y_2' \cos(2\phi) + 8(\nu - 1)(2\nu - 1)y_2' \right] \\
&\quad - \frac{1}{2} p_2 \cos(2\phi) \log(r_1'^2), \tag{62}
\end{aligned}$$

$$\begin{aligned}
 I_{322'} = & \frac{x_3}{r_2^2} \left[ \sin(4\phi)((D+x_3)y_2' + x_2y_3') - (-D^2 + x_2^2 + x_3^2) \sin(\phi) + \sin(2\phi)(-Dy_2' + x_3y_2' + 3x_2y_3') \right. \\
 & - \sin(3\phi)((D+x_3)^2 + x_2^2 + 2(y_3')^2) - \cos(2\phi)(3Dy_3' + x_2y_2' + x_3y_3') \\
 & \left. + \cos(4\phi)((D+x_3)y_3' - x_2y_2') + 2Dx_2 \cos(\phi) + 2y_2'y_3' \cos(3\phi) \right] \\
 & + 4(\nu-1)(2\nu-1) \arctan\left(\frac{p_3'}{p_2}\right) \left[ (D+x_3) \cos(\phi) + x_2 \sin(\phi) \right] \\
 & + p_3 \arctan\left(\frac{p_2}{p_3}\right) \sin(2\phi) \\
 & + \cos(\phi) \arctan\left(\frac{p_2'}{p_3}\right) \left[ \cos(2\phi)(4\nu(D+x_3) - 3D - 5x_3) \right. \\
 & \quad \left. - (4\nu-3)(D + 2 \sin(\phi)(y_3' - x_2 \cos(\phi)) - x_3) \right] \\
 & - 4(\nu-1)(2\nu-1)y_2' \arctan\left(\frac{x_2 - y_2}{x_3 + y_3}\right) \\
 & + \frac{1}{4} \log(r_2'^2) \left[ -\sin(\phi)(16\nu^2(D+x_3) - 4\nu(5D+9x_3) + 5D + 19x_3) \right. \\
 & \quad + \sin(3\phi)(4\nu(D+x_3) - 3D - 5x_3) + (4\nu(4\nu-7) + 11)x_2 \cos(\phi) \\
 & \quad \left. + (3-4\nu)x_2 \cos(3\phi) + 2(4\nu-3)y_3' \cos(2\phi) - 8(\nu-1)(2\nu-1)y_3' \right] \\
 & - \frac{1}{2} p_3 \cos(2\phi) \log(r_1'^2), \tag{63}
 \end{aligned}$$

$$\begin{aligned}
 I_{333'} = & \frac{x_3}{r_2^2} \left[ (x_2^2 + x_3^2 - D^2) \sin \phi - \sin(3\phi)((D+x_3)^2 + x_2^2 + 2(y_2')^2) \right. \\
 & + \sin(2\phi)(3Dy_2' + x_3y_2' - x_2y_3') + \sin(4\phi)((D+x_3)y_2' + x_2y_3') \\
 & + \cos(2\phi)(Dy_3' + 3x_2y_2' - x_3y_3') + \cos(4\phi)((D+x_3)y_3' - x_2y_2') \\
 & \left. - 2Dx_2 \cos(\phi) - 2y_2'y_3' \cos(3\phi) \right] \\
 & - \frac{1}{2} \arctan\left(\frac{p_3'}{p_2}\right) \left[ \cos(3\phi)(-4\nu(D+x_3) + 3D + x_3) + (4(7-4\nu)\nu - 13)x_2 \sin \phi \right. \\
 & \quad - \cos(\phi)(16\nu^2(D+x_3) - 20\nu(D+x_3) + 7D + 5x_3) \\
 & \quad \left. + (3-4\nu)x_2 \sin(3\phi) + 2(4\nu-3)y_2' \cos(2\phi) + 2(4\nu(2\nu-3) + 5)y_2' \right] \\
 & + p_2 \arctan\left(\frac{p_3}{p_2}\right) \left[ 4\nu + \cos(2\phi) - 3 \right] \\
 & + \frac{1}{4} \log(r_2'^2) \left[ \sin(3\phi)(-4\nu(D+x_3) + 3D + x_3) \right. \\
 & \quad - \sin(\phi)(16\nu^2(D+x_3) - 20\nu(D+x_3) + 7D + 5x_3) \\
 & \quad + (4\nu(4\nu-7) + 13)x_2 \cos(\phi) + (4\nu-3)x_2 \cos(3\phi) \\
 & \quad \left. + 2(4\nu-3)y_2' \sin(2\phi) - 2(4\nu(2\nu-3) + 5)y_3' \right] \\
 & + \frac{1}{4} \log(r_1'^2) \left[ 2(D-x_3) \sin(\phi)(4\nu + \cos(2\phi) - 2) \right. \\
 & \quad \left. + (7-8\nu)x_2 \cos(\phi) - x_2 \cos(3\phi) + 8\nu y_3' - 2y_2' \sin(2\phi) - 6y_3' \right], \tag{64}
 \end{aligned}$$

and finally,

$$\begin{aligned}
I_{332}' = & \frac{x_3}{r_2'^2} \left[ \sin(4\phi)(x_2 y_2' - (D + x_3) y_3') + \sin(2\phi)((3D + x_3) y_3' + x_2 y_2') - (x_2^2 + x_3^2 - D^2) \cos\phi \right. \\
& + \cos(4\phi)((D + x_3) y_2' + x_2 y_3') + \cos(2\phi)(x_3 y_2' + 3x_2 y_3' - D y_2') \\
& \left. - \cos(3\phi)((D + x_3)^2 + x_2^2 + 2(y_3')^2) - 2D x_2 \sin(\phi) - 2y_2' y_3' \sin(3\phi) \right] \\
& + \frac{1}{2} \arctan\left(\frac{p_2'}{p_3'}\right) \left[ -4\nu(4\nu - 5)(D + x_3) \sin(\phi) - \sin(3\phi)(-4\nu(D + x_3) + 3D + x_3) \right. \\
& - (7D + 5x_3) \sin(\phi) - (4(7 - 4\nu)\nu - 13)x_2 \cos(\phi) - (4\nu - 3)x_2 \cos(3\phi) \\
& \left. - 2(3 - 4\nu)y_3' \cos(2\phi) - 2(4\nu(2\nu - 3) + 5)y_3' \right] \\
& - p_3 \arctan\left(\frac{p_2'}{p_3'}\right) [3 - 4\nu + \cos(2\phi)] \\
& + \frac{1}{4} \log(r_2'^2) \left[ \cos(\phi)(16\nu^2(D + x_3) - 20\nu(D + x_3) + 7D + 5x_3) \right. \\
& + \cos(3\phi)(-4\nu(D + x_3) + 3D + x_3) + (4\nu(4\nu - 7) + 13)x_2 \sin\phi \\
& \left. + (3 - 4\nu)x_2 \sin(3\phi) + 2(4\nu - 3)y_3' \sin(2\phi) - 2(4\nu(2\nu - 3) + 5)y_2' \right] \\
& + \frac{1}{4} \log(r_1'^2) \left[ 2x_2(-4\nu + \cos(2\phi) + 4) \sin\phi \right. \\
& \left. + 2(D - x_3) \cos(\phi)(-4\nu + \cos(2\phi) + 2) + 8\nu y_2' - 2y_3' \sin(2\phi) - 6y_2' \right]. \tag{65}
\end{aligned}$$

Examples of displacement fields occasioned by distributed anelastic strain are given in Figure 4. There are two important end members, one for shear sources and the other for isotropic sources.

#### Numerical Solution with the tanh Quadrature

We use the tanh quadrature to convolve the Green's functions with the equivalent body forces. To do so, we write the integral in canonical form using the change of variable  $y_2' = u'T/2$  and  $y_3' = (1 + v')W/2$ :

$$\begin{aligned}
u_2 = & \sin\phi \left\{ (\lambda\epsilon_{kk}^i + 2\mu\epsilon_{22}^i) \frac{W}{2} \int_{-1}^1 G_{22}[y_2(T/2, (1 + v')W/2), y_3(T/2, (1 + v')W/2)] \right. \\
& - G_{22}[y_2(-T/2, (1 + v')W/2), y_3(-T/2, (1 + v')W/2)] dv' \\
& + 2\mu\epsilon_{23}^i \frac{T}{2} \int_{-1}^1 G_{22}[y_2(u'T/2, W), y_3(u'T/2, W)] - G_{22}[y_2(u'T/2, 0), y_3(u'T/2, 0)] du' \\
& + (\lambda\epsilon_{kk}^i + 2\mu\epsilon_{33}^i) \frac{T}{2} \int_{-1}^1 G_{32}[y_2(u'T/2, W), y_3(u'T/2, W)] - G_{32}[x_2(u'T/2, 0), x_3(u'T/2, 0)] du' \\
& + 2\mu\epsilon_{23}^i \frac{W}{2} \int_{-1}^1 G_{32}[y_2(T/2, (1 + v')W/2), y_3(T/2, (1 + v')W/2)] \\
& \left. - G_{32}[y_2(-T/2, (1 + v')W/2), y_3(-T/2, (1 + v')W/2)] dy_3' \right\} \\
& + \cos\phi \left\{ (\lambda\epsilon_{kk}^i + 2\mu\epsilon_{22}^i) \frac{T}{2} \int_{-1}^1 G_{22}[y_2(u'T/2, W), y_3(u'T/2, W)] - G_{22}[y_2(u'T/2, 0), y_3(u'T/2, 0)] du' \right. \\
& - 2\mu\epsilon_{23}^i \frac{W}{2} \int_{-1}^1 G_{22}[y_2(T/2, (1 + v')W/2), y_3(T/2, (1 + v')W/2)] \\
& - G_{22}[y_2(-T/2, (1 + v')W/2), y_3(-T/2, (1 + v')W/2)] dv' \\
& - (\lambda\epsilon_{kk}^i + 2\mu\epsilon_{33}^i) \frac{W}{2} \int_{-1}^1 G_{32}[y_2(T/2, (1 + v')W/2), y_3(T/2, (1 + v')W/2)] \\
& - G_{32}[y_2(-T/2, (1 + v')W/2), y_3(-T/2, (1 + v')W/2)] dv' \\
& \left. + 2\mu\epsilon_{23}^i \frac{T}{2} \int_{-1}^1 G_{32}[y_2(u'T/2, W), y_3(u'T/2, W)] - G_{32}[y_2(u'T/2, 0), y_3(u'T/2, 0)] du' \right\}. \tag{66}
\end{aligned}$$



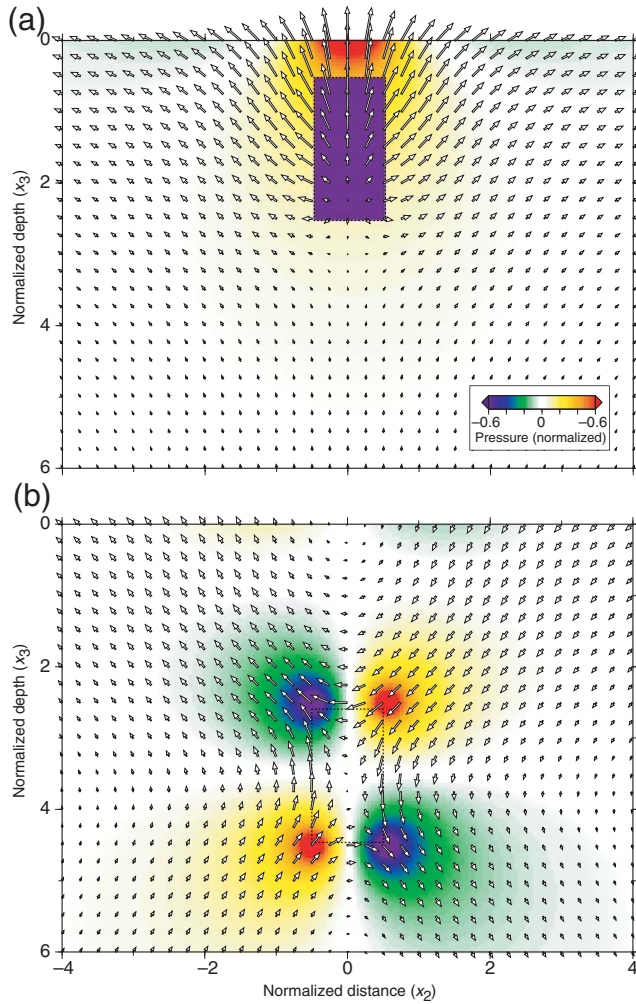


**Figure 4.** Displacements (arrows) and pressure (background color) in plane strain due to distributed anelastic strain in a rectangular strain region (black dashed box). (a) Case of isotropic anelastic strain in a shallow strain region highlighting the amplification effect of the free surface. (b) Cause of anelastic shear strain  $e_{23}^i$  in a finite strain region.

The solution for  $u_3$  can be obtained using the proper Green's functions, by substituting  $G_{22}$  for  $G_{23}$  and  $G_{32}$  to  $G_{33}$ . The analytic solution and the numerical solution with the tanh quadrature converge with increasing integration points, down to double-precision floating-point accuracy. As expected, the analytic solution can be evaluated several orders of magnitude faster.

### Stress and Strains

Given the displacement field, the stress and strain can be obtained analytically, or by finite difference, following equation (9). We generate the solutions for the displacement gradient by taking the derivatives of displacement analytically in Mathematica. We then export these expressions in forms that can be evaluated in computer programs. We validate this procedure by comparing the analytic solutions to results obtained by finite difference of the displacement field. Examples of

stress components for a deformation in plane strain are shown in Figures 5 and 6. A wide range of anelastic strain orientations and distributions are shown in  $\text{\textcircled{E}}$  Movie S2.

### Distributed Deformation of Finite Strain Volumes in 3D

The Earth's deformation occurs at all scales, from the most localized, around faults, to the most distributed, in the mantle. Understanding the effect of distributed strain on deformation and stress in the Earth's interior allows us to describe many important processes that are activated by volcanic unrest or throughout the earthquake cycle, including viscoelastic, poroelastic, and thermoelastic effects. Describing these effects in 3D is key to more realistic models of deformation data.

#### Problem Definition for Vertical Strain Volumes

We now consider deformation in a 3D half-space. We consider a cuboid volume of length  $L$ , width  $W$ , and thickness  $T$ , buried at depth  $D$ , and subjected to the six independent eigenstrain components  $e_{11}^i$ ,  $e_{12}^i$ ,  $e_{13}^i$ ,  $e_{22}^i$ ,  $e_{23}^i$ , and  $e_{33}^i$  (Fig. 7). In tensor notation, the eigenstrain is

$$\mathbf{e}^i = \begin{pmatrix} e_{11}^i & e_{12}^i & e_{13}^i \\ e_{12}^i & e_{22}^i & e_{23}^i \\ e_{13}^i & e_{23}^i & e_{33}^i \end{pmatrix}. \quad (67)$$

We write  $e_{kk}^i$ , the trace of the eigenstrain tensor. This gives rise to the moment density tensor:

$$\begin{aligned} \mathbf{m} &= \mathbf{C} : \mathbf{e}^i \\ &= \begin{pmatrix} \lambda e_{kk}^i + 2\mu e_{11}^i & 2\mu e_{12}^i & 2\mu e_{13}^i \\ 2\mu e_{12}^i & \lambda e_{kk}^i + 2\mu e_{22}^i & 2\mu e_{23}^i \\ 2\mu e_{13}^i & 2\mu e_{23}^i & \lambda e_{kk}^i + 2\mu e_{33}^i \end{pmatrix}. \end{aligned} \quad (68)$$

The deformation in the half-space due to elastic coupling can be attributed to equivalent body forces:

$$\mathbf{f} = -\nabla \cdot \mathbf{m} = - \begin{pmatrix} \lambda e_{kk,1}^i + 2\mu e_{11,1}^i + 2\mu e_{12,2}^i + 2\mu e_{13,3}^i \\ 2\mu e_{12,1}^i + \lambda e_{kk,2}^i + 2\mu e_{22,2}^i + 2\mu e_{23,3}^i \\ 2\mu e_{13,1}^i + 2\mu e_{23,2}^i + \lambda e_{kk,3}^i + 2\mu e_{33,3}^i \end{pmatrix}. \quad (69)$$

The spatial extent of the eigenstrain can be defined with the generalized boxcar function  $\Pi(x)$ , with  $\Pi'(x) = \delta(x + 1/2) - \delta(x - 1/2)$  and  $S(x) = \Pi(x - 1/2)$ , with  $S'(x) = \delta(x) - \delta(x - 1)$ . We have the eigenstrain distributions of the form:

$$e_{ij}^i(\mathbf{x}) = e_{ij}^i \Pi\left(\frac{x_1}{L}\right) \Pi\left(\frac{x_2}{T}\right) S\left(\frac{x_3}{W}\right). \quad (70)$$

So we have the equivalent body forces

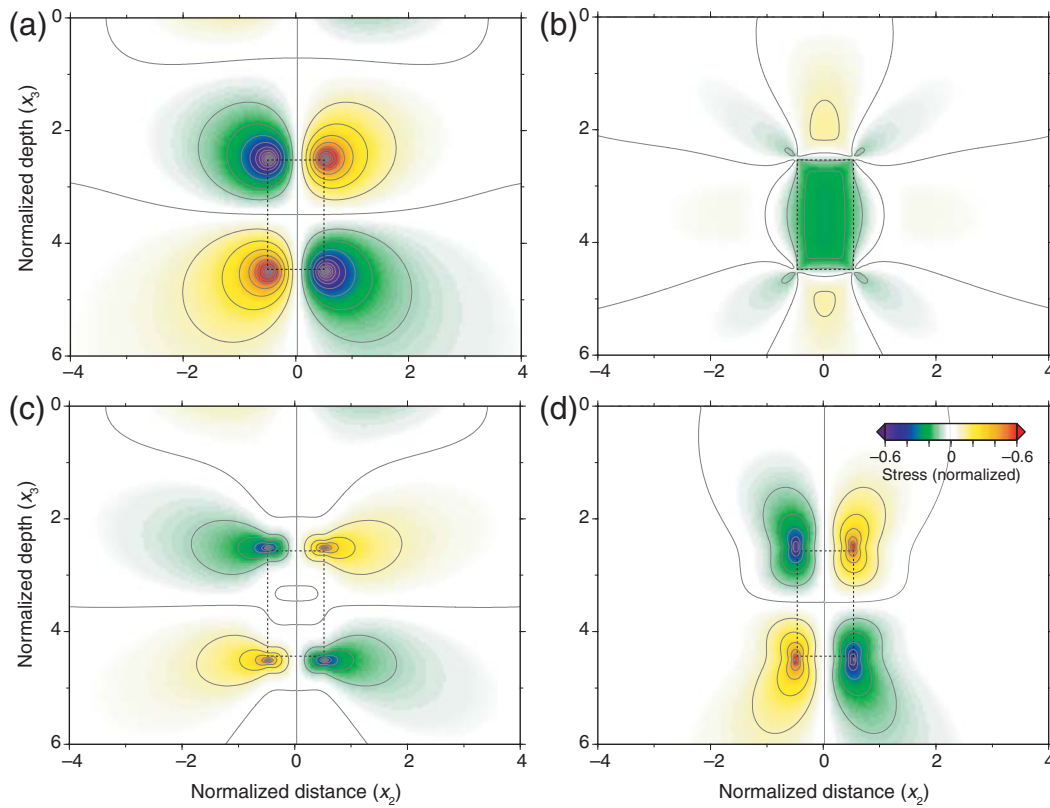


**Figure 5.** (a) Pressure and other stress components (b)  $\sigma_{23}$ , (c)  $\sigma_{22}$ , and (d)  $\sigma_{33}$  due to anelastic strain  $\epsilon_{23}^i$  in a rectangular strain region (black dashed box). The corresponding displacement field is shown at the bottom of Figure 4.

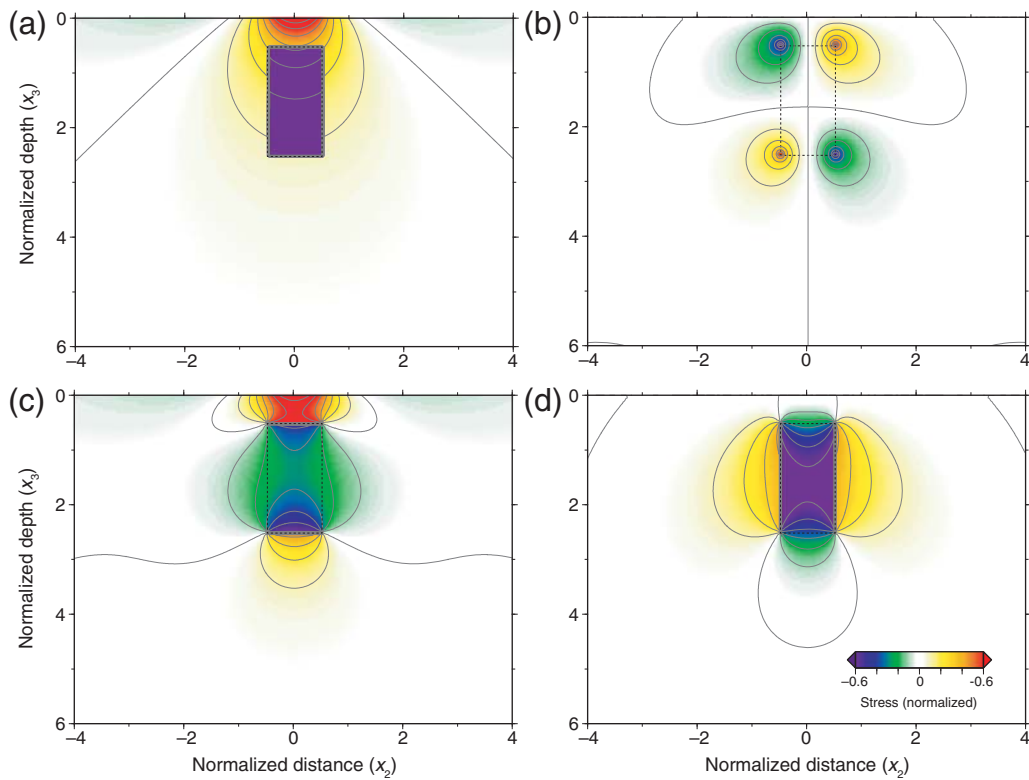


**Figure 6.** (a) Pressure and other stress components (b)  $\sigma_{23}$ , (c)  $\sigma_{22}$ , (d)  $\sigma_{33}$  due to isotropic anelastic strain  $\epsilon_{kk}^i \neq 0$  in a shallow rectangular strain region. The corresponding displacement field is shown in Figure 4a. An isotropic source of anelastic distributed deformation only pressurizes regions close to the free surface.

$$\begin{aligned}
 f_1 &= (\lambda \epsilon_{kk}^i + 2\mu \epsilon_{11}^i) \frac{1}{L} \left[ \delta \left( \frac{x_1}{L} - \frac{1}{2} \right) - \delta \left( \frac{x_1}{L} + \frac{1}{2} \right) \right] \Pi \left( \frac{x_2}{T} \right) S \left( \frac{x_3}{W} \right) \\
 &+ 2\mu \epsilon_{12}^i \Pi \left( \frac{x_1}{L} \right) \frac{1}{T} \left[ \delta \left( \frac{x_2}{T} - \frac{1}{2} \right) - \delta \left( \frac{x_2}{T} + \frac{1}{2} \right) \right] S \left( \frac{x_3}{W} \right) \\
 &+ 2\mu \epsilon_{13}^i \Pi \left( \frac{x_1}{L} \right) \Pi \left( \frac{x_2}{T} \right) \frac{1}{W} \left[ \delta \left( \frac{x_3}{W} - 1 \right) - \delta \left( \frac{x_3}{W} \right) \right] \\
 f_2 &= (\lambda \epsilon_{kk}^i + 2\mu \epsilon_{22}^i) \Pi \left( \frac{x_1}{L} \right) \frac{1}{T} \left[ \delta \left( \frac{x_2}{T} - \frac{1}{2} \right) - \delta \left( \frac{x_2}{T} + \frac{1}{2} \right) \right] S \left( \frac{x_3}{W} \right) \\
 &+ 2\mu \epsilon_{12}^i \frac{1}{L} \left[ \delta \left( \frac{x_1}{L} - \frac{1}{2} \right) - \delta \left( \frac{x_1}{L} + \frac{1}{2} \right) \right] \Pi \left( \frac{x_2}{T} \right) S \left( \frac{x_3}{W} \right) \\
 &+ 2\mu \epsilon_{23}^i \Pi \left( \frac{x_1}{L} \right) \Pi \left( \frac{x_2}{T} \right) \frac{1}{W} \left[ \delta \left( \frac{x_3}{W} - 1 \right) - \delta \left( \frac{x_3}{W} \right) \right] \\
 f_3 &= (\lambda \epsilon_{kk}^i + 2\mu \epsilon_{33}^i) \Pi \left( \frac{x_1}{L} \right) \Pi \left( \frac{x_2}{T} \right) \frac{1}{W} \left[ \delta \left( \frac{x_3}{W} - 1 \right) - \delta \left( \frac{x_3}{W} \right) \right] \\
 &+ 2\mu \epsilon_{13}^i \frac{1}{L} \left[ \delta \left( \frac{x_1}{L} - \frac{1}{2} \right) - \delta \left( \frac{x_1}{L} + \frac{1}{2} \right) \right] \Pi \left( \frac{x_2}{T} \right) S \left( \frac{x_3}{W} \right) \\
 &+ 2\mu \epsilon_{23}^i \Pi \left( \frac{x_1}{L} \right) \frac{1}{T} \left[ \delta \left( \frac{x_2}{T} - \frac{1}{2} \right) - \delta \left( \frac{x_2}{T} + \frac{1}{2} \right) \right] S \left( \frac{x_3}{W} \right). \quad (71)
 \end{aligned}$$

Green’s Function Formulation

We obtain the displacement field by solving Navier’s equation using the Green’s functions for a point source in a half-space, located at  $(y_1, y_2, y_3)$ , observed at  $(x_1, x_2, x_3)$ , in which  $x_3$  is defined positive downward. As the solution involves the method of images, we define the radial distances:

$$\begin{aligned}
 R_1 &= ((x_1 - y_1)^2 + (x_2 - y_2)^2 + (y_3 - x_3)^2)^{1/2} \\
 R_2 &= ((x_1 - y_1)^2 + (x_2 - y_2)^2 + (x_3 + y_3)^2)^{1/2}. \quad (72)
 \end{aligned}$$

The displacement in the direction  $i$  due to forces pointing in the direction  $j$  is given by the point-source Green’s functions  $G_{ji}(x_1, x_2, x_3)$ , which are described by Mindlin (1936), Press (1965), Okada (1985), and Segall (2010). We write below a formulation that is compatible with our choice of coordinates. The horizontal components are symmetric to each other

$$\begin{aligned}
 G_{11} &= \frac{1}{16\pi\mu(1-\nu)} \left[ \frac{3-4\nu}{R_1} + \frac{1}{R_2} + \frac{(x_1-y_1)^2}{R_1^3} + \frac{(3-4\nu)(x_1-y_1)^2}{R_2^3} + \frac{2x_3y_3(R_2^2-3(x_1-y_1)^2)}{R_2^5} \right. \\
 &\quad \left. + \frac{4(1-2\nu)(1-\nu)(R_2^2-(x_1-y_1)^2+R_2(x_3+y_3))}{R_2(R_2+x_3+y_3)^2} \right] \\
 G_{12} &= \frac{(x_1-y_1)(x_2-y_2)}{16\pi\mu(1-\nu)} \left[ \frac{1}{R_1^3} + \frac{3-4\nu}{R_2^3} - \frac{6x_3y_3}{R_2^5} - \frac{4(1-2\nu)(1-\nu)}{R_2(R_2+x_3+y_3)^2} \right] \\
 G_{13} &= \frac{(x_1-y_1)}{16\pi\mu(1-\nu)} \left[ \frac{x_3-y_3}{R_1^3} + \frac{(3-4\nu)(x_3-y_3)}{R_2^3} - \frac{6x_3y_3(x_3+y_3)}{R_2^5} + \frac{4(1-2\nu)(1-\nu)}{R_2(R_2+x_3+y_3)} \right] \\
 G_{21} &= \frac{(x_1-y_1)(x_2-y_2)}{16\pi\mu(1-\nu)} \left[ \frac{1}{R_1^3} + \frac{3-4\nu}{R_2^3} - \frac{6x_3y_3}{R_2^5} - \frac{4(1-2\nu)(1-\nu)}{R_2(R_2+x_3+y_3)^2} \right] \\
 G_{22} &= \frac{1}{16\pi\mu(1-\nu)} \left[ \frac{3-4\nu}{R_1} + \frac{1}{R_2} + \frac{(x_2-y_2)^2}{R_1^3} + \frac{(3-4\nu)(x_2-y_2)^2}{R_2^3} + \frac{2x_3y_3(R_2^2-3(x_2-y_2)^2)}{R_2^5} \right. \\
 &\quad \left. + \frac{4(1-2\nu)(1-\nu)(R_2^2-(x_2-y_2)^2+R_2(x_3+y_3))}{R_2(R_2+x_3+y_3)^2} \right] \\
 G_{23} &= \frac{(x_2-y_2)}{16\pi\mu(1-\nu)} \left[ \frac{x_3-y_3}{R_1^3} + \frac{(3-4\nu)(x_3-y_3)}{R_2^3} - \frac{6x_3y_3(x_3+y_3)}{R_2^5} + \frac{4(1-2\nu)(1-\nu)}{R_2(R_2+x_3+y_3)} \right], \quad (73)
 \end{aligned}$$

and the displacements due to a point force pointing in the  $e_3$  direction are

$$\begin{aligned}
 G_{31} &= \frac{(x_1-y_1)}{16\pi\mu(1-\nu)} \left[ \frac{x_3-y_3}{R_1^3} + \frac{(3-4\nu)(x_3-y_3)}{R_2^3} + \frac{6x_3y_3(x_3+y_3)}{R_2^5} - \frac{4(1-2\nu)(1-\nu)}{R_2(R_2+x_3+y_3)} \right] \\
 G_{32} &= \frac{(x_2-y_2)}{16\pi\mu(1-\nu)} \left[ \frac{x_3-y_3}{R_1^3} + \frac{(3-4\nu)(x_3-y_3)}{R_2^3} + \frac{6x_3y_3(x_3+y_3)}{R_2^5} - \frac{4(1-2\nu)(1-\nu)}{R_2(R_2+x_3+y_3)} \right] \\
 G_{33} &= \frac{1}{16\pi\mu(1-\nu)} \left[ \frac{3-4\nu}{R_1} + \frac{5-12\nu+8\nu^2}{R_2} + \frac{(x_3-y_3)^2}{R_1^3} + \frac{6x_3y_3(x_3+y_3)^2}{R_2^5} + \frac{(3-4\nu)(x_3+y_3)^2-2x_3y_3}{R_2^3} \right]. \quad (74)
 \end{aligned}$$

The displacement field is then given by

$$u_i = \iiint_{-\infty}^{\infty} f_j(y_1, y_2, y_3) G_{ji}(y_1, y_2, y_3) dy_1 dy_2 dy_3, \quad (75)$$

in which Einstein's summation convention is assumed. Each displacement component can be obtained by substituting  $i = 1, 2, 3$ .

Using the spatial distribution of equivalent body forces, we can write the displacement field explicitly:

$$\begin{aligned} u_i = & (\lambda e_{kk}^i + 2\mu e_{11}^i) \iiint_{-\infty}^{\infty} \frac{1}{L} \left[ \delta\left(\frac{y_1}{L} - 1\right) - \delta\left(\frac{y_1}{L}\right) \right] \Pi\left(\frac{y_2}{T}\right) S\left(\frac{y_3}{W}\right) G_{1i} dy_1 dy_2 dy_3 \\ & + 2\mu e_{12}^i \iiint_{-\infty}^{\infty} \frac{1}{L} \left[ \delta\left(\frac{y_1}{L} - 1\right) - \delta\left(\frac{y_1}{L}\right) \right] \Pi\left(\frac{y_2}{T}\right) S\left(\frac{y_3}{W}\right) G_{2i} dy_1 dy_2 dy_3 \\ & + 2\mu e_{13}^i \iiint_{-\infty}^{\infty} \frac{1}{L} \left[ \delta\left(\frac{y_1}{L} - 1\right) - \delta\left(\frac{y_1}{L}\right) \right] \Pi\left(\frac{y_2}{T}\right) S\left(\frac{y_3}{W}\right) G_{3i} dy_1 dy_2 dy_3 \\ & + 2\mu e_{12}^i \iiint_{-\infty}^{\infty} S\left(\frac{y_1}{L}\right) \frac{1}{T} \left[ \delta\left(\frac{y_2}{T} - \frac{1}{2}\right) - \delta\left(\frac{y_2}{T} + \frac{1}{2}\right) \right] S\left(\frac{y_3}{W}\right) G_{1i} dy_1 dy_2 dy_3 \\ & + 2\mu e_{13}^i \iiint_{-\infty}^{\infty} S\left(\frac{y_1}{L}\right) \Pi\left(\frac{y_2}{T}\right) \frac{1}{W} \left[ \delta\left(\frac{y_3}{W} - 1\right) - \delta\left(\frac{y_3}{W}\right) \right] G_{1i} dy_1 dy_2 dy_3 \\ & + (\lambda e_{kk}^i + 2\mu e_{22}^i) \iiint_{-\infty}^{\infty} S\left(\frac{y_1}{L}\right) \frac{1}{T} \left[ \delta\left(\frac{y_2}{T} - \frac{1}{2}\right) - \delta\left(\frac{y_2}{T} + \frac{1}{2}\right) \right] S\left(\frac{y_3}{W}\right) G_{2i} dy_1 dy_2 dy_3 \\ & + 2\mu e_{23}^i \iiint_{-\infty}^{\infty} S\left(\frac{y_1}{L}\right) \Pi\left(\frac{y_2}{T}\right) \frac{1}{W} \left[ \delta\left(\frac{y_3}{W} - 1\right) - \delta\left(\frac{y_3}{W}\right) \right] G_{2i} dy_1 dy_2 dy_3 \\ & + 2\mu e_{23}^i \iiint_{-\infty}^{\infty} S\left(\frac{y_1}{L}\right) \frac{1}{T} \left[ \delta\left(\frac{y_2}{T} - \frac{1}{2}\right) - \delta\left(\frac{y_2}{T} + \frac{1}{2}\right) \right] S\left(\frac{y_3}{W}\right) G_{3i} dy_1 dy_2 dy_3 \\ & + (\lambda e_{kk}^i + 2\mu e_{33}^i) \iiint_{-\infty}^{\infty} S\left(\frac{y_1}{L}\right) \Pi\left(\frac{y_2}{T}\right) \frac{1}{W} \left[ \delta\left(\frac{y_3}{W} - 1\right) - \delta\left(\frac{y_3}{W}\right) \right] G_{3i} dy_1 dy_2 dy_3. \end{aligned} \quad (76)$$

Integrating out the delta functions, we get the simplified expression

$$\begin{aligned} u_i = & (\lambda e_{kk}^i + 2\mu e_{11}^i) \int_{-T/2}^{T/2} \int_0^W G_{1i}(y_1, y_2, y_3) \Big|_{y_1=0}^{y_1=L} dy_2 dy_3 \\ & + 2\mu e_{12}^i \int_{-T/2}^{T/2} \int_0^W G_{2i}(y_1, y_2, y_3) \Big|_{y_1=0}^{y_1=L} dy_2 dy_3 \\ & + 2\mu e_{13}^i \int_{-T/2}^{T/2} \int_0^W G_{3i}(y_1, y_2, y_3) \Big|_{y_1=0}^{y_1=L} dy_2 dy_3 \\ & + 2\mu e_{12}^i \int_0^L \int_0^W G_{1i}(y_1, y_2, y_3) \Big|_{y_2=-T/2}^{y_2=T/2} dy_1 dy_3 \\ & + 2\mu e_{13}^i \int_0^L \int_{-T/2}^{T/2} G_{1i}(y_1, y_2, y_3) \Big|_{y_3=0}^{y_3=W} dy_1 dy_2 \\ & + (\lambda e_{kk}^i + 2\mu e_{22}^i) \int_0^L \int_0^W G_{2i}(y_1, y_2, y_3) \Big|_{y_2=-T/2}^{y_2=T/2} dy_1 dy_3 \\ & + 2\mu e_{23}^i \int_0^L \int_{-T/2}^{T/2} G_{2i}(y_1, y_2, y_3) \Big|_{y_3=0}^{y_3=W} dy_1 dy_2 \\ & + 2\mu e_{23}^i \int_0^L \int_0^W G_{3i}(y_1, y_2, y_3) \Big|_{y_2=-T/2}^{y_2=T/2} dy_1 dy_3 \\ & + (\lambda e_{kk}^i + 2\mu e_{33}^i) \int_0^L \int_{-T/2}^{T/2} G_{3i}(y_1, y_2, y_3) \Big|_{y_3=0}^{y_3=W} dy_1 dy_2. \end{aligned} \quad (77)$$

Analytic Solution

The displacement field is given in closed form by

$$\begin{aligned} u_i = & (\lambda e_{kk}^i + 2\mu e_{11}^i) J_{i123} + 2\mu e_{12}^i (J_{i223} + J_{i113}) \\ & + 2\mu e_{13}^i (J_{i323} + J_{i112}) + (\lambda e_{kk}^i + 2\mu e_{22}^i) J_{i213} \\ & + 2\mu e_{23}^i (J_{i212} + J_{i313}) + (\lambda e_{kk}^i + 2\mu e_{33}^i) J_{i312} \end{aligned} \quad (78)$$

in which we have used the following notation based on Chinnery's to evaluate the bounds

$$\begin{aligned} f(y_1, y_2, y_3) \Big| = & f\left(L, \frac{T}{2}, W\right) - f\left(L, -\frac{T}{2}, W\right) \\ & + f\left(L, -\frac{T}{2}, 0\right) - f\left(L, \frac{T}{2}, 0\right) \\ & - f\left(0, \frac{T}{2}, W\right) + f\left(0, -\frac{T}{2}, W\right) \\ & - f\left(0, -\frac{T}{2}, 0\right) + f\left(0, \frac{T}{2}, 0\right) \end{aligned} \quad (79)$$

and where we defined the following indefinite integrals:

$$J_{ijkl} = \iint G_{ji} dy_k dy_l. \quad (80)$$

The closed-form solutions are below:

$$\begin{aligned}
 J_{1112} = & \frac{1}{16\pi\mu(1-\nu)} \left[ -x_3 \arctan\left(\frac{x_3}{x_1-y_1}\right) \right. \\
 & - 3x_3 \arctan\left(\frac{3x_3}{x_1-y_1}\right) - 4\nu x_3 \arctan\left(\frac{\nu x_3}{x_1-y_1}\right) \\
 & - (4\nu-3)(x_1-y_1) \log(r_1+x_2-y_2) \\
 & + (4\nu(2\nu-3)+5)(x_1-y_1) \log(r_2+x_2-y_2) \\
 & - 4(\nu-1)(x_2-y_2) \log(r_1+x_1-y_1) \\
 & - 4(\nu-1)(x_2-y_2) \log(r_2+x_1-y_1) \\
 & - 4(\nu-1)(x_3-y_3) \arctan\left(\frac{r_1(x_3-y_3)}{(x_1-y_1)(x_2-y_2)}\right) \\
 & - y_3 \arctan\left(\frac{y_3}{x_1-y_1}\right) - 3y_3 \arctan\left(\frac{3y_3}{x_1-y_1}\right) \\
 & - 4\nu y_3 \arctan\left(\frac{\nu y_3}{x_1-y_1}\right) \\
 & - 4(\nu-1)(2\nu-1)(x_3+y_3) \arctan\left(\frac{x_2-y_2}{x_1-y_1}\right) \\
 & + 4(\nu-1)(2\nu-1)(x_3+y_3) \arctan\left(\frac{r_2(y_1-x_1)}{(x_2-y_2)(x_3+y_3)}\right) \\
 & - 4(\nu-1)(x_3+y_3) \arctan\left(\frac{r_2(x_3+y_3)}{(x_1-y_1)(x_2-y_2)}\right) \\
 & \left. + \frac{2x_3y_3(x_1-y_1)(x_2-y_2)}{r_2((x_1-y_1)^2+(x_3+y_3)^2)} \right], \tag{81}
 \end{aligned}$$

$$\begin{aligned}
 J_{1113} = & \frac{1}{16\pi\mu(1-\nu)} \left[ x_2 \left( -\arctan\left(\frac{x_2}{x_1-y_1}\right) \right) \right. \\
 & - 3x_2 \arctan\left(\frac{3x_2}{x_1-y_1}\right) - 4\nu x_2 \arctan\left(\frac{\nu x_2}{x_1-y_1}\right) \\
 & - (4\nu-3)(x_1-y_1) \log(r_1+x_3-y_3) \\
 & - (4\nu^2-6\nu+3)(x_1-y_1) \log(r_2+x_3+y_3) \\
 & - 4(\nu-1)(x_2-y_2) \arctan\left(\frac{r_1(x_2-y_2)}{(x_1-y_1)(x_3-y_3)}\right) \\
 & + 4(\nu-1)(x_2-y_2) \arctan\left(\frac{r_2(x_2-y_2)}{(x_1-y_1)(x_3+y_3)}\right) \\
 & - y_2 \arctan\left(\frac{y_2}{x_1-y_1}\right) - 3y_2 \arctan\left(\frac{3y_2}{x_1-y_1}\right) \\
 & - 4\nu y_2 \arctan\left(\frac{\nu y_2}{x_1-y_1}\right) \\
 & - 4(\nu-1)(x_3-y_3) \log(r_1+x_1-y_1) \\
 & + 4(\nu-1)(x_3+y_3) \log(r_2+x_1-y_1) \\
 & + 2(\nu-1)(2\nu-1)(x_1-y_1) \\
 & \times \frac{r_2y_3(2x_3+y_3)-r_2^2(x_3+y_3)}{r_2((x_1-y_1)^2+(x_2-y_2)^2)} + 2(x_1-y_1) \\
 & \left. \times \frac{x_3((x_1-y_1)^2+(x_2-y_2)^2+x_3(x_3+y_3))}{r_2((x_1-y_1)^2+(x_2-y_2)^2)} \right], \tag{82}
 \end{aligned}$$

$$\begin{aligned}
 J_{1123} = & \frac{1}{16\pi\mu(1-\nu)} \left[ x_1 \left( -\arctan\left(\frac{x_1}{x_2-y_2}\right) \right) \right. \\
 & - 3x_1 \arctan\left(\frac{3x_1}{x_2-y_2}\right) - 4\nu x_1 \arctan\left(\frac{\nu x_1}{x_2-y_2}\right) \\
 & - 2x_3 \log(r_2-x_2+y_2) \\
 & + 2(\nu-1)(2\nu-1)(x_1-y_1) \arctan\left(\frac{x_1-y_1}{x_2-y_2}\right) \\
 & + 2(2\nu-1)(x_1-y_1) \arctan\left(\frac{r_1(y_1-x_1)}{(x_2-y_2)(x_3-y_3)}\right) \\
 & + 2(1-2\nu)^2(x_1-y_1) \arctan\left(\frac{r_2(y_1-x_1)}{(x_2-y_2)(x_3+y_3)}\right) \\
 & - y_1 \arctan\left(\frac{y_1}{x_2-y_2}\right) - 3y_1 \arctan\left(\frac{3y_1}{x_2-y_2}\right) \\
 & - 4\nu y_1 \arctan\left(\frac{\nu y_1}{x_2-y_2}\right) - (4\nu-3)(x_2-y_2) \log(r_1+x_3-y_3) \\
 & - (4\nu^2-6\nu+3)(x_2-y_2) \log(r_2+x_3+y_3) \\
 & - (4\nu-3)(x_3-y_3) \log(r_1+x_2-y_2) \\
 & - (4\nu(2\nu-3)+5)(x_3+y_3) \log(r_2+x_2-y_2) \\
 & - 2(x_2-y_2)(\nu-1)(2\nu-1) \\
 & \times \frac{((x_1-y_1)^2+(x_3+y_3)^2)(y_3(2x_3+y_3)-r_2(x_3+y_3))}{((x_1-y_1)^2+(x_2-y_2)^2)((x_1-y_1)^2+(x_3+y_3)^2)} \\
 & - 2(x_2-y_2)x_3^2 \\
 & \times \frac{y_3^3+3x_3y_3^2+y_3(2(x_1-y_1)^2+(x_2-y_2)^2+3x_3^2)}{r_2((x_1-y_1)^2+(x_2-y_2)^2)((x_1-y_1)^2+(x_3+y_3)^2)} \\
 & - 2(x_2-y_2)x_3 \\
 & \times \frac{((x_1-y_1)^2+x_3^2)((x_1-y_1)^2+(x_2-y_2)^2+x_3^2)}{r_2((x_1-y_1)^2+(x_2-y_2)^2)((x_1-y_1)^2+(x_3+y_3)^2)} \left. \right], \tag{83}
 \end{aligned}$$

$$\begin{aligned}
 J_{2112} = & \frac{1}{16\pi\mu(1-\nu)} \left[ -r_1 + (8(\nu-1)\nu+1)r_2 - \frac{2x_3y_3}{r_2} \right. \\
 & \left. - 4(\nu-1)(2\nu-1)(x_3+y_3) \log(r_2+x_3+y_3) \right], \tag{84}
 \end{aligned}$$

$$\begin{aligned}
 J_{2113} = & \frac{1}{16\pi\mu(1-\nu)} \left[ -(4\nu^2-2\nu-1)(x_2-y_2) \log(r_2+x_3+y_3) \right. \\
 & + (y_2-x_2) \log(r_1+x_3-y_3) \\
 & + 2(x_2-y_2)(\nu-1)(2\nu-1) \frac{-r_2(x_3+y_3)+y_3(2x_3+y_3)}{(x_1-y_1)^2+(x_2-y_2)^2} \\
 & \left. + 2(x_2-y_2) \frac{x_3((x_1-y_1)^2+(x_2-y_2)^2+x_3(x_3+y_3))}{r_2((x_1-y_1)^2+(x_2-y_2)^2)} \right], \tag{85}
 \end{aligned}$$

$$\begin{aligned}
 J_{2123} = & \frac{1}{16\pi\mu(1-\nu)} \left[ -(4\nu^2 - 2\nu - 1)(x_1 - y_1) \log(r_2 + x_3 + y_3) \right. \\
 & + (y_1 - x_1) \log(r_1 + x_3 - y_3) \\
 & + 2(\nu - 1)(2\nu - 1)(x_1 - y_1) \frac{-r_2(x_3 + y_3) + y_3(2x_3 + y_3)}{((x_1 - y_1)^2 + (x_2 - y_2)^2)} \\
 & + 2(\nu - 1)(2\nu - 1)(x_1 - y_1) \frac{x_3((x_1 - y_1)^2 + (x_2 - y_2)^2 + x_3(x_3 + y_3))}{r_2((x_1 - y_1)^2 + (x_2 - y_2)^2)} \\
 & \left. + 2(x_1 - y_1) \frac{x_3((x_1 - y_1)^2 + (x_2 - y_2)^2 + x_3(x_3 + y_3))}{r_2((x_1 - y_1)^2 + (x_2 - y_2)^2)} \right], \tag{86}
 \end{aligned}$$

$$\begin{aligned}
 J_{3112} = & \frac{-1}{16\pi\mu(1-\nu)} \left[ 4(\nu - 1)(2\nu - 1)(x_1 - y_1) \arctan\left(\frac{x_1 - y_1}{x_2 - y_2}\right) \right. \\
 & + 4(\nu - 1)(2\nu - 1)(x_1 - y_1) \arctan\left(\frac{r_2(y_1 - x_1)}{(x_2 - y_2)(x_3 + y_3)}\right) \\
 & - 4(\nu - 1)(2\nu - 1)(x_2 - y_2) \log(r_2 + x_3 + y_3) \\
 & + (x_3 - y_3) \log(r_1 + x_2 - y_2) - \frac{2x_3y_3(x_2 - y_2)(x_3 + y_3)}{r_2((x_1 - y_1)^2 + (x_3 + y_3)^2)} \\
 & + (-8\nu^2(x_3 + y_3) + 8\nu(x_3 + 2y_3) \\
 & \left. - x_3 - 7y_3) \log(r_2 + x_2 - y_2) \right], \tag{87}
 \end{aligned}$$

$$\begin{aligned}
 J_{3113} = & \frac{-1}{16\pi\mu(1-\nu)} \left[ r_1 + (-8(\nu - 1)\nu - 1)r_2 \right. \\
 & + 2(4\nu - 3)x_3 \operatorname{arccoth}\left(\frac{x_3 + y_3}{r_2}\right) - \frac{2x_3y_3}{r_2} \\
 & + 2(4\nu^2(x_3 + y_3) - 6\nu(x_3 + y_3) + 3x_3 \\
 & \left. + 2y_3) \log(r_2 + x_3 + y_3) \right], \tag{88}
 \end{aligned}$$

$$\begin{aligned}
 J_{3123} = & \frac{-1}{16\pi\mu(1-\nu)} \left[ (x_1 - y_1) \log(r_1 + x_2 - y_2) \right. \\
 & - (8(\nu - 1)\nu + 1)(x_1 - y_1) \log(r_2 + x_2 - y_2) \\
 & + 4(\nu - 1)(2\nu - 1)(x_3 + y_3) \arctan\left(\frac{x_2 - y_2}{x_1 - y_1}\right) \\
 & + 4(2\nu - 1)(\nu x_3 + (\nu - 1)y_3) \\
 & \times \arctan\left(\frac{r_2(x_1 - y_1)}{(x_2 - y_2)(x_3 + y_3)}\right) \\
 & \left. + \frac{2x_3y_3(x_1 - y_1)(x_2 - y_2)}{r_2((x_1 - y_1)^2 + (x_3 + y_3)^2)} \right], \tag{89}
 \end{aligned}$$

$$\begin{aligned}
 J_{1212} = & \frac{1}{16\pi\mu(1-\nu)} \left[ -r_1 + (8(\nu - 1)\nu + 1)r_2 - \frac{2x_3y_3}{r_2} \right. \\
 & \left. - 4(\nu - 1)(2\nu - 1)(x_3 + y_3) \log(r_2 + x_3 + y_3) \right], \tag{90}
 \end{aligned}$$

$$\begin{aligned}
 J_{1213} = & \frac{1}{16\pi\mu(1-\nu)} \left[ -(4\nu^2 - 2\nu - 1)(x_2 - y_2) \log(r_2 + x_3 + y_3) \right. \\
 & + (y_2 - x_2) \log(r_1 + x_3 - y_3) \\
 & + 2(\nu - 1)(2\nu - 1)(x_2 - y_2) \frac{-r_2(x_3 + y_3) + y_3(2x_3 + y_3)}{((x_1 - y_1)^2 + (x_2 - y_2)^2)} \\
 & \left. + 2(x_2 - y_2) \frac{x_3((x_1 - y_1)^2 + (x_2 - y_2)^2 + x_3(x_3 + y_3))}{r_2((x_1 - y_1)^2 + (x_2 - y_2)^2)} \right], \tag{91}
 \end{aligned}$$

$$\begin{aligned}
 J_{1223} = & \frac{1}{16\pi\mu(1-\nu)} \left[ -(4\nu^2 - 2\nu - 1)(x_1 - y_1) \log(r_2 + x_3 + y_3) \right. \\
 & + (y_1 - x_1) \log(r_1 + x_3 - y_3) \\
 & + 2(\nu - 1)(2\nu - 1)(x_1 - y_1) \frac{-r_2(x_3 + y_3) + y_3(2x_3 + y_3)}{((x_1 - y_1)^2 + (x_2 - y_2)^2)} \\
 & \left. + 2(x_1 - y_1) \frac{x_3((x_1 - y_1)^2 + (x_2 - y_2)^2 + x_3(x_3 + y_3))}{r_2((x_1 - y_1)^2 + (x_2 - y_2)^2)} \right], \tag{92}
 \end{aligned}$$

$$\begin{aligned}
 J_{2212} = & \frac{1}{16\pi\mu(1-\nu)} \left[ x_3 \left( -\arctan\left(\frac{x_3}{x_1 - y_1}\right) \right) \right. \\
 & - 3x_3 \arctan\left(\frac{3x_3}{x_1 - y_1}\right) - 4\nu x_3 \arctan\left(\frac{\nu x_3}{x_1 - y_1}\right) \\
 & - 4(\nu - 1)(x_1 - y_1) \log(r_1 + x_2 - y_2) \\
 & - 4(\nu - 1)(x_1 - y_1) \log(r_2 + x_2 - y_2) \\
 & - (4\nu - 3)(x_2 - y_2) \log(r_1 + x_1 - y_1) \\
 & + (4\nu(2\nu - 3) + 5)(x_2 - y_2) \log(r_2 + x_1 - y_1) \\
 & - 4(\nu - 1)(x_3 - y_3) \arctan\left(\frac{r_1(x_3 - y_3)}{(x_1 - y_1)(x_2 - y_2)}\right) \\
 & + y_3 \left( -\arctan\left(\frac{y_3}{x_1 - y_1}\right) \right) - 3y_3 \arctan\left(\frac{3y_3}{x_1 - y_1}\right) \\
 & - 4\nu y_3 \arctan\left(\frac{\nu y_3}{x_1 - y_1}\right) \\
 & - 4(\nu - 1)(2\nu - 1)(x_3 + y_3) \arctan\left(\frac{x_1 - y_1}{x_2 - y_2}\right) \\
 & + 4(\nu - 1)(2\nu - 1)(x_3 + y_3) \arctan\left(\frac{r_2(y_2 - x_2)}{(x_1 - y_1)(x_3 + y_3)}\right) \\
 & - 4(\nu - 1)(x_3 + y_3) \arctan\left(\frac{r_2(x_3 + y_3)}{(x_1 - y_1)(x_2 - y_2)}\right) \\
 & \left. + \frac{2x_3y_3(x_1 - y_1)(x_2 - y_2)}{r_2((x_2 - y_2)^2 + (x_3 + y_3)^2)} \right], \tag{93}
 \end{aligned}$$

$$\begin{aligned}
 J_{2213} = & \frac{1}{16\pi\mu(1-\nu)} \left[ x_2 \left( -\arctan\left(\frac{x_2}{x_1 - y_1}\right) \right) \right. \\
 & - 3x_2 \arctan\left(\frac{3x_2}{x_1 - y_1}\right) - 4\nu x_2 \arctan\left(\frac{\nu x_2}{x_1 - y_1}\right) \\
 & \left. - 2x_3 \log(r_2 - x_1 + y_1) \right]
 \end{aligned}$$

$$\begin{aligned}
 & -(4\nu-3)(x_1-y_1)\log(r_1+x_3-y_3) \\
 & -(4\nu^2-6\nu+3)(x_1-y_1)\log(r_2+x_3+y_3) \\
 & +2(\nu-1)(2\nu-1)(x_2-y_2)\arctan\left(\frac{x_2-y_2}{x_1-y_1}\right) \\
 & +2(2\nu-1)(x_2-y_2)\arctan\left(\frac{r_1(y_2-x_2)}{(x_1-y_1)(x_3-y_3)}\right) \\
 & +2(1-2\nu)^2(x_2-y_2)\arctan\left(\frac{r_2(y_2-x_2)}{(x_1-y_1)(x_3+y_3)}\right) \\
 & -y_2\arctan\left(\frac{y_2}{x_1-y_1}\right)-3y_2\arctan\left(\frac{3y_2}{x_1-y_1}\right) \\
 & -4\nu y_2\arctan\left(\frac{\nu y_2}{x_1-y_1}\right) \\
 & -(4\nu-3)(x_3-y_3)\log(r_1+x_1-y_1) \\
 & -(4\nu(2\nu-3)+5)(x_3+y_3)\log(r_2+x_1-y_1) \\
 & -2(\nu-1)(2\nu-1)(x_1-y_1)\frac{-r_2(x_3+y_3)+y_3(2x_3+y_3)}{((x_1-y_1)^2+(x_2-y_2)^2)} \\
 & -2(x_1-y_1)x_3^2\frac{y_3^3+3x_3y_3^2+y_3((x_1-y_1)^2+2(x_2-y_2)^2+3x_3^2)}{r_2((x_1-y_1)^2+(x_2-y_2)^2)((x_2-y_2)^2+(x_3+y_3)^2)} \\
 & -2(x_1-y_1)x_3\frac{((x_2-y_2)^2+x_3^2)((x_1-y_1)^2+(x_2-y_2)^2+x_3^2)}{r_2((x_1-y_1)^2+(x_2-y_2)^2)((x_2-y_2)^2+(x_3+y_3)^2)} \Big], \\
 & \tag{94}
 \end{aligned}$$

$$\begin{aligned}
 J_{2223} &= \frac{1}{16\pi\mu(1-\nu)} \Big[ x_1 \left( -\arctan\left(\frac{x_1}{x_2-y_2}\right) \right) \\
 & -3x_1\arctan\left(\frac{3x_1}{x_2-y_2}\right) -4\nu x_1\arctan\left(\frac{\nu x_1}{x_2-y_2}\right) \\
 & -4(\nu-1)(x_1-y_1)\arctan\left(\frac{r_1(x_1-y_1)}{(x_2-y_2)(x_3-y_3)}\right) \\
 & +4(\nu-1)(x_1-y_1)\arctan\left(\frac{r_2(x_1-y_1)}{(x_2-y_2)(x_3+y_3)}\right) \\
 & -y_1\arctan\left(\frac{y_1}{x_2-y_2}\right) -3y_1\arctan\left(\frac{3y_1}{x_2-y_2}\right) \\
 & -4\nu y_1\arctan\left(\frac{\nu y_1}{x_2-y_2}\right) \\
 & -(4\nu-3)(x_2-y_2)\log(r_1+x_3-y_3) \\
 & -(4\nu^2-6\nu+3)(x_2-y_2)\log(r_2+x_3+y_3) \\
 & -4(\nu-1)(x_3-y_3)\log(r_1+x_2-y_2) \\
 & +4(\nu-1)(x_3+y_3)\log(r_2+x_2-y_2) \\
 & +2(\nu-1)(2\nu-1)(x_2-y_2)\frac{-r_2(x_3+y_3)+y_3(2x_3+y_3)}{((x_1-y_1)^2+(x_2-y_2)^2)} \\
 & +2(x_2-y_2)\frac{x_3((x_1-y_1)^2+(x_2-y_2)^2+x_3(x_3+y_3))}{r_2((x_1-y_1)^2+(x_2-y_2)^2)} \Big], \\
 & \tag{95}
 \end{aligned}$$

$$\begin{aligned}
 J_{3212} &= \frac{-1}{16\pi\mu(1-\nu)} \Big[ -4(\nu-1)(2\nu-1) \\
 & \times (x_1-y_1)\log(r_2+x_3+y_3) \\
 & +4(\nu-1)(2\nu-1)(x_2-y_2)\arctan\left(\frac{x_2-y_2}{x_1-y_1}\right) \\
 & +4(\nu-1)(2\nu-1)(x_2-y_2)\arctan\left(\frac{r_2(y_2-x_2)}{(x_1-y_1)(x_3+y_3)}\right) \\
 & +(x_3-y_3)\log(r_1+x_1-y_1) \\
 & -\frac{2x_3y_3(x_1-y_1)(x_3+y_3)}{r_2((x_2-y_2)^2+(x_3+y_3)^2)} \\
 & +(-8\nu^2(x_3+y_3)+8\nu(x_3+2y_3) \\
 & -x_3-7y_3)\log(r_2+x_1-y_1) \Big], \\
 & \tag{96}
 \end{aligned}$$

$$\begin{aligned}
 J_{3213} &= \frac{-1}{16\pi\mu(1-\nu)} \Big[ (x_2-y_2)\log(r_1+x_1-y_1) \\
 & -(8(\nu-1)\nu+1)(x_2-y_2)\log(r_2+x_1-y_1) \\
 & +4(\nu-1)(2\nu-1)(x_3+y_3)\arctan\left(\frac{x_1-y_1}{x_2-y_2}\right) \\
 & +4(2\nu-1)(\nu x_3+(\nu-1)y_3) \\
 & \times \arctan\left(\frac{r_2(x_2-y_2)}{(x_1-y_1)(x_3+y_3)}\right) \\
 & +\frac{2x_3y_3(x_1-y_1)(x_2-y_2)}{r_2((x_2-y_2)^2+(x_3+y_3)^2)} \Big], \\
 & \tag{97}
 \end{aligned}$$

$$\begin{aligned}
 J_{3223} &= \frac{-1}{16\pi\mu(1-\nu)} \Big[ r_1+(-8(\nu-1)\nu-1)r_2 \\
 & +2(4\nu-3)x_3\operatorname{arccoth}\left(\frac{x_3+y_3}{r_2}\right) -\frac{2x_3y_3}{r_2} \\
 & +2(4\nu^2(x_3+y_3)-6\nu(x_3+y_3) \\
 & +3x_3+2y_3)\log(r_2+x_3+y_3) \Big], \\
 & \tag{98}
 \end{aligned}$$

$$\begin{aligned}
 J_{1312} &= \frac{-1}{16\pi\mu(1-\nu)} \Big[ -4(\nu-1)(2\nu-1)(x_1-y_1)\arctan\left(\frac{x_1-y_1}{x_2-y_2}\right) \\
 & +4(\nu-1)(2\nu-1)(x_1-y_1)\arctan\left(\frac{r_2(x_1-y_1)}{(x_2-y_2)(x_3+y_3)}\right) \\
 & +4(\nu-1)(2\nu-1)(x_2-y_2)\log(r_2+x_3+y_3) \\
 & +(x_3-y_3)\log(r_1+x_2-y_2)+((8(\nu-2)\nu+7)x_3 \\
 & +8(\nu-1)\nu y_3+y_3)\log(r_2+x_2-y_2) \\
 & +\frac{2x_3y_3(x_2-y_2)(x_3+y_3)}{r_2((x_1-y_1)^2+(x_3+y_3)^2)} \Big], \\
 & \tag{99}
 \end{aligned}$$

$$\begin{aligned}
J_{1313} = & \frac{-1}{16\pi\mu(1-\nu)} \left[ r_1 + 2(4\nu-3)x_3 \operatorname{arccoth}\left(\frac{x_3+y_3}{r_2}\right) \right. \\
& + \frac{(8(\nu-2)\nu+7)r_2^2+2x_3y_3}{r_2} \\
& + 2(-4\nu^2(x_3+y_3)+6\nu(x_3+y_3) \\
& \left. - 3x_3-2y_3) \log(r_2+x_3+y_3) \right], \quad (100)
\end{aligned}$$

$$\begin{aligned}
J_{2323} = & \frac{-1}{16\pi\mu(1-\nu)} \left[ r_1 + 2(4\nu-3)x_3 \operatorname{arccoth}\left(\frac{x_3+y_3}{r_2}\right) \right. \\
& + \frac{(8(\nu-2)\nu+7)r_2^2+2x_3y_3}{r_2} \\
& + 2(-4\nu^2(x_3+y_3)+6\nu(x_3+y_3) \\
& \left. - 3x_3-2y_3) \log(r_2+x_3+y_3) \right], \quad (104)
\end{aligned}$$

$$\begin{aligned}
J_{1323} = & \frac{-1}{16\pi\mu(1-\nu)} \left[ (x_1-y_1) \log(r_1+x_2-y_2) \right. \\
& + (8(\nu-2)\nu+7)(x_1-y_1) \log(r_2+x_2-y_2) \\
& - 4(\nu-1)(2\nu-1)(x_3+y_3) \arctan\left(\frac{x_2-y_2}{x_1-y_1}\right) \\
& - 4(\nu-1)(2\nu(x_3+y_3)-3x_3-y_3) \\
& \times \arctan\left(\frac{r_2(x_1-y_1)}{(x_2-y_2)(x_3+y_3)}\right) \\
& \left. - \frac{2x_3y_3(x_1-y_1)(x_2-y_2)}{r_2((x_1-y_1)^2+(x_3+y_3)^2)} \right], \quad (101)
\end{aligned}$$

$$\begin{aligned}
J_{3312} = & \frac{1}{16\pi\mu(1-\nu)} \left[ -3x_3 \arctan\left(\frac{3x_3}{x_1-y_1}\right) \right. \\
& - 4\nu x_3 \arctan\left(\frac{\nu x_3}{x_1-y_1}\right) - 5x_3 \arctan\left(\frac{5x_3}{x_2-y_2}\right) \\
& - 12\nu x_3 \arctan\left(\frac{3\nu x_3}{x_2-y_2}\right) - 8\nu^2 x_3 \arctan\left(\frac{\nu^2 x_3}{x_2-y_2}\right) \\
& - (4\nu-3)(x_1-y_1) \log(r_1+x_2-y_2) \\
& + (4\nu(2\nu-3)+5)(x_1-y_1) \log(r_2+x_2-y_2) \\
& - (4\nu-3)(x_2-y_2) \log(r_1+x_1-y_1) \\
& + (4\nu(2\nu-3)+5)(x_2-y_2) \log(r_2+x_1-y_1) \\
& + 2(2\nu-1)(x_3-y_3) \arctan\left(\frac{r_1(y_3-x_3)}{(x_1-y_1)(x_2-y_2)}\right) \\
& - 3y_3 \arctan\left(\frac{3y_3}{x_1-y_1}\right) - 4\nu y_3 \arctan\left(\frac{\nu y_3}{x_1-y_1}\right) \\
& - 5y_3 \arctan\left(\frac{5y_3}{x_2-y_2}\right) - 12\nu y_3 \arctan\left(\frac{3\nu y_3}{x_2-y_2}\right) \\
& - 8\nu^2 y_3 \arctan\left(\frac{\nu^2 y_3}{x_2-y_2}\right) + 2(1-2\nu)^2(x_3+y_3) \\
& \times \arctan\left(\frac{r_2(x_3+y_3)}{(x_1-y_1)(x_2-y_2)}\right) \\
& \left. + \frac{2x_3y_3(x_1-y_1)(x_2-y_2)((x_1-y_1)^2+(x_2-y_2)^2+2(x_3+y_3)^2)}{r_2((x_1-y_1)^2+(x_3+y_3)^2)((x_2-y_2)^2+(x_3+y_3)^2)} \right], \quad (105)
\end{aligned}$$

$$\begin{aligned}
J_{2312} = & \frac{-1}{16\pi\mu(1-\nu)} \left[ 4(\nu-1)(2\nu-1)(x_1-y_1) \log(r_2+x_3+y_3) \right. \\
& - 4(\nu-1)(2\nu-1)(x_2-y_2) \arctan\left(\frac{x_2-y_2}{x_1-y_1}\right) \\
& + 4(\nu-1)(2\nu-1)(x_2-y_2) \arctan\left(\frac{r_2(x_2-y_2)}{(x_1-y_1)(x_3+y_3)}\right) \\
& + (x_3-y_3) \log(r_1+x_1-y_1) \\
& + ((8(\nu-2)\nu+7)x_3+8(\nu-1)\nu y_3+y_3) \\
& \left. \times \log(r_2+x_1-y_1) + \frac{2x_3y_3(x_1-y_1)(x_3+y_3)}{r_2((x_2-y_2)^2+(x_3+y_3)^2)} \right], \quad (102)
\end{aligned}$$

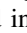
$$\begin{aligned}
J_{2313} = & \frac{-1}{16\pi\mu(1-\nu)} \left[ (x_2-y_2) \log(r_1+x_1-y_1) \right. \\
& + (8(\nu-2)\nu+7)(x_2-y_2) \log(r_2+x_1-y_1) \\
& - 4(\nu-1)(2\nu-1)(x_3+y_3) \arctan\left(\frac{x_1-y_1}{x_2-y_2}\right) \\
& - 4(\nu-1)(2\nu(x_3+y_3)-3x_3-y_3) \\
& \times \arctan\left(\frac{r_2(x_2-y_2)}{(x_1-y_1)(x_3+y_3)}\right) \\
& \left. - \frac{2x_3y_3(x_1-y_1)(x_2-y_2)}{r_2((x_2-y_2)^2+(x_3+y_3)^2)} \right], \quad (103)
\end{aligned}$$

$$\begin{aligned}
J_{3313} = & \frac{1}{16\pi\mu(1-\nu)} \left[ -3x_2 \arctan\left(\frac{3x_2}{x_1-y_1}\right) \right. \\
& - 5x_2 \arctan\left(\frac{5x_2}{x_1-y_1}\right) - 4\nu x_2 \arctan\left(\frac{\nu x_2}{x_1-y_1}\right) \\
& - 12\nu x_2 \arctan\left(\frac{3\nu x_2}{x_1-y_1}\right) - 8\nu^2 x_2 \arctan\left(\frac{\nu^2 x_2}{x_1-y_1}\right) \\
& - 4x_3 \log(r_2-x_1+y_1) \\
& - 4(\nu-1)(x_1-y_1) \log(r_1+x_3-y_3) \\
& - 8(\nu-1)^2(x_1-y_1) \log(r_2+x_3+y_3) \\
& \left. - 4(\nu-1)(x_2-y_2) \arctan\left(\frac{r_1(x_2-y_2)}{(x_1-y_1)(x_3+y_3)}\right) \right]
\end{aligned}$$



$$\begin{aligned}
 & -8(\nu - 1)^2(x_2 - y_2) \arctan\left(\frac{r_2(x_2 - y_2)}{(x_1 - y_1)(x_3 + y_3)}\right) \\
 & -3y_2 \arctan\left(\frac{3y_2}{x_1 - y_1}\right) - 5y_2 \arctan\left(\frac{5y_2}{x_1 - y_1}\right) \\
 & -4\nu y_2 \arctan\left(\frac{\nu y_2}{x_1 - y_1}\right) - 12\nu y_2 \arctan\left(\frac{3\nu y_2}{x_1 - y_1}\right) \\
 & -8\nu^2 y_2 \arctan\left(\frac{\nu^2 y_2}{x_1 - y_1}\right) \\
 & - (4\nu - 3)(x_3 - y_3) \log(r_1 + x_1 - y_1) + (-8\nu^2(x_3 + y_3) \\
 & + 12\nu(x_3 + y_3) - 7x_3 - 5y_3) \log(r_2 + x_1 - y_1) \\
 & + \frac{2x_3 y_3 (x_1 - y_1)(x_3 + y_3)}{r_2((x_2 - y_2)^2 + (x_3 + y_3)^2)}, \tag{106}
 \end{aligned}$$

$$\begin{aligned}
 J_{3323} = & \frac{1}{16\pi\mu(1 - \nu)} \left[ -3x_1 \arctan\left(\frac{3x_1}{x_2 - y_2}\right) \right. \\
 & - 5x_1 \arctan\left(\frac{5x_1}{x_2 - y_2}\right) - 4\nu x_1 \arctan\left(\frac{\nu x_1}{x_2 - y_2}\right) \\
 & - 12\nu x_1 \arctan\left(\frac{3\nu x_1}{x_2 - y_2}\right) - 8\nu^2 x_1 \arctan\left(\frac{\nu^2 x_1}{x_2 - y_2}\right) \\
 & - 4x_3 \log(r_2 - x_2 + y_2) \\
 & - 4(\nu - 1)(x_1 - y_1) \arctan\left(\frac{r_1(x_1 - y_1)}{(x_2 - y_2)(x_3 - y_3)}\right) \\
 & - 8(\nu - 1)^2(x_1 - y_1) \arctan\left(\frac{r_2(x_1 - y_1)}{(x_2 - y_2)(x_3 + y_3)}\right) \\
 & - 3y_1 \arctan\left(\frac{3y_1}{x_2 - y_2}\right) - 5y_1 \arctan\left(\frac{5y_1}{x_2 - y_2}\right) \\
 & - 4\nu y_1 \arctan\left(\frac{\nu y_1}{x_2 - y_2}\right) - 12\nu y_1 \arctan\left(\frac{3\nu y_1}{x_2 - y_2}\right) \\
 & - 8\nu^2 y_1 \arctan\left(\frac{\nu^2 y_1}{x_2 - y_2}\right) \\
 & - 4(\nu - 1)(x_2 - y_2) \log(r_1 + x_3 - y_3) \\
 & - 8(\nu - 1)^2(x_2 - y_2) \log(r_2 + x_3 + y_3) \\
 & - (4\nu - 3)(x_3 - y_3) \log(r_1 + x_2 - y_2) \\
 & + (-8\nu^2(x_3 + y_3) + 12\nu(x_3 + y_3) - 7x_3 - 5y_3) \\
 & \left. \times \log(r_2 + x_2 - y_2) + \frac{2x_3 y_3 (x_2 - y_2)(x_3 + y_3)}{r_2((x_1 - y_1)^2 + (x_3 + y_3)^2)} \right]. \tag{107}
 \end{aligned}$$

Examples of surface displacements are given in Figures 8–12 and in  Movie S3.

### Stress and Strains

Strains can be obtained by differentiating the total displacement by finite difference or analytically. The displacement gradient is written analytically as

$$\begin{aligned}
 u_{i,j} = & (\lambda e_{kk}^i + 2\mu e_{11}^i) J_{i123,j} + 2\mu e_{12}^i (J_{i223,j} + J_{i113,j}) \\
 & + 2\mu e_{13}^i (J_{i323,j} + J_{i112,j}) + (\lambda e_{kk}^i + 2\mu e_{22}^i) J_{i213,j} \\
 & + 2\mu e_{23}^i (J_{i212,j} + J_{i313,j}) + (\lambda e_{kk}^i + 2\mu e_{33}^i) J_{i312,j}. \tag{108}
 \end{aligned}$$

We generate the 81 independent components  $J_{ijkl,m}$  using Mathematica and then export the expressions in forms that can be evaluated by computer programs, making sure to avoid mathematical artifacts, with the exception of the unavoidable singularities at the eight corners of each strain volume. Then, the stress components are obtained following equation (9). Examples of stress fields generated by anelastic strain are shown in Figures 8–13.

Figure 9 illustrates that isotropic sources of anelastic strain create little isotropic stress in the surrounding rocks. This property may be exploited to decouple the governing equations of poroelasticity in a full-space (Rice and Cleary, 1976). Our solutions illustrate the remaining isotropic stress interaction resulting from the presence of the free surface. This effect vanishes with increasing depth of the source.

### Problem Definition for Dipping Strain Volumes

We consider the case of dipping strain volumes in a half-space. We define two systems of coordinates. The unprimed system of coordinates is aligned with the free surface and in the strike direction of the strain volume (Fig. 14). The primed system of coordinates is aligned with the fault. We consider a cuboid volume of length  $L$  in the strike direction  $\mathbf{e}_1$ , of width  $W$  in the dip direction  $\mathbf{e}'_3$ , and thickness  $T$  in the normal direction  $\mathbf{e}'_2$ . The relationships between the primed and unprimed coordinates are

$$\begin{aligned}
 x'_1 & = x_1 \\
 x'_2 & = x_2 \sin \phi - (x_3 - D) \cos \phi \\
 x'_3 & = x_2 \cos \phi + (x_3 - D) \sin \phi \tag{109}
 \end{aligned}$$

and

$$\begin{aligned}
 x_1 & = x'_1 \\
 x_2 & = +x'_2 \sin \phi + x'_3 \cos \phi \\
 x_3 & = -x'_2 \cos \phi + x'_3 \sin \phi + D. \tag{110}
 \end{aligned}$$

The volume is buried at a depth  $D$  and is subjected to six independent eigenstrain components  $e_{11}^i, e_{12}^i, e_{13}^i, e_{22}^i, e_{23}^i,$  and  $e_{33}^i$  expressed in the unprimed system of coordinates.

The spatial extent of the eigenstrain can be written as

$$e_{ij}^i(x_1, x_2, x_3) = e_{ij}^i S\left(\frac{x_1}{L}\right) \Pi\left(\frac{x'_2}{T}\right) S\left(\frac{x'_3}{W}\right) \equiv e_{ij}^i \Omega(x_1, x_2, x_3), \tag{111}$$

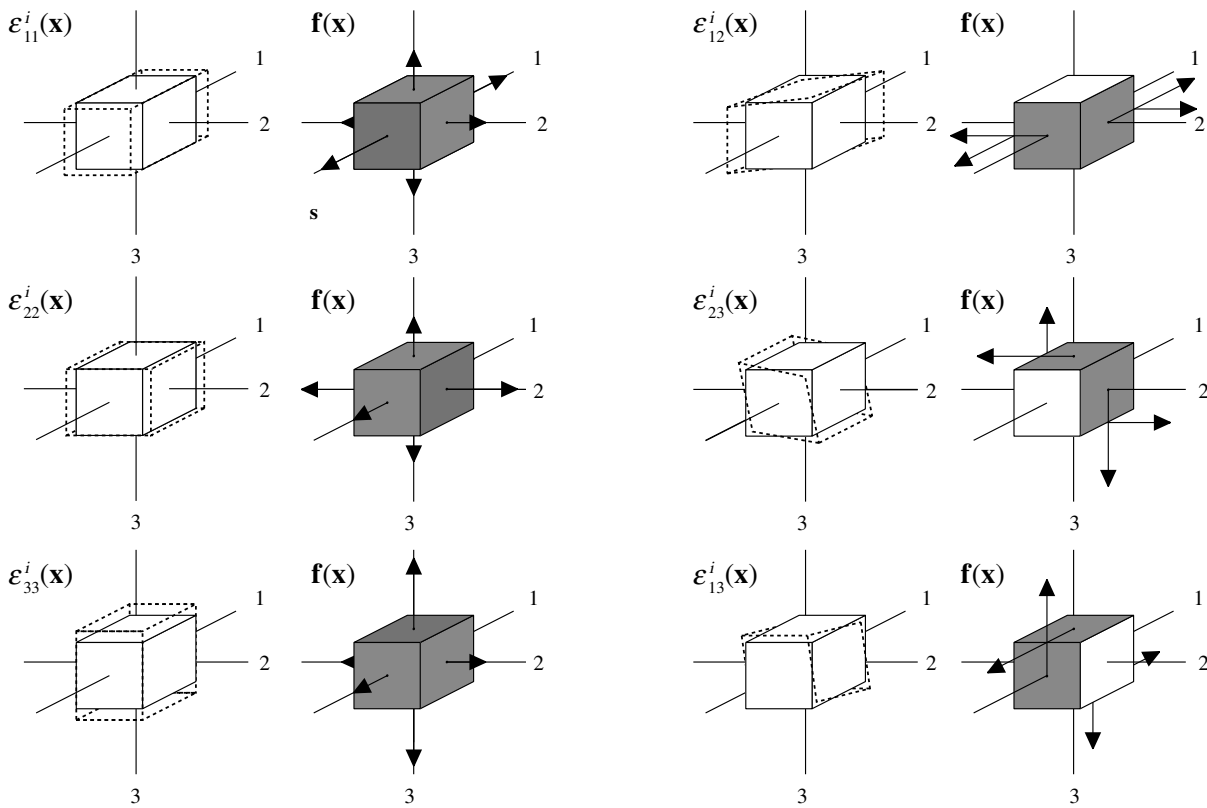


**Figure 7.** Six independent strain components on a finite cuboid volume and associated distribution of equivalent body forces. The dashed volume represents the anelastic deformation.

with  $x'_2 = x'_2(x_2, x_3)$  and  $x'_3 = x'_3(x_2, x_3)$ . Or, more explicitly

$$\epsilon^i_{ij}(x_1, x_2, x_3) = \epsilon^i_{22} S\left(\frac{x_1}{L}\right) \Pi\left(\frac{x_2 \sin \phi - (x_3 - D) \cos \phi}{T}\right) \times S\left(\frac{x_2 \cos \phi + (x_3 - D) \sin \phi}{W}\right). \quad (112)$$

We have defined

$$\Omega(x_1, x_2, x_3) = S\left(\frac{x_1}{L}\right) \Pi\left(\frac{x'_2(x_2, x_3)}{T}\right) S\left(\frac{x'_3(x_2, x_3)}{W}\right) \\ \Omega'(x'_1, x'_2, x'_3) = S\left(\frac{x'_1}{L}\right) \Pi\left(\frac{x'_2}{T}\right) S\left(\frac{x'_3}{W}\right), \quad (113)$$

which describes where the strain is applied. The deformation in the half-space due to elastic coupling can be attributed to the equivalent body forces

$$\mathbf{f} = -\nabla \cdot \mathbf{m} = - \begin{pmatrix} \lambda \epsilon^i_{kk,1} + 2\mu \epsilon^i_{11,1} + 2\mu \epsilon^i_{12,2} + 2\mu \epsilon^i_{13,3} \\ 2\mu \epsilon^i_{12,1} + \lambda \epsilon^i_{kk,2} + 2\mu \epsilon^i_{22,2} + 2\mu \epsilon^i_{23,3} \\ 2\mu \epsilon^i_{13,1} + 2\mu \epsilon^i_{23,2} + \lambda \epsilon^i_{kk,3} + 2\mu \epsilon^i_{33,3} \end{pmatrix}. \quad (114)$$

So we have

$$f_1(x_1, x_2, x_3) = (\lambda \epsilon^i_{kk} + 2\mu \epsilon^i_{11}) \frac{1}{L} \left[ \delta\left(\frac{x_1}{L} - 1\right) - \delta\left(\frac{x_1}{L}\right) \right] \Pi\left(\frac{x'_2}{T}\right) S\left(\frac{x'_3}{W}\right) \\ + \sin \phi \left\{ 2\mu \epsilon^i_{12} S\left(\frac{x_1}{L}\right) \frac{1}{T} \left[ \delta\left(\frac{x'_2}{T} - \frac{1}{2}\right) - \delta\left(\frac{x'_2}{T} + \frac{1}{2}\right) \right] S\left(\frac{x'_3}{W}\right) \right. \\ \left. + 2\mu \epsilon^i_{13} S\left(\frac{x_1}{L}\right) \Pi\left(\frac{x'_2}{T}\right) \frac{1}{W} \left[ \delta\left(\frac{x'_3}{W} - 1\right) - \delta\left(\frac{x'_3}{W}\right) \right] \right\} \\ + \cos \phi \left\{ 2\mu \epsilon^i_{12} S\left(\frac{x_1}{L}\right) \Pi\left(\frac{x'_2}{T}\right) \frac{1}{W} \left[ \delta\left(\frac{x'_3}{W} - 1\right) - \delta\left(\frac{x'_3}{W}\right) \right] \right. \\ \left. - 2\mu \epsilon^i_{13} S\left(\frac{x_1}{L}\right) \frac{1}{T} \left[ \delta\left(\frac{x'_2}{T} - \frac{1}{2}\right) - \delta\left(\frac{x'_2}{T} + \frac{1}{2}\right) \right] S\left(\frac{x'_3}{W}\right) \right\} \quad (115)$$

and

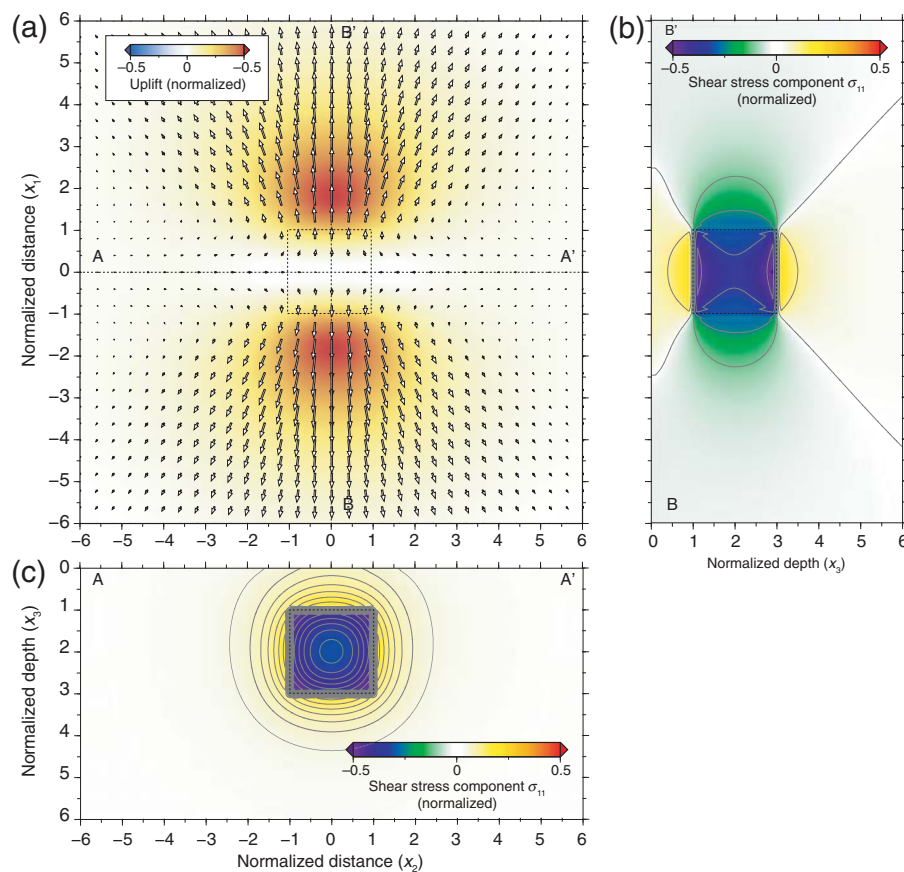


**Figure 8.** (a) Surface displacement and (b,c) stress component field  $\sigma_{11}$  for anelastic strain component  $\epsilon_{11}^i$ , representative of tectonic rifting. The cross sections are taken along the dashed profiles (A–A' for the bottom cross section and B–B' for the right one). The projection of the contour of the strain volume in the field of view is shown with the black dashed box. The displacement field is scaled by half of the maximum value. Similar results for anelastic strain component  $\epsilon_{22}^i$  can be obtained by symmetry.

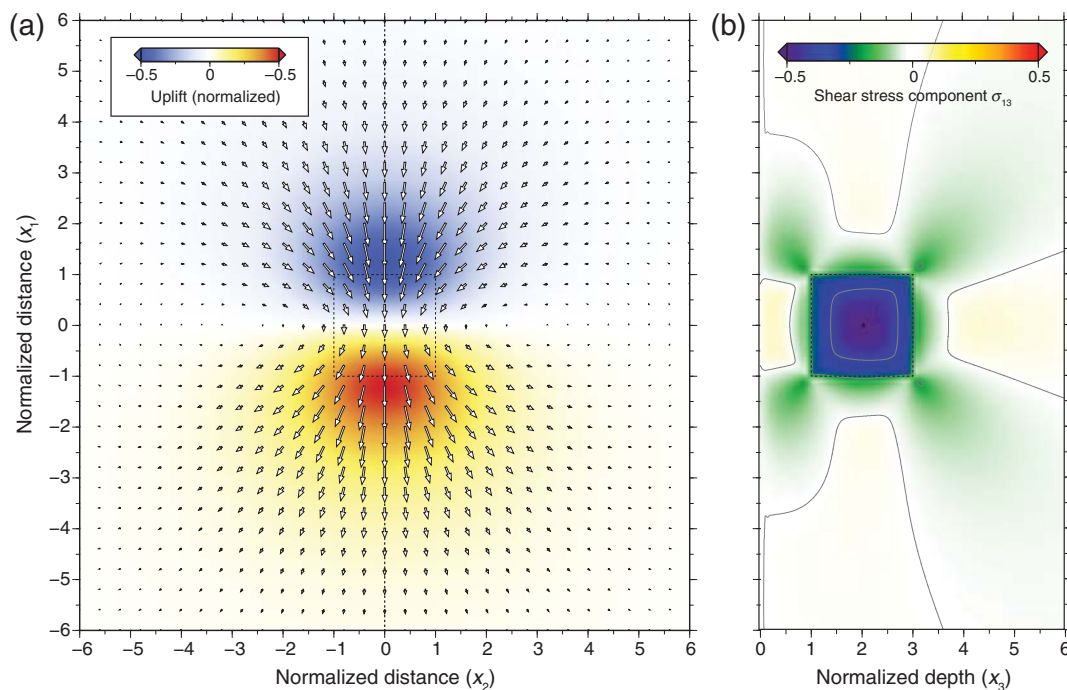


**Figure 9.** (a) Surface displacements and (b) stress component  $\sigma_{13}$  for anelastic strain component  $\epsilon_{13}^i$ , representative of channel flow. The cross section is taken along the dashed profile running north–south.

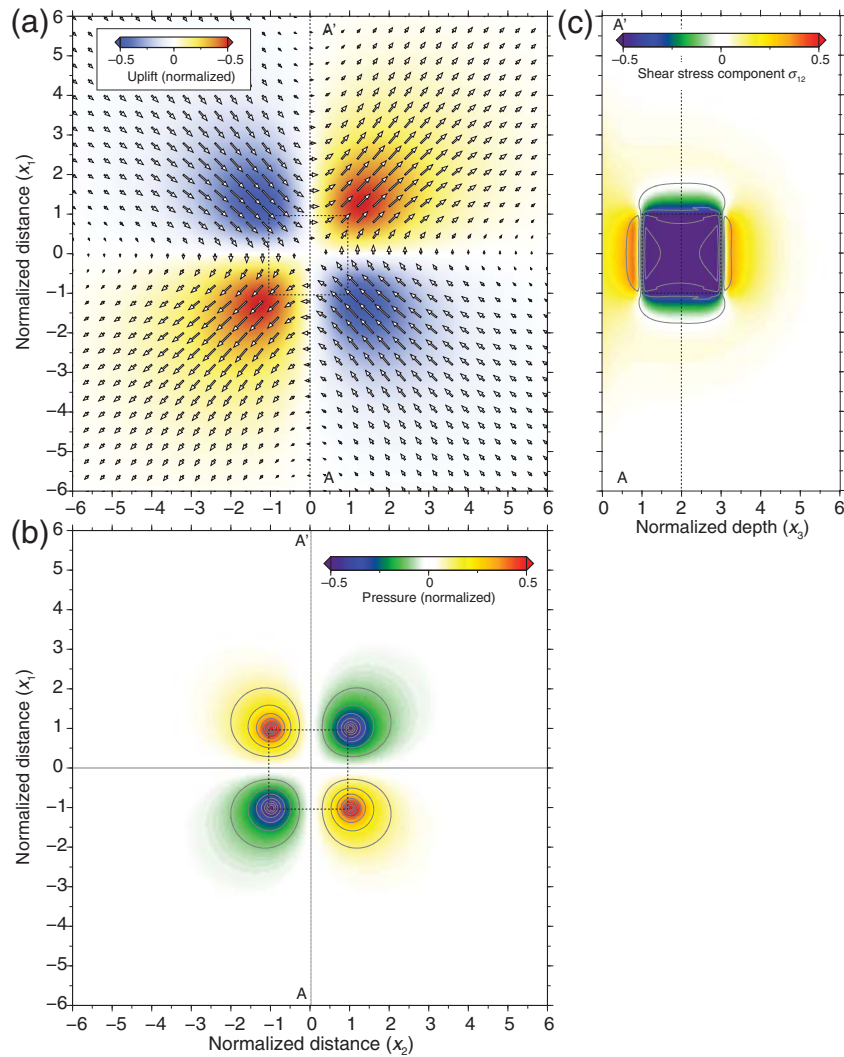


**Figure 10.** (a) Surface displacement, (b) stress component  $\sigma_{12}$ , and (c) pressure fields due to anelastic shear strain  $\epsilon_{12}^i$ . The map view of pressure is at the center of the strain volume ( $x_3 = 2$ ). The cross section is taken along the profile A–A'. Horizontal anelastic strain occurs in viscoelastic relaxation following strike-slip earthquakes.

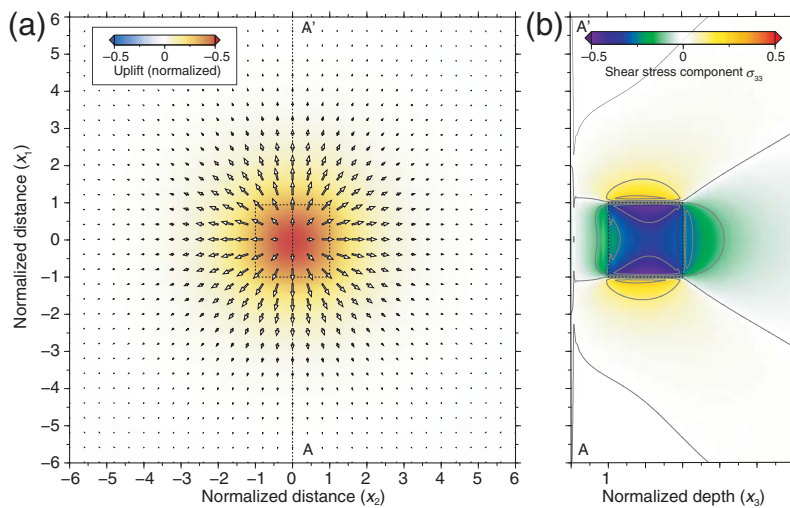


**Figure 11.** (a) Displacement and (b) stress component  $\sigma_{33}$  for anelastic strain component  $\epsilon_{33}^i$ . The cross section is running along the profile A–A'. Anelastic strain components  $\epsilon_{11}^i$  (Fig. 8),  $\epsilon_{13}^i$  (Fig. 9), and  $\epsilon_{33}^i$  are relevant to model viscoelastic deformation at convergent margins or transform boundaries.

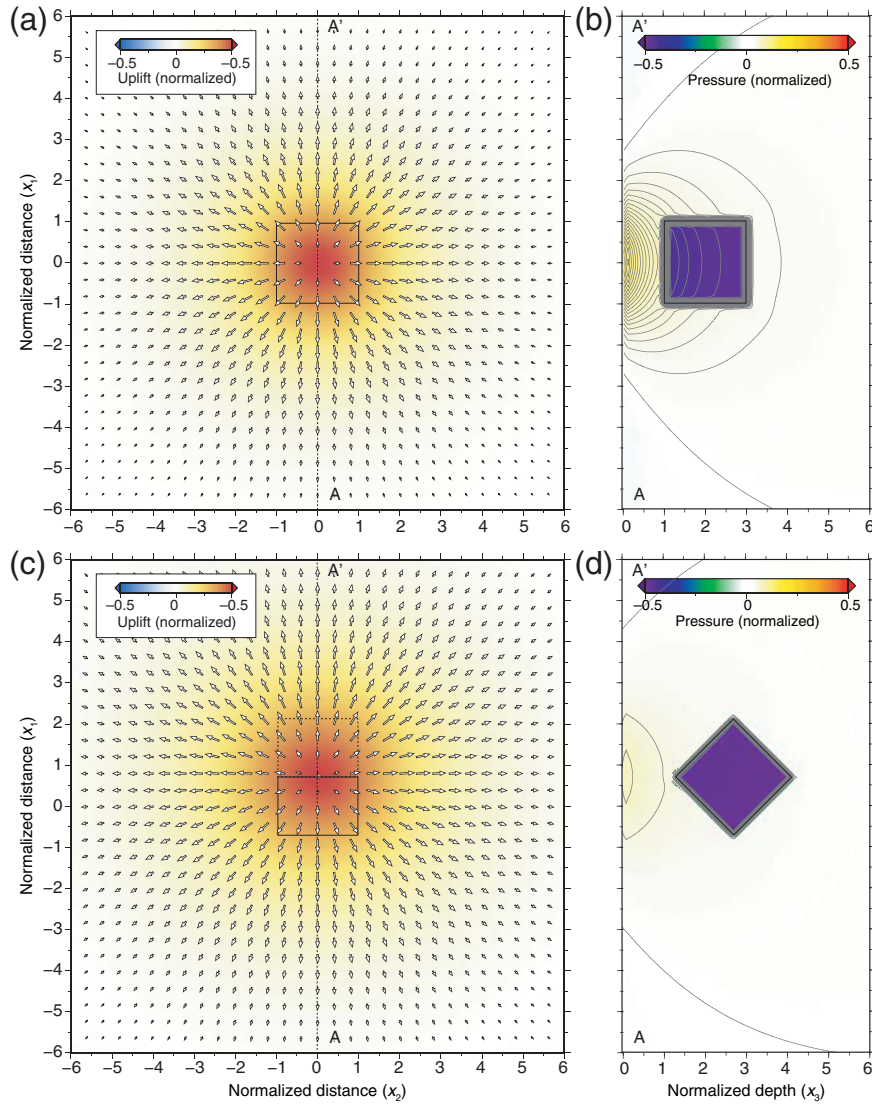


**Figure 12.** (a,c) Surface displacement and (b,d) cross section along profile A–A′ of isotropic stress for isotropic anelastic strain in (a,b) vertical and (c,d) 45°-dipping strain volume. The top and bottom of the strain volume are shown in map view with a solid and dashed profile, respectively. The cross sections are running along the A–A′ profiles (dashed lines in map view). Isotropic sources of deformation are relevant to represent the effects of thermoelasticity or poroelasticity, in which thermal expansion of fluid injection in a porous matrix causes the solid matrix to expand. Isotropic anelastic strain does not incur isotropic stress in the surrounding rocks except for the effect of the free surface, which disappears with increasing depth of the source.

$$\begin{aligned}
 f_2(x_1, x_2, x_3) = & 2\mu\epsilon_{12}^i \frac{1}{L} \left[ \delta\left(\frac{x_1}{L} - 1\right) - \delta\left(\frac{x_1}{L}\right) \right] \Pi\left(\frac{x_2}{T}\right) S\left(\frac{x_3}{W}\right) \\
 & + \sin\phi \left\{ (\lambda\epsilon_{kk}^i + 2\mu\epsilon_{22}^i) S\left(\frac{x_1}{L}\right) \frac{1}{T} \left[ \delta\left(\frac{x_2}{T} - \frac{1}{2}\right) - \delta\left(\frac{x_2}{T} + \frac{1}{2}\right) \right] S\left(\frac{x_3}{W}\right) \right. \\
 & \quad \left. + 2\mu\epsilon_{23}^i S\left(\frac{x_1}{L}\right) \Pi\left(\frac{x_2}{T}\right) \frac{1}{W} \left[ \delta\left(\frac{x_3 - W}{W}\right) - \delta\left(\frac{x_3}{W}\right) \right] \right\} \\
 & + \cos\phi \left\{ (\lambda\epsilon_{kk}^i + 2\mu\epsilon_{22}^i) S\left(\frac{x_1}{L}\right) \Pi\left(\frac{x_2}{T}\right) \frac{1}{W} \left[ \delta\left(\frac{x_3 - W}{W}\right) - \delta\left(\frac{x_3}{W}\right) \right] \right. \\
 & \quad \left. - 2\mu\epsilon_{23}^i S\left(\frac{x_1}{L}\right) \frac{1}{T} \left[ \delta\left(\frac{x_2}{T} - \frac{1}{2}\right) - \delta\left(\frac{x_2}{T} + \frac{1}{2}\right) \right] S\left(\frac{x_3}{W}\right) \right\}, \tag{116}
 \end{aligned}$$

$$\begin{aligned}
 f_3(x_1, x_2, x_3) = & 2\mu\epsilon_{13}^i \frac{1}{L} \left[ \delta\left(\frac{x_1}{L} - 1\right) - \delta\left(\frac{x_1}{L}\right) \right] \Pi\left(\frac{x_2}{T}\right) S\left(\frac{x_3}{W}\right) \\
 & + \sin\phi \left\{ 2\mu\epsilon_{23}^i S\left(\frac{x_1}{L}\right) \frac{1}{T} \left[ \delta\left(\frac{x_2}{T} - \frac{1}{2}\right) - \delta\left(\frac{x_2}{T} + \frac{1}{2}\right) \right] S\left(\frac{x_3}{W}\right) \right. \\
 & \quad \left. + (\lambda\epsilon_{kk}^i + 2\mu\epsilon_{33}^i) S\left(\frac{x_1}{L}\right) \Pi\left(\frac{x_2}{T}\right) \frac{1}{W} \left[ \delta\left(\frac{x_3 - W}{W}\right) - \delta\left(\frac{x_3}{W}\right) \right] \right\} \\
 & + \cos\phi \left\{ 2\mu\epsilon_{23}^i S\left(\frac{x_1}{L}\right) \Pi\left(\frac{x_2}{T}\right) \frac{1}{W} \left[ \delta\left(\frac{x_3 - W}{W}\right) - \delta\left(\frac{x_3}{W}\right) \right] \right. \\
 & \quad \left. - (\lambda\epsilon_{kk}^i + 2\mu\epsilon_{33}^i) S\left(\frac{x_1}{L}\right) \frac{1}{T} \left[ \delta\left(\frac{x_2}{T} - \frac{1}{2}\right) - \delta\left(\frac{x_2}{T} + \frac{1}{2}\right) \right] S\left(\frac{x_3}{W}\right) \right\}. \tag{117}
 \end{aligned}$$

## Green's Function Formulation

The displacement field can be obtained by the convolution of the body forces with the Green's function as follows:

$$u_i(\mathbf{x}) = \iiint_{-\infty}^{\infty} f_j(\mathbf{y}) G_{ji}(\mathbf{x}, \mathbf{y}) d\mathbf{y}. \quad (118)$$

Using the spatial distribution of equivalent body forces, we can write the displacement field explicitly:

$$\begin{aligned} u_i = & (\lambda e_{kk}^i + 2\mu e_{11}^i) \iiint_{-\infty}^{\infty} \frac{1}{L} \left[ \delta\left(\frac{y_1}{L} - 1\right) - \delta\left(\frac{y_1}{L}\right) \right] \Pi\left(\frac{y_2'}{T}\right) S\left(\frac{y_3'}{W}\right) G_{1i} dy_1 dy_2 dy_3 \\ & + 2\mu e_{12}^i \iiint_{-\infty}^{\infty} \frac{1}{L} \left[ \delta\left(\frac{y_1}{L} - 1\right) - \delta\left(\frac{y_1}{L}\right) \right] \Pi\left(\frac{y_2'}{T}\right) S\left(\frac{y_3'}{W}\right) G_{2i} dy_1 dy_2 dy_3 \\ & + 2\mu e_{13}^i \iiint_{-\infty}^{\infty} \frac{1}{L} \left[ \delta\left(\frac{y_1}{L} - 1\right) - \delta\left(\frac{y_1}{L}\right) \right] \Pi\left(\frac{y_2'}{T}\right) S\left(\frac{y_3'}{W}\right) G_{3i} dy_1 dy_2 dy_3 \\ & + \sin \phi \left\{ 2\mu e_{12}^i \iiint_{-\infty}^{\infty} S\left(\frac{y_1}{L}\right) \frac{1}{T} \left[ \delta\left(\frac{y_2'}{T} - \frac{1}{2}\right) - \delta\left(\frac{y_2'}{T} + \frac{1}{2}\right) \right] S\left(\frac{y_3'}{W}\right) G_{1i} dy_1 dy_2 dy_3 \right. \\ & + 2\mu e_{13}^i \iiint_{-\infty}^{\infty} S\left(\frac{y_1}{L}\right) \Pi\left(\frac{y_2'}{T}\right) \frac{1}{W} \left[ \delta\left(\frac{y_3'}{W} - 1\right) - \delta\left(\frac{y_3'}{W}\right) \right] G_{1i} dy_1 dy_2 dy_3 \\ & + (\lambda e_{kk}^i + 2\mu e_{22}^i) \iiint_{-\infty}^{\infty} S\left(\frac{y_1}{L}\right) \frac{1}{T} \left[ \delta\left(\frac{y_2'}{T} - \frac{1}{2}\right) - \delta\left(\frac{y_2'}{T} + \frac{1}{2}\right) \right] S\left(\frac{y_3'}{W}\right) G_{2i} dy_1 dy_2 dy_3 \\ & + 2\mu e_{23}^i \iiint_{-\infty}^{\infty} S\left(\frac{y_1}{L}\right) \Pi\left(\frac{y_2'}{T}\right) \frac{1}{W} \left[ \delta\left(\frac{y_3'}{W} - 1\right) - \delta\left(\frac{y_3'}{W}\right) \right] G_{2i} dy_1 dy_2 dy_3 \\ & + 2\mu e_{23}^i \iiint_{-\infty}^{\infty} S\left(\frac{y_1}{L}\right) \frac{1}{T} \left[ \delta\left(\frac{y_2'}{T} - \frac{1}{2}\right) - \delta\left(\frac{y_2'}{T} + \frac{1}{2}\right) \right] S\left(\frac{y_3'}{W}\right) G_{3i} dy_1 dy_2 dy_3 \\ & + (\lambda e_{kk}^i + 2\mu e_{33}^i) \iiint_{-\infty}^{\infty} S\left(\frac{y_1}{L}\right) \Pi\left(\frac{y_2'}{T}\right) \times \frac{1}{W} \left[ \delta\left(\frac{y_3'}{W} - 1\right) - \delta\left(\frac{y_3'}{W}\right) \right] G_{3i} dy_1 dy_2 dy_3 \left. \right\} \\ & + \cos \phi \left\{ 2\mu e_{12}^i \iiint_{-\infty}^{\infty} S\left(\frac{y_1}{L}\right) \Pi\left(\frac{y_2'}{T}\right) \frac{1}{W} \left[ \delta\left(\frac{y_3'}{W} - 1\right) - \delta\left(\frac{y_3'}{W}\right) \right] G_{1i} dy_1 dy_2 dy_3 \right. \\ & - 2\mu e_{13}^i \iiint_{-\infty}^{\infty} S\left(\frac{y_1}{L}\right) \frac{1}{T} \left[ \delta\left(\frac{y_2'}{T} - \frac{1}{2}\right) - \delta\left(\frac{y_2'}{T} + \frac{1}{2}\right) \right] S\left(\frac{y_3'}{W}\right) G_{1i} dy_1 dy_2 dy_3 \\ & + (\lambda e_{kk}^i + 2\mu e_{22}^i) \iiint_{-\infty}^{\infty} S\left(\frac{y_1}{L}\right) \Pi\left(\frac{y_2'}{T}\right) \frac{1}{W} \left[ \delta\left(\frac{y_3'}{W} - 1\right) - \delta\left(\frac{y_3'}{W}\right) \right] G_{2i} dy_1 dy_2 dy_3 \\ & - 2\mu e_{23}^i \iiint_{-\infty}^{\infty} S\left(\frac{y_1}{L}\right) \frac{1}{T} \left[ \delta\left(\frac{y_2'}{T} - \frac{1}{2}\right) - \delta\left(\frac{y_2'}{T} + \frac{1}{2}\right) \right] S\left(\frac{y_3'}{W}\right) G_{2i} dy_1 dy_2 dy_3 \\ & + 2\mu e_{23}^i \iiint_{-\infty}^{\infty} S\left(\frac{y_1}{L}\right) \Pi\left(\frac{y_2'}{T}\right) \frac{1}{W} \left[ \delta\left(\frac{y_3'}{W} - 1\right) - \delta\left(\frac{y_3'}{W}\right) \right] G_{3i} dy_1 dy_2 dy_3 \\ & \left. - (\lambda e_{kk}^i + 2\mu e_{33}^i) \iiint_{-\infty}^{\infty} S\left(\frac{y_1}{L}\right) \frac{1}{T} \left[ \delta\left(\frac{y_2'}{T} - \frac{1}{2}\right) - \delta\left(\frac{y_2'}{T} + \frac{1}{2}\right) \right] S\left(\frac{y_3'}{W}\right) G_{3i} dy_1 dy_2 dy_3 \right\}, \quad (119) \end{aligned}$$

in which each component can be obtained by substituting  $i = 1, 2, 3$ , and the Green's function  $G_{ij}$  is for  $G_{ij}(y_1, y_2, y_3)$ . To simplify the problem, we now change the variables of integration from  $dx_2 dx_3$  to  $dx_2' dx_3'$  as follows:

$$\begin{aligned} u_i = & (\lambda e_{kk}^i + 2\mu e_{11}^i) \iiint_{-\infty}^{\infty} \frac{1}{L} \left[ \delta\left(\frac{y_1}{L} - 1\right) - \delta\left(\frac{y_1}{L}\right) \right] \Pi\left(\frac{y_2'}{T}\right) S\left(\frac{y_3'}{W}\right) G_{1i}(y_1, y_2, y_3) dy_2' dy_3' \\ & + 2\mu e_{12}^i \iiint_{-\infty}^{\infty} \frac{1}{L} \left[ \delta\left(\frac{y_1}{L} - 1\right) - \delta\left(\frac{y_1}{L}\right) \right] \Pi\left(\frac{y_2'}{T}\right) S\left(\frac{y_3'}{W}\right) G_{2i}(y_1, y_2, y_3) dy_2' dy_3' \\ & + 2\mu e_{13}^i \iiint_{-\infty}^{\infty} \frac{1}{L} \left[ \delta\left(\frac{y_1}{L} - 1\right) - \delta\left(\frac{y_1}{L}\right) \right] \Pi\left(\frac{y_2'}{T}\right) S\left(\frac{y_3'}{W}\right) G_{3i}(y_1, y_2, y_3) dy_2' dy_3' \end{aligned}$$

$$\begin{aligned}
 & + \sin \phi \left\{ 2\mu\epsilon_{12}^i \iint_{-\infty}^{\infty} S\left(\frac{y_1}{L}\right) \frac{1}{T} \left[ \delta\left(\frac{y_2'}{T} - \frac{1}{2}\right) - \delta\left(\frac{y_2'}{T} + \frac{1}{2}\right) \right] S\left(\frac{y_3'}{W}\right) G_{1i}(y_1, y_2, y_3) dy_1' dy_3' \right. \\
 & \quad + 2\mu\epsilon_{13}^i \iint_{-\infty}^{\infty} S\left(\frac{y_1}{L}\right) \Pi\left(\frac{y_2'}{T}\right) \frac{1}{W} \left[ \delta\left(\frac{y_3'}{W} - 1\right) - \delta\left(\frac{y_3'}{W}\right) \right] G_{1i}(y_1, y_2, y_3) dy_1' dy_2' \\
 & + (\lambda\epsilon_{kk}^i + 2\mu\epsilon_{22}^i) \iint_{-\infty}^{\infty} S\left(\frac{y_1}{L}\right) \frac{1}{T} \left[ \delta\left(\frac{y_2'}{T} - \frac{1}{2}\right) - \delta\left(\frac{y_2'}{T} + \frac{1}{2}\right) \right] S\left(\frac{y_3'}{W}\right) G_{2i}(y_1, y_2, y_3) dy_1' dy_3' \\
 & \quad + 2\mu\epsilon_{23}^i \iint_{-\infty}^{\infty} S\left(\frac{y_1}{L}\right) \Pi\left(\frac{y_2'}{T}\right) \frac{1}{W} \left[ \delta\left(\frac{y_3' - W}{W}\right) - \delta\left(\frac{y_3'}{W}\right) \right] G_{2i}(y_1, y_2, y_3) dy_1' dy_2' \\
 & \quad + 2\mu\epsilon_{23}^i \iint_{-\infty}^{\infty} S\left(\frac{y_1}{L}\right) \frac{1}{T} \left[ \delta\left(\frac{y_2'}{T} - \frac{1}{2}\right) - \delta\left(\frac{y_2'}{T} + \frac{1}{2}\right) \right] S\left(\frac{y_3'}{W}\right) G_{3i}(y_1, y_2, y_3) dy_1' dy_3' \\
 & + (\lambda\epsilon_{kk}^i + 2\mu\epsilon_{33}^i) \iint_{-\infty}^{\infty} S\left(\frac{y_1}{L}\right) \Pi\left(\frac{y_2'}{T}\right) \frac{1}{W} \left[ \delta\left(\frac{y_3'}{W} - 1\right) - \delta\left(\frac{y_3'}{W}\right) \right] G_{3i}(y_1, y_2, y_3) dy_1' dy_2' \left. \right\} \\
 & + \cos \phi \left\{ 2\mu\epsilon_{12}^i \iint_{-\infty}^{\infty} S\left(\frac{y_1}{L}\right) \Pi\left(\frac{y_2'}{T}\right) \frac{1}{W} \left[ \delta\left(\frac{y_3'}{W} - 1\right) - \delta\left(\frac{y_3'}{W}\right) \right] G_{1i}(y_1, y_2, y_3) dy_1' dy_2' \right. \\
 & \quad - 2\mu\epsilon_{13}^i \iint_{-\infty}^{\infty} S\left(\frac{y_1}{L}\right) \frac{1}{T} \left[ \delta\left(\frac{y_2'}{T} - \frac{1}{2}\right) - \delta\left(\frac{y_2'}{T} + \frac{1}{2}\right) \right] S\left(\frac{y_3'}{W}\right) G_{1i}(y_1, y_2, y_3) dy_1' dy_3' \\
 & + (\lambda\epsilon_{kk}^i + 2\mu\epsilon_{22}^i) \iint_{-\infty}^{\infty} S\left(\frac{y_1}{L}\right) \Pi\left(\frac{y_2'}{T}\right) \frac{1}{W} \left[ \delta\left(\frac{y_3'}{W} - 1\right) - \delta\left(\frac{y_3'}{W}\right) \right] G_{2i}(y_1, y_2, y_3) dy_1' dy_2' \\
 & \quad - 2\mu\epsilon_{23}^i \iint_{-\infty}^{\infty} S\left(\frac{y_1}{L}\right) \frac{1}{T} \left[ \delta\left(\frac{y_2'}{T} - \frac{1}{2}\right) - \delta\left(\frac{y_2'}{T} + \frac{1}{2}\right) \right] S\left(\frac{y_3'}{W}\right) G_{2i}(y_1, y_2, y_3) dy_1' dy_3' \\
 & \quad + 2\mu\epsilon_{23}^i \iint_{-\infty}^{\infty} S\left(\frac{y_1}{L}\right) \Pi\left(\frac{y_2'}{T}\right) \frac{1}{W} \left[ \delta\left(\frac{y_3'}{W} - 1\right) - \delta\left(\frac{y_3'}{W}\right) \right] G_{3i}(y_1, y_2, y_3) dy_1' dy_2' \\
 & \left. - (\lambda\epsilon_{kk}^i + 2\mu\epsilon_{33}^i) \iint_{-\infty}^{\infty} S\left(\frac{y_1}{L}\right) \frac{1}{T} \left[ \delta\left(\frac{y_2'}{T} - \frac{1}{2}\right) - \delta\left(\frac{y_2'}{T} + \frac{1}{2}\right) \right] S\left(\frac{y_3'}{W}\right) G_{3i}(y_1, y_2, y_3) dy_1' dy_3' \right\}, \tag{120}
 \end{aligned}$$

in which the expression  $G_{ij}(y_1, y_2, y_3)$  is short for  $G_{ij}[y_1', y_2(y_2', y_3'), y_3(y_2', y_3')]$ . We simplify the bounds of integration again

$$\begin{aligned}
 u_i = & (\lambda\epsilon_{kk}^i + 2\mu\epsilon_{11}^i) \int_{-T/2}^{T/2} \int_0^W G_{1i}[y_1', y_2(y_2', y_3'), y_3(y_2', y_3')] \Big|_{y_1'=0}^{y_1'=L} dy_2' dy_3' \\
 & + 2\mu\epsilon_{12}^i \int_{-T/2}^{T/2} \int_0^W G_{2i}[y_1', y_2(y_2', y_3'), y_3(y_2', y_3')] \Big|_{y_1'=0}^{y_1'=L} dy_2' dy_3' \\
 & + 2\mu\epsilon_{13}^i \int_{-T/2}^{T/2} \int_0^W G_{3i}[y_1', y_2(y_2', y_3'), y_3(y_2', y_3')] \Big|_{y_1'=0}^{y_1'=L} dy_2' dy_3' \\
 & + \sin \phi \left\{ 2\mu\epsilon_{12}^i \int_0^L \int_0^W G_{1i}[y_1', y_2(y_2', y_3'), y_3(y_2', y_3')] \Big|_{y_2'=-T/2}^{y_2'=T/2} dy_1' dy_3' \right. \\
 & \quad + 2\mu\epsilon_{13}^i \int_0^L \int_{-T/2}^{T/2} G_{1i}[y_1', y_2(y_2', y_3'), y_3(y_2', y_3')] \Big|_{y_3'=0}^{y_3'=W} dy_1' dy_2' \\
 & + (\lambda\epsilon_{kk}^i + 2\mu\epsilon_{22}^i) \int_0^L \int_0^W G_{2i}[y_1', y_2(y_2', y_3'), y_3(y_2', y_3')] \Big|_{y_2'=-T/2}^{y_2'=T/2} dy_1' dy_3' \\
 & \quad + 2\mu\epsilon_{23}^i \int_0^L \int_{-T/2}^{T/2} G_{2i}[y_1', y_2(y_2', y_3'), y_3(y_2', y_3')] \Big|_{y_3'=0}^{y_3'=W} dy_1' dy_2' \\
 & \quad + 2\mu\epsilon_{23}^i \int_0^L \int_0^W G_{3i}[y_1', y_2(y_2', y_3'), y_3(y_2', y_3')] \Big|_{y_2'=-T/2}^{y_2'=T/2} dy_1' dy_3' \\
 & \left. + (\lambda\epsilon_{kk}^i + 2\mu\epsilon_{33}^i) \int_0^L \int_{-T/2}^{T/2} G_{3i}[y_1', y_2(y_2', y_3'), y_3(y_2', y_3')] \Big|_{y_3'=0}^{y_3'=W} dy_1' dy_2' \right\}
 \end{aligned}$$

$$\begin{aligned}
& + \cos \phi \left\{ 2\mu\epsilon_{12}^i \int_0^L \int_{-T/2}^{T/2} G_{1i} \left[ y_1', y_2(y_2', y_3'), y_3(y_2', y_3') \right] \Big|_{y_3'=0}^{y_3'=W} dy_1' dy_2' \right. \\
& \quad - 2\mu\epsilon_{13}^i \int_0^L \int_0^W G_{1i} \left[ y_1', y_2(y_2', y_3'), y_3(y_2', y_3') \right] \Big|_{y_2'=-T/2}^{y_2'=T/2} dy_1' dy_3' \\
& + (\lambda\epsilon_{kk}^i + 2\mu\epsilon_{22}^i) \int_0^L \int_{-T/2}^{T/2} G_{2i} \left[ y_1', y_2(y_2', y_3'), y_3(y_2', y_3') \right] \Big|_{y_3'=0}^{y_3'=W} dy_1' dy_2' \\
& \quad - 2\mu\epsilon_{23}^i \int_0^L \int_0^W G_{2i} \left[ y_1', y_2(y_2', y_3'), y_3(y_2', y_3') \right] \Big|_{y_2'=-T/2}^{y_2'=T/2} dy_1' dy_3' \\
& \quad + 2\mu\epsilon_{23}^i \int_0^L \int_{-T/2}^{T/2} G_{3i} \left[ y_1', y_2(y_2', y_3'), y_3(y_2', y_3') \right] \Big|_{y_3'=0}^{y_3'=W} dy_1' dy_2' \\
& \quad \left. - (\lambda\epsilon_{kk}^i + 2\mu\epsilon_{33}^i) \int_0^L \int_0^W G_{3i} \left[ y_1', y_2(y_2', y_3'), y_3(y_2', y_3') \right] \Big|_{y_2'=-T/2}^{y_2'=T/2} dy_1' dy_3' \right\}. \tag{121}
\end{aligned}$$

The solution for each  $u_i$  can be obtained using the proper Green's functions, defined in equations (73) and (74).

#### Numerical Solution with the tanh Quadrature

We use the tanh quadrature to convolve the Green's functions with the equivalent body forces (equations 115 and 116).

To do so, we write the integral in canonical form using the change of variable  $y_1' = (1 + u')L/2$ ,  $y_2' = v'T/2$ , and  $y_3' = (1 + w')W/2$ :

$$\begin{aligned}
u_i = & (\lambda\epsilon_{kk}^i + 2\mu\epsilon_{11}^i) \frac{T}{2} \frac{W}{2} \int_{-1}^1 \int_{-1}^1 G_{1i} \left[ y_1', y_2(v'T/2, (1 + w')W/2), y_3(v'T/2, (1 + w')W/2) \right] \Big|_{y_1'=0}^{y_1'=L} dv' dw' \\
& + 2\mu\epsilon_{12}^i \frac{T}{2} \frac{W}{2} \int_{-1}^1 \int_{-1}^1 G_{2i} \left[ y_1', y_2(v'T/2, (1 + w')W/2), y_3(v'T/2, (1 + w')W/2) \right] \Big|_{y_1'=0}^{y_1'=L} dv' dw' \\
& + 2\mu\epsilon_{13}^i \frac{T}{2} \frac{W}{2} \int_{-1}^1 \int_{-1}^1 G_{3i} \left[ y_1', y_2(v'T/2, (1 + w')W/2), y_3(v'T/2, (1 + w')W/2) \right] \Big|_{y_1'=0}^{y_1'=L} dv' dw' \\
& + \sin \phi \left\{ 2\mu\epsilon_{12}^i \frac{L}{2} \frac{W}{2} \int_{-1}^1 \int_{-1}^1 G_{1i} \left[ (1 + u')L/2, y_2(y_2', (1 + w')W/2), y_3(y_2', (1 + w')W/2) \right] \Big|_{y_2'=-T/2}^{y_2'=T/2} du' dw' \right. \\
& \quad + 2\mu\epsilon_{13}^i \frac{L}{2} \frac{T}{2} \int_{-1}^1 \int_{-1}^1 G_{1i} \left[ (1 + u')L/2, y_2(v'T/2, y_3'), y_3(v'T/2, y_3') \right] \Big|_{y_3'=0}^{y_3'=W} du' dv' \\
& + (\lambda\epsilon_{kk}^i + 2\mu\epsilon_{22}^i) \frac{L}{2} \frac{W}{2} \int_{-1}^1 \int_{-1}^1 G_{2i} \left[ (1 + u')L/2, y_2(y_2', (1 + w')W/2), y_3(y_2', (1 + w')W/2) \right] \Big|_{y_2'=-T/2}^{y_2'=T/2} du' dw' \\
& \quad + 2\mu\epsilon_{23}^i \frac{L}{2} \frac{T}{2} \int_{-1}^1 \int_{-1}^1 G_{2i} \left[ (1 + u')L/2, y_2(v'T/2, y_3'), y_3(v'T/2, y_3') \right] \Big|_{y_3'=0}^{y_3'=W} du' dv' \\
& \quad + 2\mu\epsilon_{23}^i \frac{L}{2} \frac{W}{2} \int_{-1}^1 \int_{-1}^1 G_{3i} \left[ (1 + u')L/2, y_2(y_2', (1 + w')W/2), y_3(y_2', (1 + w')W/2) \right] \Big|_{y_2'=-T/2}^{y_2'=T/2} du' dw' \\
& \quad \left. + (\lambda\epsilon_{kk}^i + 2\mu\epsilon_{33}^i) \frac{L}{2} \frac{T}{2} \int_{-1}^1 \int_{-1}^1 G_{3i} \left[ (1 + u')L/2, y_2(v'T/2, y_3'), y_3(v'T/2, y_3') \right] \Big|_{y_3'=0}^{y_3'=W} du' dv' \right\} \\
& + \cos \phi \left\{ 2\mu\epsilon_{12}^i \frac{L}{2} \frac{T}{2} \int_{-1}^1 \int_{-1}^1 G_{1i} \left[ (1 + u')L/2, y_2(v'T/2, y_3'), y_3(v'T/2, y_3') \right] \Big|_{y_3'=0}^{y_3'=W} du' dv' \right. \\
& \quad - 2\mu\epsilon_{13}^i \frac{L}{2} \frac{W}{2} \int_{-1}^1 \int_{-1}^1 G_{1i} \left[ (1 + u')L/2, y_2(y_2', (1 + w')W/2), y_3(y_2', (1 + w')W/2) \right] \Big|_{y_2'=-T/2}^{y_2'=T/2} du' dw' \\
& + (\lambda\epsilon_{kk}^i + 2\mu\epsilon_{22}^i) \frac{L}{2} \frac{T}{2} \int_{-1}^1 \int_{-1}^1 G_{2i} \left[ (1 + u')L/2, y_2(v'T/2, y_3'), y_3(v'T/2, y_3') \right] \Big|_{y_3'=0}^{y_3'=W} du' dv' \\
& \quad - 2\mu\epsilon_{23}^i \frac{L}{2} \frac{W}{2} \int_{-1}^1 \int_{-1}^1 G_{2i} \left[ (1 + u')L/2, y_2(y_2', (1 + w')W/2), y_3(y_2', (1 + w')W/2) \right] \Big|_{y_2'=-T/2}^{y_2'=T/2} du' dw' \\
& \quad + 2\mu\epsilon_{23}^i \frac{L}{2} \frac{T}{2} \int_{-1}^1 \int_{-1}^1 G_{3i} \left[ (1 + u')L/2, y_2(v'T/2, y_3'), y_3(v'T/2, y_3') \right] \Big|_{y_3'=0}^{y_3'=W} du' dv' \\
& \quad \left. - (\lambda\epsilon_{kk}^i + 2\mu\epsilon_{33}^i) \frac{L}{2} \frac{W}{2} \int_{-1}^1 \int_{-1}^1 G_{3i} \left[ (1 + u')L/2, y_2(y_2', (1 + w')W/2), y_3(y_2', (1 + w')W/2) \right] \Big|_{y_2'=-T/2}^{y_2'=T/2} du' dw' \right\}. \tag{122}
\end{aligned}$$



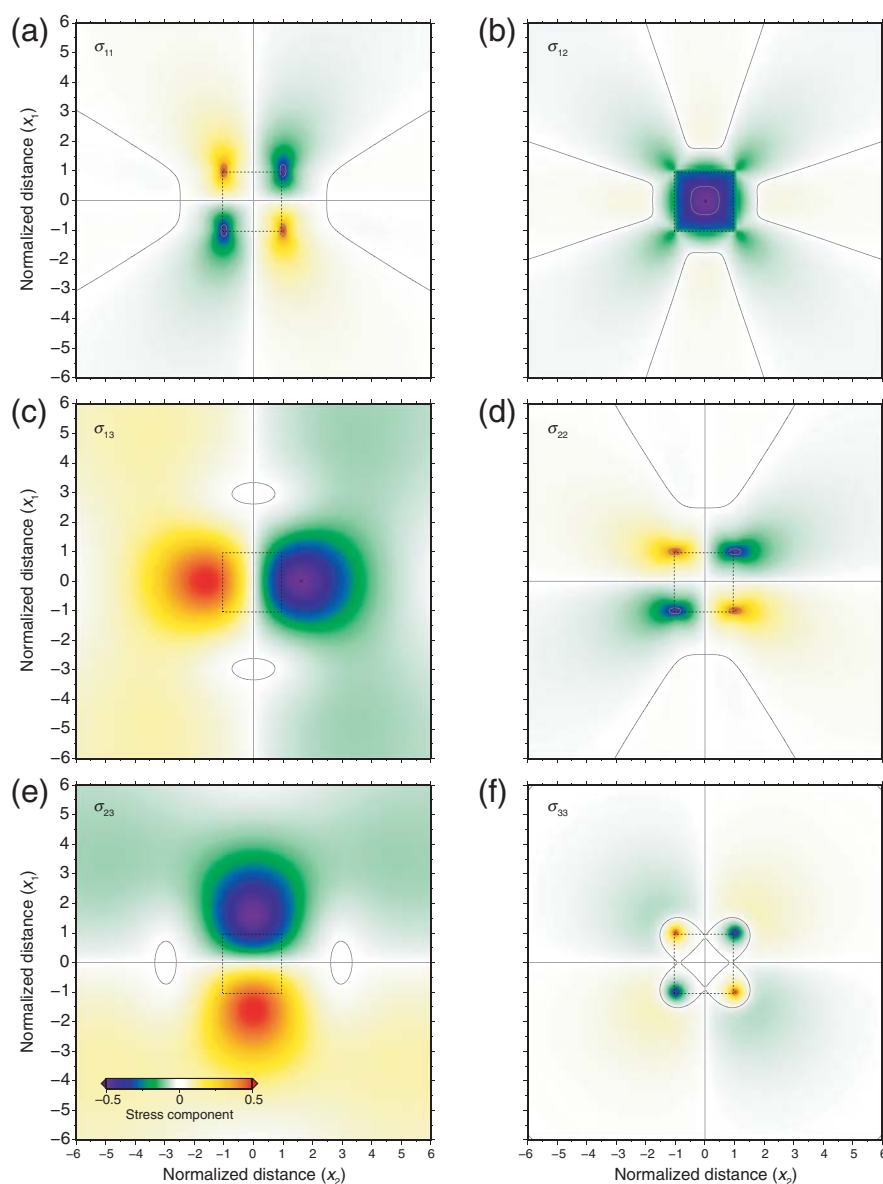


**Figure 13.** (a–f) Six independent stress components in map view at the center of the strain volume due to anelastic strain  $\epsilon_{12}^i$ . The dashed boxes represent the contour of the strain volume. The corresponding displacement and pressure fields are shown in Figure 10.

In this form, the classic algorithms for numerical integration can be directly applied. We accompany this article with computer codes that provide the numerical solution with arbitrary accuracy, free of any numerical artifacts, with the exception of singularities at the precise location of the eight strain volume corners. Examples of displacement and stress for distributed anelastic strain in dipping strain volumes in 3D are shown in Figures 15 and 16. Displacement and stress for dipping pressure sources are shown in Figure 12.

#### Semianalytic Solution with a Spectral Method

We use the spectral method *Relax* (Barbot and Fialko, 2010a,b) to solve Navier's equation numerically. The method relies on an analytical solution in the Fourier domain for the displacement field due to an arbitrary distribution of body

forces. We use the body forces defined in equations (115) and (116) for 3D dipping strain volumes. The total strain is obtained by finite difference, and the stress is obtained by combining the total strain with the eigenstrain following equation (9). The displacement and stress fields using the spectral method agree with other solutions within a 1% error, which is due to the undesirable periodicity of the discrete Fourier transform, and the necessity of smoothing the equivalent body forces to avoid spurious oscillations.

#### Conclusions

We presented fundamental solutions for the displacement and stress caused by distributed anelastic deformation in a half-space. The solutions are valid under the infinitesimal strain approximation and linear isotropic elasticity.

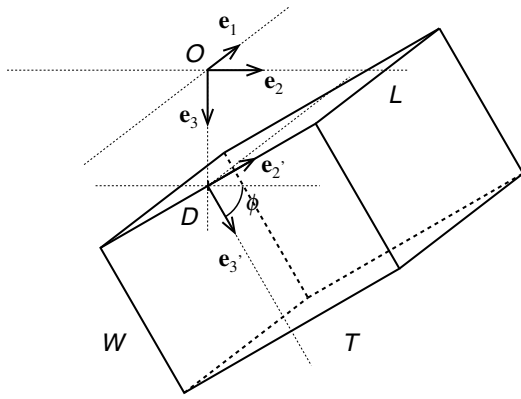


**Figure 14.** Position, dimension, and orientation of a dipping strain volume of length  $L$ , thickness  $T$ , and width  $W$ , buried at depth  $D$ , and dipping an angle  $\phi$ . The primed coordinate system is aligned with the strain volume. Both systems of coordinates point in the strike direction, such as  $\mathbf{e}'_1 = \mathbf{e}_1$ . For  $\phi = \pi/2$ , the two systems are identical except for a translation.

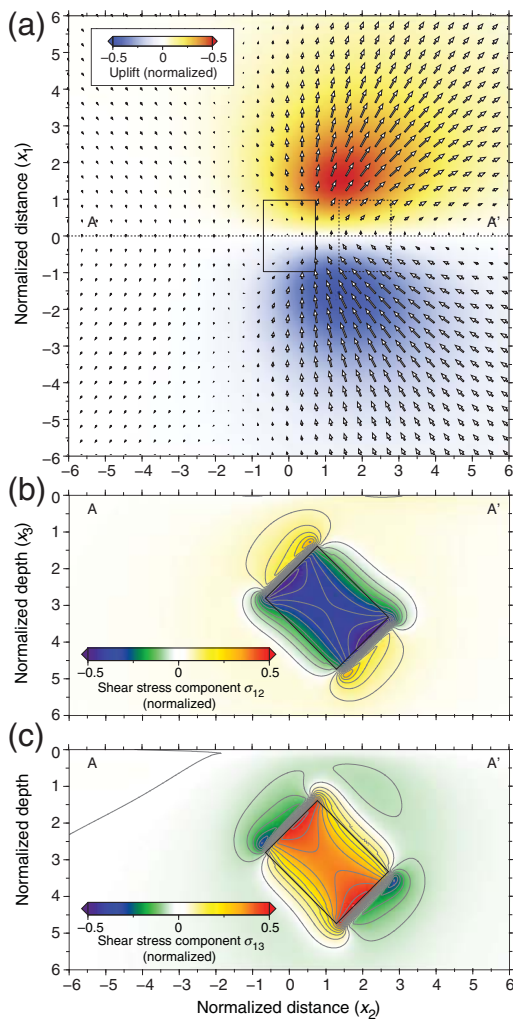


**Figure 15.** (a) Surface displacement in map view, (b) stress components  $\sigma_{12}$ , and (c)  $\sigma_{13}$  in a cross section along the A–A' profile due to anelastic shear strain  $\epsilon_{12}^i$ , defined in the primed system of coordinates tied with the strain volume. The map projection of the bottom of the strain volume is shown with the dashed rectangle in map view.

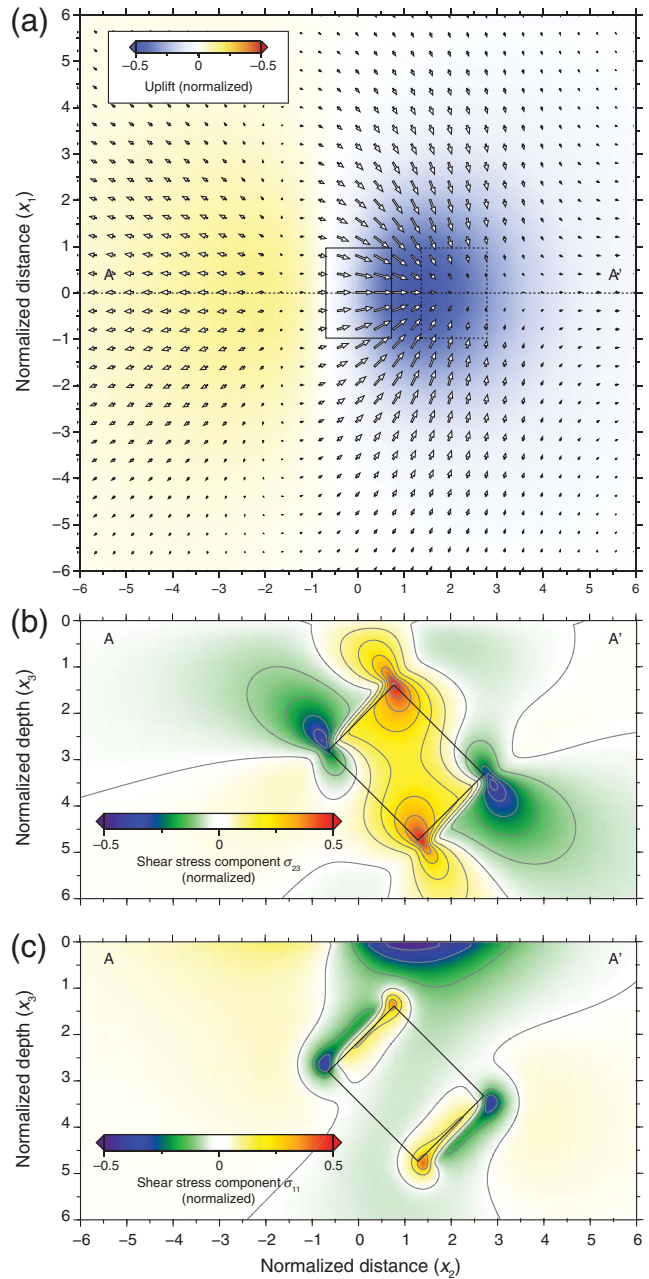


**Figure 16.** (a) Surface displacement in map view, (b) stress components  $\sigma_{23}$ , and (c)  $\sigma_{11}$  in a cross section along the A–A' profile due to anelastic shear strain  $\epsilon_{23}^i$ , defined in the primed system of coordinates tied with the strain volume. The map projection of the bottom of the strain volume is shown with the dashed rectangle in map view.

These solutions represent much-needed tools to probe the distributed deformation in the Earth's interior using geodetic and other geophysical observations. The description of the stress interactions provide the building blocks to simulate the dynamics of stress evolution around plate boundaries, incorporating off-fault and distributed deformation, including the viscoelastic and poroelastic effects. The solutions presented here are limited to uniform elastic properties. This assumption

allows closed-form analytic solutions. Admittedly, more realistic representations of the Earth's constitutive properties should be included, which we postpone to future work.

### Data and Resources

The MATLAB computer programs used in the article are available at <https://bitbucket.org/sbarbot> (last accessed February 2017). The *Relax* modeling software is hosted at [www.geodynamics.org](http://www.geodynamics.org) (last accessed February 2017) with support from the Computational Infrastructure for Geodynamics.

### Acknowledgments

This research was supported by the National Research Foundation (NRF) of Singapore under the NRF Fellowship scheme (National Research Fellow Awards Number NRF-NRFF2013-04) and by the Earth Observatory of Singapore, the NRF, and the Singapore Ministry of Education under the Research Centres of Excellence initiative.

### References

- Barbot, S., and Y. Fialko (2010a). A unified continuum representation of postseismic relaxation mechanisms: Semi-analytic models of afterslip, poroelastic rebound and viscoelastic flow, *Geophys. J. Int.* **182**, no. 3, 1124–1140, doi: [10.1111/j.1365-246X.2010.04678.x](https://doi.org/10.1111/j.1365-246X.2010.04678.x).
- Barbot, S., and Y. Fialko (2010b). Fourier-domain Green's function for an elastic semi-infinite solid under gravity, with applications to earthquake and volcano deformation, *Geophys. J. Int.* **182**, no. 2, 568–582, doi: [10.1111/j.1365-246X.2010.04655.x](https://doi.org/10.1111/j.1365-246X.2010.04655.x).
- Barbot, S., Y. Fialko, and D. Sandwell (2008). Effect of a compliant fault zone on the inferred earthquake slip distribution, *J. Geophys. Res.* **113**, no. B6, doi: [10.1029/2007JB005256](https://doi.org/10.1029/2007JB005256).
- Chinnery, M. (1963). The stress changes that accompany strike-slip faulting, *Bull. Seismol. Soc. Am.* **53**, no. 5, 921–932.
- Haber, S. (1977). The tanh rule for numerical integration, *SIAM J. Numer. Anal.* **14**, no. 4, 668–685.
- Iwasaki, T., and R. Sato (1979). Strain field in a semi-infinite medium due to an inclined rectangular fault, *J. Phys. Earth* **27**, no. 4, 285–314.
- Lambert, V., and S. Barbot (2016). Contribution of viscoelastic flow in earthquake cycles within the lithosphere–asthenosphere system, *Geophys. Res. Lett.* **43**, no. 19, 142–154.
- Masuti, S., S. Barbot, S. Karato, L. Feng, and P. Banerjee (2016). Upper mantle water stratification inferred from the 2012  $M_w$  8.6 Indian Ocean earthquake, *Nature* **538**, 373–377.
- Mindlin, R. D. (1936). Force at a point in the interior of a semi-infinite solid, *J. Appl. Phys.* **7**, 195–202.
- Moore, J. D., and B. Parsons (2015). Scaling of viscous shear zones with depth-dependent viscosity and power-law stress–strain-rate dependence, *Geophys. J. Int.* **202**, no. 1, 242–260.
- Okada, Y. (1985). Surface deformation due to shear and tensile faults in a half-space, *Bull. Seismol. Soc. Am.* **75**, no. 4, 1135–1154.
- Okada, Y. (1992). Internal deformation due to shear and tensile faults in a half-space, *Bull. Seismol. Soc. Am.* **82**, 1018–1040.
- Press, F. (1965). Displacements, strains, and tilts at teleseismic distances, *J. Geophys. Res.* **70**, no. 10, 2395–2412.
- Rice, J. R., and M. P. Cleary (1976). Some basic stress-diffusion solutions for fluid-saturated elastic porous media with compressible constituents, *Rev. Geophys.* **14**, 227–241.
- Sato, R., and M. Matsu'ura (1974). Strains and tilts on the surface of a semi-infinite medium, *J. Phys. Earth* **22**, no. 2, 213–221.
- Savage, J. C., and L. M. Hastie (1966). Surface deformation associated with dip-slip faulting, *J. Geophys. Res.* **71**, no. 20, 4897–4904.
- Segall, P. (2010). *Earthquake and Volcano Deformation*, Princeton University Press, Princeton, New Jersey.
- Steketee, J. A. (1958). Some geophysical applications of the elasticity theory of dislocations, *Can. J. Phys.* **36**, 1168–1198.

Earth Observatory of Singapore  
Nanyang Technological University  
50 Nanyang Avenue  
Singapore 639798, Singapore  
sylbar.vainbot@gmail.com

Manuscript received 22 July 2016;  
Published Online 23 March 2017